DISSERTATION

submitted to the

Combined Faculties for the Natural Sciences and for Mathematics
of the Ruperta-Carola University of Heidelberg

for the degree of

Doctor of Natural Sciences

Put forward by

M. Sc. Carsten Littek

born in
Essen

Oral examination: 29.06.2018

KINETIC FIELD THEORY:
MOMENTUM-DENSITY CORRELATIONS AND FUZZY DARK MATTER

Referees:

Prof. Dr. Matthias Bartelmann
Prof. Dr. Manfred Salmhofer

ABSTRACT

Building upon the recent developments of Kinetic Field Theory (KFT) for cosmic structure formation we develop a systematic way to calculate correlation functions of the momentum-density field. We show that these correlators can be calculated from the factorised generating functional after application of partial derivatives with respect to the momentum shift. For visual aid and in order to facilitate an automatic evaluation of corrections by particle interactions we introduce a diagrammatic representation of terms.
We employ this formalism to calculate the 2-point momentum-density correlation tensor including initial correlations to quadratic order and completely. A comparison of the results shows that the initial correlations are responsible for the deformation of the power-spectrum on small scales rather than the particle interactions. In the spirit of the Born approximation we use an effective force term to calculate the corrections due to gravity. Our results are in good agreement with previous analytic and simulation results.
Recently, Fuzzy Dark Matter models such as Ultra-Light Axions have caught a lot of interest. Their dynamics is described by the classical equations of a condensate. This introduces a quantum potential in the Euler equation and is generally repulsive. We have developed an extension to KFT treating the effects of the quantum potential on the dynamics and on the initial density fluctuation power-spectrum. We find the effects to be largest on scales in the range of $3h/\mathrm{Mpc} \gtrsim k \gtrsim 0.3h/\mathrm{Mpc}$, close to the onset of non-linear structures.

Auf Grundlage jüngster Entwicklungen in der Kinetischen Feldtheorie (KFT) für kosmische Strukturbildung erarbeiten wir eine systematische Herangehensweise zur Berechnung von Korrelationen des Geschwindigkeitsdichte-Feldes. Diese Korrelationsfunktionen können durch partielle Ableitungen nach der Impulsverschiebung von dem faktorisierten generierenden Funktional berechnet werden. Wir führen eine diagrammatische Repräsentation der durch Wechselwirkungen zwischen Teilchen auftretenden Korrekturen als visuelles Hilfsmittel ein. Diese Diagramme ermöglichen auch eine automatische Berechnung dieser Korrekturen.
Wir benutzen diesen Formalismus, um den 2-Punkt Korrelationstensor der Impulsdichte zu berechnen. Die anfänglichen Korrelationen berücksichtigen wir dabei entweder bis zur quadratischen Ordnung oder vollständig. Ein Vergleich der Ergebnisse lässt den Schluss zu, dass die anfänglichen Korrelationen wichtiger sind für die Deformation des Power-Spektrums auf kleinen Skalen als die Wechselwirkungen zwischen Teilchen. Zusätzlich berechnen wir die Auswirkung von gravitativer Wechselwirkungen durch einen effektiven Kraft-Term im Sinne der Born-Näherung. Unsere Ergebnisse stimmen mit vorigen analytischen und Simulationsergebnissen überein.
In letzter Zeit hat das Interesse an Fuzzy Dark Matter Modellen, wie z.B. Ultra-Leichte Axionen, stark zugenommen. Zur Beschreibung der Dynamik werden die klassichen Gleichungen eines Kondensats genutzt. Dies führt zu einem Quantenpotential in der Euler-Gleichung, welches im Allgemeinen abstoßend wirkt. Wir haben KFT um die Effekte des Quantenpotentials auf die Dynamik und auf das anfängliche Dichtefluktuations Power-Spektrum erweitert. Unsere Ergebnisse zeigen, dass diese Effekte auf Skalen im Bereich $3h/\mathrm{Mpc} \gtrsim k \gtrsim 0.3h/\mathrm{Mpc}$ am größten sind. Dies ist nahe der Skala der nicht-linearen Strukturbildung.

PUBLICATIONS

Some ideas have appeared previously in the following publications:

M. Bartelmann, F. Fabis, S. Konrad, E. Kozlikin, R. Lilow, C. Littek, and J. Dombrowski. "Analytic calculation of the non-linear cosmic density-fluctuation power spectrum in the Born approximation." In: ArXiv e-prints (Oct. 2017). arXiv: 1710.07522.

Aah, you mean EFFFECKT

— Prof. Dr. Matthias Bartelmann

ACKNOWLEDGEMENTS

Foremost, I want to thank my advisor Matthias Bartelmann for his support, his jokes and ideas in the time of need. I have enjoyed our discussions on physics and life very much (Dat sind ja Ehrensachen). His deep fascination for physics make him an excellent teacher.
I would like to thank Björn Malte Schäfer for dropping by my office every then and again for dopping some knowledge or just some target practice.
I am very grateful for the help provided by David (Doddy) Marsh on Fuzzy Dark Matter. Visiting Göttingen brought the project a big leap forwards.
My special thanks go to the ancient and not-so-ancient Fieldworkers in the group. The ancients being Dr. Felix Fabis, Elena Kozlikin, Robert Lilow and Celia Viermann who helped me get started. The not-so-ancient Fieldworkers include Sara Konrad, Igor Böttcher, and many more. I would like to thank you for very useful discussions on Kinetic Field Theory and any other topic. A special thanks to Christian Sorgenfrei who helped including the Born approximation in momentum-density correlations and to Leander Fischer for providing calculations on the Born approximated quantum force on FDM particles.
I would like to thank the whole Cosmology group at ITA for just being the way they are, open-minded and always in for a joke. Especially people like Tim Tugendhat or Robert Reischke whose comments may sometimes be hilarious.
I want to thank Anna Zacheus for her dedicated work to keep any administrative problems out of the way.
I am most grateful for the support of my parents who made it possible for me to go my way and become who I am now. They supported me in so many ways that I cannot thank them enough.
Last but not least I want to thank my girlfriend Jessi and my friends for providing necessary diversions through dancing, boardgames, sports, and the occasional barbecue.

CONTENTS

LIST OF FIGURES

ACRONYMS

BEC Bose-Einstein Condensate

CMB Cosmic Microwave Background

CDM Cold Dark Matter

FDM Fuzzy Dark Matter

KFT Kinetic Field Theory

kSZ kinetic Sunyaev-Zel'dovich effect

QFT Quantum Field Theory

SPT Standard Perturbation Theory

tSZ thermal Sunyaev-Zel'dovich effect

ULA Ultra-Light Axion

WDM Warm Dark Matter

1 INTRODUCTION AND MOTIVATION

Standard analytical tools of cosmic structure formation are based on the Boltzmann equation or the hydrodynamical equations (cf. Bernardeau et al. [7] for a review). The dynamical fields in those theories are continuous, namely the phase-space density, or mass-density and velocity field of the fluid. For collisionless dark matter those theories generally break down, as soon as streams cross leading to an ill-defined velocity field. Bartelmann et al. [6] recently developed an alternative to the common fluid approaches called Kinetic Field Theory (KFT). In the spirit of Martin, Siggia, and Rose [23] KFT describes structures as ensembles of correlated microscopic particles obeying Hamiltonian dynamics. The dynamical fields in this approach are the phase-space coordinates of the microscopic particles and the ensemble is completely described by a generating functional that contains information about the initial phase-space distribution and the dynamics of the particles. Structurally, this approach is closely related to the path integral formulation of Quantum Field Theory (QFT). Correlators of macroscopic fields, e. g. the density, are calculated from the generating functional by application of appropriate functional derivatives.

Problems arising in conventional analytic approaches to cosmic structure formation are avoided by the use of particle dynamics rather than smooth fields. The Hamiltonian flow in phase-space is symplectic, i. e. volume conserving by Liouille's theorem, and diffeomorphic. Therefore each particle moves on a unique trajectory in phase-space. This avoids problems of crossing streams and ill-defined smooth fields. One can think of KFT as the analytical analogue of the N-body simulation commonly used in cosmology.

Recent publications (Bartelmann et al. [5], Bartelmann et al. [4]) have developed KFT further and applied the formalism to the calculation of the density fluctuation power-spectrum. In this work we extend the analysis of previous publications to the calculation of momentum-density correlations. In the first part we review the formalism to KFT. Based on that we derive a systematic way to calculate n-point momentum-density correlators from the generating functional employing diagrams as a visual aid. The derivation involves the factorisation of the generating functional. The factorisation is possible due to the statistical homogeneity and isotropy of the initial correlations. As a result, correlators can be calculated from convolutions of power-spectra.

We apply the developed formalism to calculate the 2-point momentum-density correlation tensor in Chapter 4. For the calculation we will first consider initial momentum correlations only quadratically as Bartelmann et al. [6] did for the density power-spectrum. Then we give expressions using the factorised form of the generating functional. In the spirit of Bartelmann et al. [4] we employ the Born approximation in order to estimate the effect of gravitational particle interactions.

As an application of our calculations we look at secondary anisotropies in the Cosmic Microwave Background (CMB) radiation. The CMB was released when the Universe became electrically neutral and the optical depth dropped to zero. The radiation field is highly isotropic with small anisotropies, either primordially seeded during inflation or secondarily due to interactions of photons along their journey. The formation of astrophysical objects, such as stars and galaxies, in halos of dark matter causes the reionisation of the intergalactic medium by radiation. One possible secondary anisotropy is caused by inverse Compton scattering off free electrons, called the Sunyaev-Zel'dovich effect. We can distinguish the thermal Sunyaev-Zel'dovich effect (tSZ) caused by random motion

of electrons and the kinetic Sunyaev-Zel'dovich effect (kSZ) caused by electrons moving with the bulk. Here we investigate the kSZ effect which is directly related to the power-spectrum of the momentum-density.
In the last Chapter we extend the formalism of KFT towards Fuzzy Dark Matter (FDM). The particle nature of dark matter is unproven and the variety of particle candidates is vast. As we have described above, in KFT we treat the dark matter as classical microscopic particles following the Hamiltonian equations of motion. That description is valid for Cold Dark Matter (CDM), whose particles have low velocity dispersions and interact only gravitationally. Apart from the great success of CDM in predicting the large scale structure in the Universe, there exist some discrepancies between simulations and observations:

- The cusp/core problem (cf. de Blok [37]): simulations predict cuspy density profiles at the centers of galaxies, while observations of rotation curves favor flat profiles.
- The missing satellites problem (cf. Bullock [11]): the abundance of low-mass halos is larger in simulations than observations around the Milky Way suggest.

These problems may be related to problems with the implementation of baryonic physics in the simulations (Brooks et al. [10]) or in the nature of the dark matter itself.
Here we direct our attention to FDM models, such as the axion or axion-like particles (e. g. Marsh [22]). The term was coined by Hu, Barkana, and Gruzinov [16] who proposed an extremely light, non-thermally produced boson whose de-Broglie wavelength would be relevant on cosmological scales. For a typical mass of $m_a \simeq 10^{-22}\mathrm{eV}/c^2$ the de-Broglie wavelength is of the order of 1kpc.
The small particle mass implies large occupation numbers in galactic halos. Thus, the classical field equations of a condensate describe the dynamics of FDM. In the context of structure formation the scales under consideration are much smaller than the Hubble horizon and larger than the de-Broglie wavelength, so that we can work in the Newtonian limit. The set of equations describing the dynamics of a self-gravitating condensate is the Gross-Pitaevskii-Poisson system (Gross [15], Pitaevskii [31]), which can be transformed into a set of hydrodynamical equations using the Madelung form of the wavefunction (Madelung [20]). The difference to a pressureless fluid is an additional force which is in general repulsive on small scales. The force is the gradient of the quantum potential (Bohm [8]) and stems from Heisenberg's uncertainty principle. While large scales behave as CDM, the quantum potential can stabilise small scale perturbations and thus alleviate conflicts between simulations and observations.
In this thesis we work out how the effects of the quantum potential can be included in the framework of KFT. In other words, we do not change the degrees of freedom of KFT, i. e. the phase-space coordinates of classical particles, but we add the quantum potential gradient to the dynamics. In fact, we need to adapt the dynamics as well as the initial power-spectrum, since the quantum potential stabilises structures below the so-called quantum Jeans scale. Thus, the initial FDM power-spectrum is truncated with respect to the initial CDM power-spectrum.

Part I

THE FRAMEWORK

2

KINETIC FIELD THEORY

In this Chapter we review the key concepts and mathematical structure of KFT developed by Bartelmann et al. [6]. The basic idea is to describe structures as canonical ensembles of correlated classical particles. In analogy to the path integral formulation of QFT (cf. Peskin and Schroeder [30]), a generating functional is at the center of the theory which includes all information on the initial correlations and dynamics of the particles in phase-space.
Here we review the construction of the generating functional $Z[\mathbf{J}]$ for an ensemble of classical particles and how correlations of macroscopic quantities, such as the density, can be obtained from it. In a first step we have a look at the Hamiltonian dynamics of the particles and give a general solution to their trajectories in phase-space by means of a Green's function. In a second step we make use of the deterministic nature of the Hamiltonian flow to write down the probability of the transition from an initial set of phase-space coordinates $\mathbf{x}^{(i)}$ to a set at a later time $\mathbf{x}(t)$ with $t > t_0$. Then the generating functional is given by an integral over the initial distribution of particles in phase-space weighted by the transition probability. In cosmological applications the initial distribution is completely specified by the density-fluctuation power-spectrum at CMB release.
In order to calculate correlation functions of the microscopic degrees of freedom and of macroscopic/collective fields, such as the density, we construct operators including functional derivatives with respect to generator fields. We include interactions by a multiplicative operator and conclude the general description of KFT with a formal analogy to Statistical Mechanics.
The second part of this Chapter is dedicated to a more thorough discussion of the Green's function in a cosmological setting. For that purpose we will transform the time coordinate from physical time to the linear growth factor of structures $D_+(t)$, which solves the second order differential equation for the density contrast in the linear hydrodynamics description (cf. (A.32)). We discuss ballistic motion in this new time coordinate and a deviation from this that was suggested by Bartelmann [3].

2.1 GENERATING FUNCTIONAL

2.1.1 *Hamiltonian Particle Dynamics*

The dynamical fields of KFT are the phase-space coordinates $\vec{x}_j(t) = \left(\vec{q}_j(t), \vec{p}_j(t)\right)^T$ of all $j = 1 \dots N$ microscopic particles. We adopt the notation of Bartelmann et al. [6] and organise the phase-space coordinates of all particles in tensors

$$\mathbf{x}(t) = \vec{x}_j(t) \otimes \vec{e}_j = \begin{pmatrix} \vec{q}_j(t) \\ \vec{p}_j(t) \end{pmatrix} \otimes \vec{e}_j, \tag{2.1}$$

where summation over repeated indices is implied. The properties and a scalar product of these tensors are defined in Appendix B.1.1.
For each particle j the phase-space coordinates obey the Hamiltonian equations of motion

$$\dot{\vec{q}}_j = \nabla_{p_j} \mathcal{H}(\mathbf{x}, t), \quad \dot{\vec{p}}_j = -\nabla_{q_j} \mathcal{H}(\mathbf{x}, t), \tag{2.2}$$

with the Hamiltonian $\mathcal{H}(\mathbf{x}, t)$ and the gradients acting on the position and momentum of the j-th particle. The Hamiltonian equations are symplectic and thus preserve the phase-space volume of the collection of particles by Liouville's theorem. In addition, trajectories of particles in phase-space will never cross, since the solution to the Hamiltonian equations is unique. This is a decisive advantage over standard methods in cosmic structure formation which break down as soon as (fluid) streams cross since one of the dynamical fields, namely the fluid velocity, becomes ill-defined.
We bundle the equations of motion (2.2) for the position and momentum of each particle into one simple equation with the use of our tensor notation (2.1):

$$\dot{\mathbf{x}} = \mathbb{J}\boldsymbol{\nabla}\mathcal{H}(\mathbf{x}, t), \tag{2.3}$$

with the $6N$-dimensional phase-space gradient $\boldsymbol{\nabla} = \nabla_j \otimes \vec{e}_j$ (cf. B.8) and the symplectic matrix

$$\mathbb{J} = \begin{pmatrix} 0 & I_3 \\ -I_3 & 0 \end{pmatrix} \otimes I_N. \tag{2.4}$$

Here I_d represents the identity in d dimensions. Without loss of generality we can split the Hamiltonian of the system into a free and a non-linear/interaction part. In the example of Section B.2.3 the former is the ballistic motion of particles according to their initial momentum and the latter is a potential-gradient force. Then the Hamiltonian equations of motion assume the form

$$\dot{\mathbf{x}}(t) = \mathbb{J}\boldsymbol{\nabla}\mathcal{H}_{\text{free}}(\mathbf{x}, t) + E_I(\mathbf{x}, t). \tag{2.5}$$

Here the inhomogeneity $E_I(\mathbf{x}, t) = \mathbb{J}\boldsymbol{\nabla}\mathcal{H}_I(\mathbf{x}, t)$ represents the interaction that we have split off the full Hamiltonian $\mathcal{H}(\mathbf{x}, t)$.

2.1.2 *The Generating Functional*

In analogy to the path integral formulation of QFT, we aim at the probability of the transition from an initial configuration of particles $\mathbf{x}(t_0) = \mathbf{x}^{(i)}$ to a configuration later in time $t > t_0$. The Hamiltonian equations are deterministic. Therefore the transition probability must be unity if and only if the phase-space trajectories of the particles follow the solution of (2.5).
The translation of this concept into a path integral is

$$P[\mathbf{x}^{(i)} \mapsto \mathbf{x}(t)] = \int_{\mathbf{x}^{(i)}} d\mathbf{x}(t)\delta_D\left[\dot{\mathbf{x}}(t) - \mathbb{J}\boldsymbol{\nabla}\mathcal{H}_{\text{free}}(\mathbf{x}, t) - E_I(\mathbf{x}, t)\right] \tag{2.6}$$

where we introduced a functional Dirac delta distribution. The path integral is to be taken over all possible phase-space trajectories $\mathbf{x}(t)$ starting with the initial configuration $\mathbf{x}^{(i)}$. The functional delta distribution ensures that only the Hamiltonian trajectories solving the equation of motion (2.5) contribute to the transition probability. In other words, fixing the initial positions also fixes all subsequent positions of the classical particles in phase-space.
Since the evolution of the microscopic degrees of freedom is deterministic, the only random element are the initial conditions for the ensemble of particles. Therefore in the construction of the generating functional of KFT we need to integrate over the initially available phase-space, i. e. the complete $6N$-dimensional phase-space weighted by a suitable probability distribution function. We express the initial phase-space measure as

$$d\Gamma = d\mathbf{q}^{(i)} d\mathbf{p}^{(i)} P[\mathbf{q}^{(i)}, \mathbf{p}^{(i)}], \tag{2.7}$$

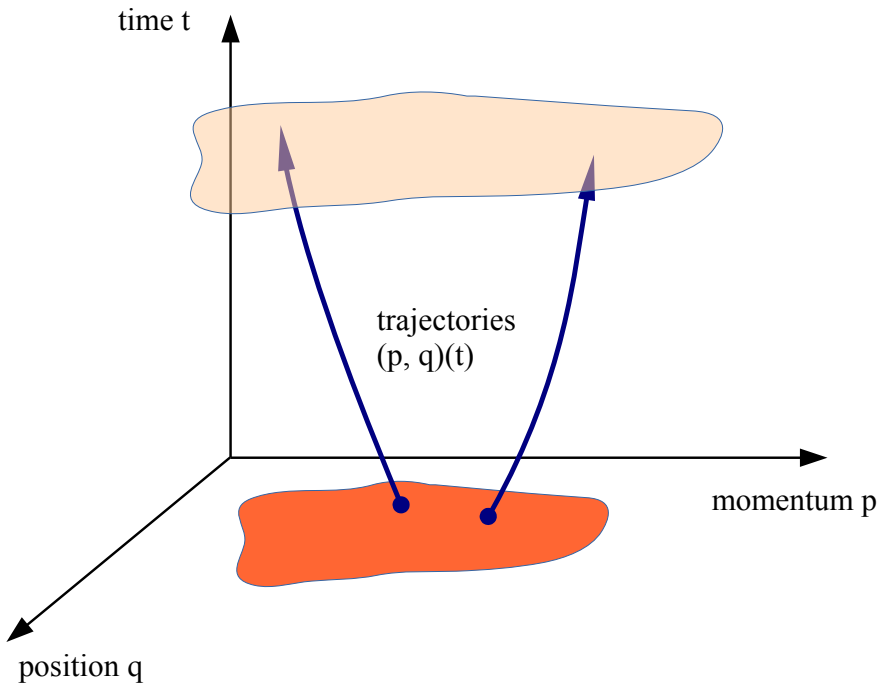

Figure 1: Shown is the principle idea of the generating functional $Z[\mathbf{J}]$. The initial configuration of particles in phase-space (light blue) is mapped to a configuration later in time (dark blue) by the classical solution $\mathbf{x}_{cl}(t)$. Courtesy of Matthias Bartelmann.

with the probability distribution $P[\mathbf{q}^{(i)}, \mathbf{p}^{(i)}]$ properly adapted to the system at hand. We will specify the distribution for cosmological initial conditions shortly.
The generating functional is now readily constructed from the transition probability and an integral over the initial phase-space distribution

$$\begin{aligned} Z[\mathbf{J}] &= \int d\Gamma P[\mathbf{x}^{(i)} \mapsto \mathbf{x}(t)] \exp\left(i \int_{t_0}^{t} dt' \left\langle \mathbf{J}(t'), \mathbf{x}(t') \right\rangle\right) \\ &= \int d\Gamma \int_{\mathbf{x}^{(i)}} d\mathbf{x}(t) \delta_D \left[\dot{\mathbf{x}}(t) - \mathbb{J}\nabla \mathcal{H}_{\text{free}}(\mathbf{x}, t) - E_I(\mathbf{x}, t)\right] \exp\left(i \int_{t_0}^{t} dt' \left\langle \mathbf{J}(t'), \mathbf{x}(t') \right\rangle\right) \\ &= \int d\Gamma \exp\left(i \int_{t_0}^{t} dt' \left\langle \mathbf{J}(t'), \mathbf{x}_{cl}(t') \right\rangle\right). \end{aligned} \tag{2.8}$$

In the last step we have carried out the path integral and replaced the trajectory in the phase factor by $\mathbf{x}_{cl}(t)$, i. e. the retarded solution of the classical equations of motion (2.5). We have also introduced the 6N-dimensional source field $\mathbf{J}(t)$ in the sense of (B.9) that couples to the position and momentum vectors of each particle.
The general idea of $Z[\mathbf{J}]$ is shown in Figure 1. The initial configuration of particles $\mathbf{x}^{(i)}$ occupies a volume in phase-space specified by the initial phase-space measure $d\Gamma$. Each particle in the configuration follows the classical path, i. e. the solution to (2.3), which propagates the configuration forward in time. Information on the ensemble or macroscopic properties can be deduced from the propagated phase-space configuration.
The functional derivative of the generating functional $Z[\mathbf{J}]$ with respect to $\vec{J}_{q_j}(t)$ evaluated at $\mathbf{J} = 0$ returns

$$\frac{\delta}{i\delta \vec{J}_{q_j}(t)} Z[\mathbf{J}]\bigg|_{\mathbf{J}=0} = \int d\Gamma \, \vec{q}_j(t) = \left\langle \vec{q}_j(t) \right\rangle, \tag{2.9}$$

i. e. the position of the j-th particle at time t averaged over all initial phase-space configurations drawn from the distribution $P[\mathbf{q}^{(i)}, \mathbf{p}^{(i)}]$. This corresponds to an ensemble average. In principle, the ensemble average of any observable Q can be calculated, if the observable is a function of the phase-space coordinates, i. e. $Q = Q(\mathbf{x})$. Replacing $\mathbf{x}$ by the functional derivative with respect to the source field $\mathbf{J}$ defines an operator and the expectation value for any observable can be written as

$$\langle Q(\mathbf{x}(t))\rangle = Q\left(\frac{\delta}{i\delta\mathbf{J}(t)}\right) Z[\mathbf{J}]\bigg|_{\mathbf{J}=0}. \tag{2.10}$$

Higher order correlation functions of the microscopic degrees of freedom or observables are computed from $Z[\mathbf{J}]$ by consecutive application of suitable operators and evaluation at $\mathbf{J} = 0$.

2.1.3 *Macroscopic Quantities*

So far we only considered the microscopic degrees of freedom of the particle ensemble, since those are the dynamical fields of KFT. For our discussion of structure formation we will need to define macroscopic or collective quantities of the ensemble. Each particle contributes to these collective quantities.
The most straightforward example of a collective quantity is the density

$$\rho(\vec{q}, t) = \sum_{j=1}^{N} \delta_D(\vec{q} - \vec{q}_j(t)), \tag{2.11}$$

which is a sum over the densities of all particles $j = 1 \dots N$. The density of a point particle is a Dirac delta distribution peaked at its respective position. The position of the j-th particle is given by the classical trajectory.
As the second collective quantity we introduce the momentum field or rather the momentum-density field. From the considerations of the previous paragraph the velocity field is naively constructed

$$\vec{p}(t) = \sum_{j=1}^{N} \vec{p}_j(t) = m \sum_{j=1}^{N} \vec{u}_j(t), \tag{2.12}$$

where $\vec{u}_j(t)$ is the velocity of one particle and we assume all particles to have the same mass m. Unfortunately this definition lacks all information about the spatial dependence of the momentum field, since the microscopic degrees of freedom are the phase-space coordinates of all particles. Our aim is the calculation of spatial correlation functions of the momentum field. So in order to recover the spatial information we have to impose that a particle can contribute to the momentum at a position $\vec{q}$ if and only if it is at that position

$$\vec{\Pi}(\vec{q}, t) = \sum_{j=1}^{N} \vec{p}_j(t)\delta_D(\vec{q} - \vec{q}_j(t)) = \sum_{j=1}^{N} \vec{p}_j(t)\rho_j(\vec{q}, t), \tag{2.13}$$

expressed by a Dirac delta distribution. This field is no longer the momentum field, but we recognise the delta distribution as the density of particle j at position $\vec{q}$ and time t, which means that the new field $\vec{\Pi}(\vec{q}, t)$ is a momentum-density.
In this thesis we will consider only interactions between the particles that can be described by a potential, such as gravity, and external potentials are neglected. Each par-

ticle experiences the interaction potential $V(\vec{q},t)$ at position $\vec{q}$ and time t as a sum over one-particle potentials v,

$$V(\vec{q},t) = \sum_{j=1}^{N} v(\vec{q} - \vec{q}_j(t)). \tag{2.14}$$

Using the definition of the density we can turn the sum into an integral expression

$$V(\vec{q},t) = \int d^3y v(\vec{q}-\vec{y}) \sum_{j=1}^{N} \delta_D(\vec{y} - \vec{q}_j(t)) = \int_y v(\vec{q}-\vec{y})\rho(\vec{y},t), \tag{2.15}$$

which will be helpful when we construct the interaction operator.
For the calculation of correlation functions of the macroscopic quantities defined in this Section we need to construct operators that can act on the generating functional as we have described at the end of the last section. Throughout this work we will calculate correlation functions in Fourier-space. Therefore we construct the operators for the density $\rho(\vec{q},t)$ (2.11) and momentum-density field $\vec{\Pi}(\vec{q},t)$ (2.13) from their Fourier-transforms. Each particle contributes to the density $\rho(\vec{q},t)$ by a delta distribution. The one-particle contribution of particle j to the density at the point $1 := (\vec{k}_1, t_1)$ in Fourier-space is

$$\rho_j(1) = \exp(-i\vec{k}_1 \cdot \vec{q}_j(t_1)). \tag{2.16}$$

The one-particle density operator is thus readily constructed by replacing the position of the j-th particle by a functional derivative

$$\rho_j(1) = \exp\left(-i\vec{k}_1 \cdot \frac{\delta}{i\delta\vec{J}_{q_j}(t_1)}\right). \tag{2.17}$$

The complete density operator is a sum over the one-particle operators.
The momentum-density operator is constructed from the density operator in a simple way. We first realise that the Fourier transformation leaves the momentum of particle j unchanged and the second factor in (2.13) is the one-particle density. Therefore by replacing the momentum $\vec{p}_j(t)$ by a suitable functional derivative with respect to the source and our previous result we get

$$\vec{\Pi}_j(1) = \frac{\delta}{i\delta\vec{J}_{p_j}(t_1)} \exp\left(-i\vec{k}_1 \cdot \frac{\delta}{i\delta\vec{J}_{q_j}(t_1)}\right) = \frac{\delta}{i\delta\vec{J}_{p_j}(t_1)}\rho_j(1) \tag{2.18}$$

for the one-particle momentum-density. The momentum-density for the ensemble is obtained by summing over the one-particle contributions.

2.1.4 *Interaction Operator*

In equation (2.15) we introduced the interaction potential $V(\vec{q},t)$ experienced by each particle as the sum of all N one-particle potentials v. This makes the interaction term $E_I(\mathbf{x},t)$ non-linear: all particles in the ensemble are connected by their mutual interactions and an individual treatment of each particle trajectory is not possible. We aim at the form

$$Z[\mathbf{J},\mathbf{K}] = e^{iS_I} \int d\mathbf{\Gamma} \exp\left(i\int_{t_0}^{t} dt' \left\langle \mathbf{J}(t'), \bar{\mathbf{x}}(t')\right\rangle\right) \tag{2.19}$$

of the generating functional. This form includes an additional source field $\mathbf{K}(t)$. Since the inclusion of the full non-linear interaction in our calculations is not feasible, we aim at a perturbative ansatz by expanding e^{iS_I} in a Taylor series

$$\exp(iS_I) = 1 + iS_I - \frac{1}{2}S_I \cdot S_I + \mathcal{O}(S_I^3). \tag{2.20}$$

The function S_I encodes the interaction term $E_I(\mathbf{x}, t)$ and the terms in this series can be interpreted as the free motion (0-th order), one interaction/scattering happens along the trajectories (linear), two scattering/interaction events happen along the trajectories (quadratic), and so on.
The first step in the construction of equation (2.19) is to introduce a new source field $\mathbf{K}(t)$ which formally replaces the non-linear term $E_I(\mathbf{x}, t)$ in the classical equations of motion (2.5)

$$\dot{\mathbf{x}} = \mathbb{J}\nabla\mathcal{H}_{\text{free}}(\mathbf{x}, t) + \mathbf{K}(t). \tag{2.21}$$

The source $\mathbf{K}(t)$ represents an inhomogeneity. Using a retarded Green's function $G_R(t, t')$ we can solve the equations of motion

$$\bar{\mathbf{x}}(t) = G_R(t, t_0)\mathbf{x}^{(i)} + \int_{t_0}^{t} dt' G_R(t, t')\mathbf{K}(t'), \tag{2.22}$$

as we described in Appendix B.2.3. The Green's function for the 6N-dimensional phase-space is symbolically given by

$$G_R(t, t') = \begin{pmatrix} g_{qq}(t, t')I_3 & g_{qp}(t, t')I_3 \\ g_{pq}(t, t')I_3 & g_{pp}(t, t')I_3 \end{pmatrix} \theta(t - t') \otimes I_N. \tag{2.23}$$

The scalar functions $g_{ab}(t, t')$ are propagators describing the free motion of particles through phase-space, such that

$$\vec{q}_j(t) = g_{qq}(t, t_0)\vec{q}_j^{(i)} + g_{qp}(t, t_0)\vec{p}_j^{(i)} \tag{2.24}$$

is the position of particle j due to its inertial motion only. An example for classical particles in static Euclidean space is given in (B.34). We will specify these propagators to expanding space-time in the next section.
We substitute the classical solution $\mathbf{x}_{cl}(t)$ in $Z[\mathbf{J}]$ in equation (2.8) by the solution $\bar{\mathbf{x}}(t)$ including the inhomogeneity $\mathbf{K}(t)$ and construct the interaction operator e^{iS_I} to (perturbatively) recover the non-linear term $E_I(\mathbf{x}, t)$ using a functional derivative. We define

$$S_I = \int dt' \left\langle E_I(\mathbf{x}, t'), \frac{\delta}{i\delta\mathbf{K}(t')} \right\rangle, \tag{2.25}$$

as the action operator associated with the interaction. Application of this operator to the phase-space trajectories returns

$$\begin{aligned} iS_I\bar{\mathbf{x}}(t) &= iS_I \left(G_R(t, t_0)\mathbf{x}^{(i)} + \int_{t_0}^{t} dt' G_R(t, t')\mathbf{K}(t') \right) \\ &= \int dt_1 E_I(\mathbf{x}, t_1) \cdot \int dt' G_R(t, t')\delta_D(t' - t_1) \begin{pmatrix} 1 \\ 1 \end{pmatrix} \\ &= \int dt_1 G_R(t, t_1)E_I(\mathbf{x}, t_1), \end{aligned} \tag{2.26}$$

which is the correct form of the inhomogeneous term as seen by a comparison with equation (B.35).
In this thesis we consider solely interactions of the particles with a potential $V(\vec{q}, t)$ that is a sum of one-particle contributions. The equations of motion for particle j due to the interaction are

$$\dot{\vec{q}}_j = 0, \quad \dot{\vec{p}}_j = -\nabla_{q_j} V(\vec{q}, t). \tag{2.27}$$

We rewrite the momentum change in the following way

$$\begin{aligned}\dot{\vec{p}}_j(\vec{q}, t) &= -\nabla_q V(\vec{q}, t)|_{\vec{q}=\vec{q}_j(t)} = -\int_q \delta_D(\vec{q} - \vec{q}_j(t)) \nabla_q V(\vec{q}, t) \\ &= \int_q \left[\nabla_q \delta_D(\vec{q} - \vec{q}_j(t))\right] V(\vec{q}, t),\end{aligned} \tag{2.28}$$

where we used that the boundary terms vanish. In the last expression we can again identify the delta distribution with the one-particle density ρ_j at position $\vec{q}$ and time t of the j-th particle.
To arrive at the operator S_I for the potential interaction, we replace the function $E_I(\mathbf{x}, t)$ in (2.25) by the rates of change for the position and momentum

$$S_I = \int dt \int_q \left(\sum_{j=1}^{N} \frac{\delta}{i\delta \vec{K}_{p_j}(t')} \cdot \left[\nabla_q \delta_D(\vec{q} - \vec{q}_j(t))\right] \right) V(\vec{q}, t). \tag{2.29}$$

The term in brackets defines the response field $B(\vec{q}, t)$. With our definition of the interaction potential using the one-particle potentials v the action operator turns out to be

$$S_I = \int dt \int_q \int_y B(\vec{q}, t) v(\vec{q} - \vec{y}, t) \rho(\vec{y}, t). \tag{2.30}$$

From this equation the meaning of the response field becomes apparent: it quantifies the response of particles at position $\vec{q}$ to an interaction with the density field at position $\vec{y}$.
An operator expression in the sense of the previous paragraph can be constructed by transforming (2.30) into Fourier-space. We will assume that the one-particle interaction potentials are translation invariant, depend on the difference $\vec{q} - \vec{y}$ only and acts instantaneously. The Fourier tranform is

$$S_I = \int dt_1 \int_k B(-1) v(1) \rho(1) \tag{2.31}$$

with $-1 := (-\vec{k}_1, t_1)$ as introduced in Section B.1.2. The one-particle contribution to the response field $B(1)$ in Fourier-space is given by

$$\begin{aligned}B_j(1) &= \mathcal{F}\left(\frac{\delta}{i\delta \vec{K}_{p_j}(t_1)} \cdot \nabla_q \delta_D(\vec{q} - \vec{q}_j(t)) \right) \\ &= \left[-i\vec{k}_1 \cdot \frac{\delta}{i\delta \vec{K}_{p_j}(t_1)} \right] \rho_j(1).\end{aligned} \tag{2.32}$$

This serves as our operator expression for the response field.
In summary the complete generating functional for an ensemble of classical microscopic particles drawn from a probability distribution $P[\mathbf{q}^{(i)}, \mathbf{p}^{(i)}]$ is given by

$$Z[\mathbf{J}, \mathbf{K}] = e^{iS_I} \int d\mathbf{q}^{(i)} d\mathbf{p}^{(i)} P[\mathbf{q}^{(i)}, \mathbf{p}^{(i)}] \exp\left(i \int_{t_0}^{t} dt' \left\langle \mathbf{J}(t'), \bar{\mathbf{x}}(t') \right\rangle \right). \tag{2.33}$$

The trajectories $\bar{\mathbf{x}}(t)$ solve the inhomogeneous equations of motion (2.21) by means of a Green's function and the potential interaction between particles is included by the form of S_I in equation (2.31). In practical calculations we expand the interaction operator into a Taylor series as described in the beginning of this paragraph.

2.1.5 *Initially Correlated Particles*

For the generating functional $Z[\mathbf{J}, \mathbf{K}]$ to be fully specified we need to give an expression for the initial distribution of the microscopic particles in phase-space. Here we review the main steps to find the initial probability distribution and a more detailed calculation can be found in Bartelmann et al. [6]. For the sake of readability we omit the upper index (i) and understand that we construct the probability distribution for the initial phase-space coordinates.
In the context of cosmology we demand spatial correlations of the particles such that their number density is a homogeneous and isotropic Gaussian random field. The spatial correlations imply correlations of momenta and cross-correlations of the spatial and momentum degrees of freedom by continuity.
The microscopic particles sample the number density. Therefore the probability to find a particle j at position $\vec{q}_j$ has to be proportional to the density at that point

$$P(\vec{q}_j|\rho_j) = \frac{\rho_j}{N}. \tag{2.34}$$

Here $\rho_j = \rho(\vec{q}_j)$ and the normalisation N is set by the volume integral over the density.
In the hydrodynamical treatment of cosmic structure formation to linear order in the perturbations (cf. Appendix A.2) we find that the rotational part of the peculiar velocity $\delta\vec{u}$ decays proportional to one over the scale-factor a. It is thus reasonable to assume that the initial velocities of the particles are irrotational and given by the gradient of a velocity potential ψ

$$\delta\vec{u}_j = \vec{p}_j = \nabla\psi_j, \tag{2.35}$$

where we assumed the same mass $m = 1$ for all particles and $\nabla\psi_j = \nabla\psi(\vec{q}_j)$. Therefore the conditional probability for the momentum $\vec{p}_j$ is given by

$$P(\vec{p}_j|\nabla\psi_j) = \delta_D(\vec{p}_j - \nabla\psi_j). \tag{2.36}$$

By means of the linear continuity equation (A.27) we find a relation between the density contrast $\delta = (\rho - \rho_b)/\rho$ and the velocity potential

$$\delta_j = -\nabla\delta\vec{u}_j = -\nabla^2\psi_j \tag{2.37}$$

at position $\vec{q}_j$. With the use of the conditional probabilities (2.34) and (2.36) the probability for finding a particle at $(\vec{q}_j, \vec{p}_j)^T$ in phase-space

$$P(\vec{q}_j, \vec{p}_j) = \int d\delta_j \int d(\nabla\psi_j) P(\vec{q}_j|\rho_j) P(\vec{p}_j|\nabla\psi_j) P(\delta_j, \nabla\psi_j) \tag{2.38}$$

can be calculated from the probability distribution $P(\delta_j, \nabla\psi_j)$ for the density contrast and the gradient of the velocity potential. For the ensemble of N particles the probability is given by

$$P[\mathbf{q}, \mathbf{p}] = V^{-N} \int d^N\delta \prod_{j=1}^{N} (1 + \delta_j) P(\delta_j, \vec{p}_j), \tag{2.39}$$

where we used the definition of the density contrast and the identity (2.35).
The density contrast and the velocity potential are related by the continuity equation, and hence ψ and its derivatives are homogeneous and isotropic Gaussian random fields that are fully specified by their respective power-spectra. For the density fluctuations the power-spectrum is defined by

$$\left\langle \delta(\vec{k})\delta(\vec{k}')\right\rangle = (2\pi)^3\delta_D(\vec{k}+\vec{k}')P_\delta(k), \tag{2.40}$$

with the Fourier-transform of the density contrast $\delta(\vec{k})$. Statistical homogeneity is ensured by the delta distribution and for a statistically isotropic field the power-spectrum can only depend on the absolute value of the wave vector k rather than its direction. By continuity, the power-spectrum for the velocity potential is given by

$$P_\psi(k) = k^{-4}P_\delta(k). \tag{2.41}$$

Bartelmann et al. [6] have shown that the full initial phase-space distribution is given by

$$P[\mathbf{q},\mathbf{p}] = \frac{V^{-N}}{\sqrt{(2\pi)^{3N}\det C_{pp}}}\mathcal{C}(\mathbf{p})\exp\left(-\frac{1}{2}\mathbf{p}^\intercal C_{pp}^{-1}\mathbf{p}\right), \tag{2.42}$$

with the polynomial

$$\begin{aligned}\mathcal{C}(\mathbf{p}) = &\prod_{j=1}^{N}\left(1 - C_{\delta_j p_k}\frac{\partial}{\partial p_k}\right) + \sum_{(j,k)} C_{\delta_j\delta_k}\prod_{\{l\}'}\left(1 - C_{\delta_l p_k}\frac{\partial}{\partial p_k}\right)\\ &+ \sum_{(j,k)} C_{\delta_j\delta_k}\sum_{(a,b)'} C_{\delta_a\delta_b}\prod_{\{l\}''}\left(1 - C_{\delta_l p_k}\frac{\partial}{\partial p_k}\right) + \dots\end{aligned} \tag{2.43}$$

depending on the density fluctuation and momentum auto-correlations and the cross-correlations, $C_{\delta\delta}$, C_{pp}, and $C_{\delta p}$ respectively.
These correlations are completely determined by the initial power-spectrum of the density contrast and we give the definitions here. The two-point correlation function of the density fluctuation is given by the Fourier-transform of its power-spectrum

$$\left\langle \delta_j\delta_k\right\rangle = C_{\delta_j\delta_k} = \int_k P_\delta(k)e^{i\vec{k}\cdot(\vec{q}_j-\vec{q}_k)}. \tag{2.44}$$

The indices j and k indicate that the correlation is evaluated between two different points $\vec{q}_j$ and $\vec{q}_k$. For the cross-correlation we get

$$\left\langle \delta_j\vec{p}_k\right\rangle = C_{\delta_j p_k} = i\int_k k^2\vec{k}P_\psi(k)e^{i\vec{k}\cdot(\vec{q}_j-\vec{q}_k)}, \tag{2.45}$$

and for the momentum correlation

$$\left\langle \vec{p}_j\otimes\vec{p}_k\right\rangle = C_{p_j p_k} = \int_k \vec{k}\otimes\vec{k}P_\psi(k)e^{i\vec{k}\cdot(\vec{q}_j-\vec{q}_k)}. \tag{2.46}$$

Evaluating the correlation functions at the same position we obtain the one-point variances

$$\left\langle \delta_j\delta_j\right\rangle = \sigma_2^2, \quad \left\langle \delta_j\vec{p}_j\right\rangle = 0, \quad \left\langle \vec{p}_j\vec{p}_k\right\rangle = \frac{\sigma_1^2}{3}I_3, \tag{2.47}$$

with the definition

$$\sigma_n^2 = \int_k k^{2(n-2)} P_\delta(k). \tag{2.48}$$

In the early Universe the density fluctuation auto-correlations and the cross-correla-tions are weak compared to the momentum auto-correlations. We will therefore assume the correlation polynomial $\mathcal{C}(\mathbf{p}) \simeq 1$ in our calculations. For the initial power-spectrum we will use the one provided by Bardeen et al. [2] for CDM and a truncated power-spectrum for FDM (cf. Chapter 5).

2.1.6 *Similarities to Equilibrium Statistical Physics*

Conceptually, KFT is largely different from Statistical Physics, because the former describes a system that is far from equilibrium. The generating functional $Z[\mathbf{J}]$ is constructed from the joint probability density $P[\mathbf{x}^{(i)}, \mathbf{x}^{(f)}]$ that the system starts in the configuration $\mathbf{x}^{(i)}$ and takes the configuration $\mathbf{x}^{(f)}$ at the final time. We have expressed this by the probability distribution of the initial phase-space coordinates of all particles (2.42) and the conditional probability for the system to evolve from an initial configuration to one later in time, i. e. the transition probability (2.6). We adopt the notion of an ensemble since we consider the number of particles and the volume of the system fixed, and draw the initial configuration from a continuous probability distribution. The calculation of correlators from the generating functional is then analogous to an ensemble average, i. e. an average over many realisations of the initial distribution.
Statistical physics on the other hand mostly describes systems in equilibrium, i. e. fluctuations of macroscopic quantities about the mean are small, and ergodic, such that time averages are equivalent to ensemble averages. In this sense macroscopic quantities are sufficient to describe the system and knowledge about the microscopic configuration in phase-space is irrelevant. The canonical ensemble describes systems that are in equilibrium with a heat bath, i. e. the mean energy (temperature) per degree of freedom is fixed. The canonical partition function is given by

$$Z_C = \int d\mathbf{\Gamma} \exp(-\beta \mathcal{H}(\mathbf{x})), \tag{2.49}$$

where $\beta = (k_B T)^{-1}$ is the energy scale of the system with temperature T. The exponential function is the Boltzmann factor which compares the total energy of a configuration $\mathbf{x}$ with the temperature of the system. Thus, it represents the probability distribution for configurations in phase-space. Averages of macroscopic quantities can be calculated from the canonical partition function by taking the appropriate derivatives, for instance the mean energy is given by $\langle E \rangle = -\frac{\partial}{\partial \beta} Z_C$.
The canonical partition function Z_C and the generating functional $Z[\mathbf{J}]$ build the formal analogy between statistical physics and KFT. Although one describes an equilibrium and the other a non-equilibrium system both contain the initial phase-space distribution and the dynamics of the microscopic degrees of freedom. Macroscopic quantities are calculated from partial derivatives of the partition function/generating functional.

2.2 PARTICLE TRAJECTORIES

2.2.1 *Lagrangian in an Expanding Space-Time*

Along the lines of Peebles [29] we briefly discuss the effective Lagrangian for a point particle moving in expanding space-time. The motion of a classical particle in an expanding space-time is described by the Lagrangian

$$L(\vec{r}, \dot{\vec{r}}, t) = \frac{m}{2}\dot{\vec{r}}^2 - m\Phi(\vec{r}), \tag{2.50}$$

where $\vec{r}$ are the physical coordinates of the particle. The gravitational potential $\Phi(\vec{r})$ obeys the Poisson equation

$$\nabla_r^2\Phi = 4\pi G\rho - \Lambda c^2, \tag{2.51}$$

with a cosmological constant Λ. The transformation to comoving coordinates $\vec{q} = a\vec{r}$ leads to

$$L(\vec{q}, \dot{\vec{q}}, t) = \frac{m}{2}\left(\dot{a}^2\vec{q} + a^2\dot{\vec{q}}^2 + 2a\dot{a}\vec{q}\dot{\vec{q}}\right) - m\Phi(\vec{q}) \tag{2.52}$$

with all functions depending on the new coordinates.
Since the addition of the total time derivative of a function leaves the equations of motion invariant, we define an effective Lagrangian

$$L \mapsto L - \frac{d}{dt}\frac{m}{2}a\dot{a}\vec{q}^2 = \frac{m}{2}a^2\dot{\vec{q}}^2 - m\phi \tag{2.53}$$

with an effective potential

$$\phi = \Phi + \frac{a\ddot{a}}{2}\vec{q}^2. \tag{2.54}$$

The effective potential obeys the Poisson equation

$$\nabla_q^2\phi = 4\pi G a^2\rho - a^2\Lambda c^2 + 3a\ddot{a} = 4\pi G a^2(\rho - \rho_b), \tag{2.55}$$

where in the second step we used the second Friedmann equation (A.9b) with the mean background density $\rho_b(t)$ and neglected the pressure term.
In a next step we introduce the dimensionless time coordinate $\tau = D_+ - D_+^{(i)}$ using the linear growth factor, i. e. the growing solution to the linearised hydrodynamic equations (cf. Section A.2). The initial value is $\tau^{(i)} = 0$ and we choose $D_+^{(i)} = 1$. The transformation of differentials is given by

$$d\tau = dD_+ = \frac{da}{dt}\frac{dD_+}{da}dt = HD_+ f dt, \tag{2.56}$$

with the usual definitions for the Hubble function $H := \dot{a}/a$ and the growth rate $f := \frac{d\ln D_+}{d\ln a}$.
The classical action S must be invariant under this transformation. We demand

$$S = \int dt L(\vec{q}, \dot{\vec{q}}, t) = \int d\tau L'(\vec{q}, \vec{q}', \tau) = \int dt \frac{d\tau}{dt} L'(\vec{q}, \vec{q}', \tau), \tag{2.57}$$

where the prime on $\vec{q}$ denotes a derivative with respect to the dimensionless time coordinate τ. The effective Lagrangian is given by

$$L'(\vec{q}, \vec{q}', \tau) = \frac{dt}{d\tau}L(\vec{q}, \dot{\vec{q}}, t) = \frac{m}{2}a^2 HD_+ f\vec{q}'^2 - \frac{m\phi}{HD_+ f}. \tag{2.58}$$

We divide the effective Lagrangian by mH_i with $H_i = H(\tau = 0)$ and change our notation such that the dot over a quantity now denotes a derivative with respect to τ rather than physical time, i. e. we replace $\vec{q}'$ by $\dot{\vec{q}}$. The motion of a particle in expanding space-time in comoving coordinates and the dimensionless time coordinate τ is given by the effective Lagrangian

$$\mathcal{L} = \frac{g(\tau)}{2}\dot{\vec{q}}^2 - \nu(\vec{q}, \tau), \tag{2.59}$$

and the effective potential

$$\nu(\vec{q}, \tau) = \frac{\phi}{HD_+ fH_i} = \frac{a^2\phi}{H_i^2 g(\tau)}, \tag{2.60}$$

with the function

$$g(\tau) = \frac{H}{H_i} a^2 D_+ f. \tag{2.61}$$

From (2.55) we find the Poisson equation for the effective potential

$$\nabla^2\nu(\vec{q}, \tau) = \frac{4\pi G a}{H_i^2 g(\tau)}(\rho - \rho_b), \tag{2.62}$$

where we replaced the physical densities by their comoving values $\rho \mapsto \rho a^3$. We can rewrite the Poisson equation by using the definition for the comoving background density of matter. It is given by

$$\rho_b = \frac{3H_i^2}{8\pi G}\Omega_{mi}, \tag{2.63}$$

where we multiplied the critical density (A.14) by the matter density parameter at the initial time. Then introducing the density contrast $\delta = (\rho - \rho_b)/\rho$ we find

$$\nabla^2\nu(\vec{q}, \tau) = \frac{3}{2}\frac{a}{g(\tau)}\Omega_{mi}\delta \tag{2.64}$$

for the Poisson equation. The canonically conjugate momentum is

$$\vec{p}_c = \frac{\partial\mathcal{L}}{\partial\dot{\vec{q}}} = g(\tau)\dot{\vec{q}}, \tag{2.65}$$

and the Hamiltonian is

$$\mathcal{H}(\vec{q}, \dot{\vec{q}}, \tau) = \vec{p}_c \cdot \dot{\vec{q}} - \mathcal{L} = \frac{\vec{p}_c^2}{2g(\tau)} + \nu(\vec{q}, \tau). \tag{2.66}$$

The Hamiltonian equations of motion are

$$\dot{\vec{q}} = \frac{\vec{p}_c}{g(\tau)}, \quad \dot{\vec{p}}_c = -\nabla\nu. \tag{2.67}$$

2.2.2 *Zel'dovich Approximation*

The comoving particle trajectories are often modelled according to the Zel'dovich approximation (cf. Zel'dovich [35]). In our choice of coordinates these trajectories are equivalent to inertial motion of the particles due to their initial momenta. The Green's function (2.23) is then given by

$$G_R(\tau, \tau') = \begin{pmatrix} I_3 & (\tau - \tau')I_3 \\ 0 & I_3 \end{pmatrix} \theta(\tau - \tau') \otimes I_N. \tag{2.68}$$

Then the equations of motion have the form

$$\dot{\vec{q}} = \vec{p} = \frac{\vec{p}_c}{g(\tau)} \tag{2.69}$$

$$\dot{\vec{p}} = -\frac{\nabla v}{g(\tau)} - \frac{\dot{g}(\tau)}{g(\tau)}\vec{p}, \tag{2.70}$$

where initially $\vec{p} = \vec{p}_c$. We see that due to this choice of free motion an additional contribution to the change of momentum arises.

2.2.3 *Improved Zel'dovich Approximation*

The motion in the Zel'dovich approximation is unbounded. The particles will first move towards each other and thereby form structures, since their initial momenta point into the direction of the gravitational potential gradient. But structures/particles are again driven apart by the inertial motion. Bartelmann [3] has suggested how this removal of structure can be reduced by effectively adding a zero to the equations of motion and a reinterpertation of the free and interaction parts of the motion.
We do not change the equation of motion for the position but for the momentum

$$\begin{aligned}\dot{\vec{p}} &= \dot{h}\vec{p} - \dot{h}\vec{p} - -\frac{\nabla v}{g(\tau)} - \frac{\dot{g}(\tau)}{g(\tau)}\vec{p} \\ &= \dot{h}\vec{p} - \frac{\nabla v}{g(\tau)} + \frac{\dot{g}(\tau)}{g(\tau)}h\vec{p},\end{aligned} \tag{2.71}$$

where we introduced the function

$$h(\tau) = g^{-1}(\tau) - 1. \tag{2.72}$$

To arrive at a Green's function we interpret the first term in this equation as the free motion of particles. We call the solution the improved Zel'dovich approximation, because it reduces the removal of structures compared to the Zel'dovich approximation. Therefore the scalar functions in the Green's function (2.23) are

$$g_{qq}(\tau,\tau') = I_3, \quad g_{qp}(\tau,\tau') = \int_{\tau'}^{\tau} d\bar{\tau} e^{h(\bar{\tau})-h(\tau')}, \tag{2.73}$$

$$g_{pq}(\tau,\tau') = 0, \quad g_{pp}(\tau,\tau') = e^{h(\tau)-h(\tau')}. \tag{2.74}$$

3

MOMENTUM-DENSITY CORRELATION FUNCTIONS

In this Chapter we show how correlation functions for the momentum-density field are calculated from the generating functional in the free and in the interacting theory. In the free theory the microscopic degrees of freedom evolve according to their initial configuration in phase-space and the retarded Green's function that solves the homogeneous equations of motion. Interactions are included perturbatively via an interaction operator as described in the previous Chapter.
We derive general expressions for n-point correlation functions and review the factorisation of the generating functional (Bartelmann et al. [5]) if initial density correlations and density-momentum cross-correlations can be neglected. To calculate perturbative corrections due to particle interactions systematically, we present a diagrammatic approach to represent the terms contributing to those corrections at arbitrary order.

3.1 GENERAL FORM OF CORRELATION FUNCTIONS

3.1.1 *Collective Quantities*

As is usual in a statistical field theory, n-point correlation functions of any field are calculated by applying n field operators to the generating functional $Z[\mathbf{J}, \mathbf{K}]$ and setting the source fields $\mathbf{J}$ and $\mathbf{K}$ to zero. For the density we write

$$G_{\rho\dots\rho}(1\dots n) = \rho(1)\dots\rho(n)Z[\mathbf{J},\mathbf{K}] \tag{3.1}$$

with the abbreviation $1 = (\vec{k}_1, t_1)$. In this Section we derive general expressions for correlation functions of the density ρ, momentum-density $\vec{\Pi}$ and response field B. The operator expressions for those fields are

$$\rho(1) = \sum_{j=1}^{N} \rho_j(1) = \sum_j \exp\left(-i\vec{k}_1 \cdot \frac{\delta}{i\delta\vec{J}_{q_j}(t_1)}\right), \tag{3.2}$$

$$\vec{\Pi}(1) = \sum_{j=1}^{N} \vec{\Pi}_j(1) = \sum_j \frac{\delta}{i\delta\vec{J}_{p_j}(t_1)}\rho_j(1), \tag{3.3}$$

$$B(1) = \sum_{j=1}^{N} B_j(1) = \sum_j \left(-i\vec{k}_1 \cdot \frac{\delta}{i\delta\vec{K}_{p_j}(t_1)}\right)\rho_j(1). \tag{3.4}$$

Since each operator contains a one-particle density operator ρ_j, we work out the effect of n such operators on the generating functional first. We enumerate the operators in accordance with the contributing particles by $j_s = 1\dots N$

$$\rho_{j_1}(1)\dots\rho_{j_n}(n)Z[\mathbf{J},\mathbf{K}] = Z[\mathbf{J}+\mathbf{L},\mathbf{K}]. \tag{3.5}$$

We notice that each $\rho_{j_s}(s)$ amounts to a shift $\mathbf{L}$ of the source $\mathbf{J}$, since derivatives are the generators of the translation group. Working out the functional derivative we find

$$\mathbf{L}(t) = -\sum_{s=1}^{n} \begin{pmatrix} \vec{k}_s \\ 0 \end{pmatrix} \delta_D(t-t_s) \otimes \vec{e}_{j_s} \tag{3.6}$$

for the shift. Here t_s denotes the time when the s-th one-particle density operator is evaluated and $\vec{e}_{j_s}$ picks out the particle corresponding to that operator. The full density correlation function is obtained after summing (3.5) over all j_s particles with $\mathbf{J} = \mathbf{K} = 0$. For the sake of brevity we define projections of the shift vectors into the position and momentum subspaces

$$\vec{L}_{q_j}(t_1) = \int dt \left\langle \mathbf{L}, G_R(t, t_1) \begin{pmatrix} I_3 \\ 0 \end{pmatrix} \otimes \vec{e}_j \right\rangle, \tag{3.7a}$$

$$\vec{L}_{p_j}(t_1) = \int dt \left\langle \mathbf{L}, G_R(t, t_1) \begin{pmatrix} 0 \\ I_3 \end{pmatrix} \otimes \vec{e}_j \right\rangle, \tag{3.7b}$$

including the free Green's function $G_R(t, t')$. Using the form of the shift tensor and the scalar components of the Green's function we arrive at the shift tensors

$$\mathbf{L}_q(t_1) = -\sum_{s=1}^{n} \vec{k}_s \otimes \vec{e}_{j_s}, \quad \mathbf{L}_p(t_1) = -\sum_{s=1}^{n} g_{qp}(t_s, t_1)\vec{k}_s \otimes \vec{e}_{j_s}, \tag{3.8}$$

in position and momentum space, respectively. Here we used that $g_{qq} = 1$ for the trajectories considered and we will omit the time-dependence of the shift tensors whenever t_1 is the initial time t_0. Notice that the only non-vanishing components of the shift tensors are those of the particles j_s of the corresponding one-particle operators. If we ignore interactions and set the source fields to zero, then the free n-point density correlation function is

$$G^{(0)}_{\rho\ldots\rho}(1\ldots n) = \sum_{(j_1,\ldots j_n)}^{N} \int d\Gamma \exp\left(i\langle \mathbf{L}_q, \mathbf{q}\rangle + i\langle \mathbf{L}_p, \mathbf{p}\rangle\right), \tag{3.9}$$

where the superscript (0) denotes the free evolution, and the tensors $\mathbf{q}$ and $\mathbf{p}$ denote the initial positions and momenta of the particles. We call $Z_0[\mathbf{L}, 0]$ the free generating functional with shifts $\mathbf{L}$. The integral over the initial phase-space measure has still to be carried out and we will show that this integral factorises due to the homogeneity and isotropy of the initial Gaussian random fields.

The next field we consider is the momentum-density field $\vec{\Pi}$. Following the same steps as for the density field, we apply n one-particle momentum-density operators to the generating functional. Since each operator involves a one-particle density, the application leads to shifts $(\mathbf{L}_q, \mathbf{L}_p)^\intercal$ and pulls down the momentum trajectories from the phase factor:

$$\begin{aligned} &\Pi^{\alpha_1}_{j_1}(1)\ldots\Pi^{\alpha_n}_{j_n}(n)Z[\mathbf{J},\mathbf{K}] \\ =&e^{iS_I}\int d\Gamma \left[\prod_{s=1}^{n}\left(g_{pp}(t_s,t_0)p^{\alpha_s}_{j_s} + \int dt' g_{pp}(t_s,t')K^{\alpha_s}_{p_{j_s}}(t')\right)\right] e^{i\langle \mathbf{J}(t)+\mathbf{L}(t),\bar{\mathbf{x}}(t)\rangle} \end{aligned} \tag{3.10}$$

where all indices j_s are different and with the definition of the classical solution $\bar{\mathbf{x}}(t)$ (2.22) including an inhomogeneity. The greek indices α_s refer to the components of the momentum. In calculations we will substitute the initial momentum $\vec{p}_{j_s}$ by a partial derivative with respect to the corresponding momentum shift vector of particle j_s. Again, ignoring interactions and setting the source fields to zero we get the n-point momentum-correlation function for an ensemble of freely moving particles

$$G^{(0),\alpha_1\ldots\alpha_n}_{\Pi\ldots\Pi}(1\ldots n) = \sum_{j_1,\ldots j_n}\left[\prod_{s=1}^{n}\left(g_{pp}(t_s,t_0)\frac{\partial}{i\partial L^{\alpha_s}_{p_{j_s}}}\right)\right] Z[\mathbf{L},0], \tag{3.11}$$

where the integration over the initial phase-space distribution remains to be carried out. The last field we need to discuss is the response field B. For that purpose we take the definition of the one-particle response field operator and split it into the one-particle density operator ρ_j and another operator that we write as

$$b_j(1) = \left(-i\vec{k}_1 \cdot \frac{\delta}{i\delta \vec{K}_{p_j}(t_1)} \right). \tag{3.12}$$

Let us consider an n-point density correlation function and apply the new operator to it. This is formally equivalent to a correlation function of $(n-1)$ density fields and one response field. We write

$$b_j(n)\rho_j(n)\rho_{j_1}(1)\dots\rho_{j_{n-1}}(n-1)Z[\mathbf{J},\mathbf{K}] = \underline{b}_j(n)Z[\mathbf{L},\mathbf{K}], \tag{3.13}$$

where on the right-hand side we applied the shift $\mathbf{L}$ as shown in (3.5) and set the source field $\mathbf{J} = 0$ since b_j only acts on $\mathbf{K}(t)$. After evaluation of the functional derivative we find for the b-factor

$$\underline{b}_j(n) = i\sum_{s=1}^{n-1} g_{qp}(t_s,t_n)\vec{k}_s \cdot \vec{k}_n \delta_{jj_s} \tag{3.14}$$

with the Kronecker delta ensuring that the particles j and j_s are identical. For this example we have the same argument for the n-th density operator as for the b_j operator, since we considered a correlation of a response field with $(n-1)$ density fields. Therefore the term with $j = j_n$ is zero because of the Green's function.
The situation is different if the response field acts on a momentum-density correlation. We will only give an example in the case of a 2-point correlation of the response field and the response field, but this is easily extended to higher orders. We can write for the free correlation

$$B_j(1)\Pi_k^\alpha(2)Z[\mathbf{J},\mathbf{K}] = \left[\underline{b}_j(1) g_{pp}(t_2,t_0) \frac{\partial}{i\partial L^\alpha_{p_k}} + i g_{pp}(t_2,t_1) k_1^\alpha \delta_{jk} \right] Z[\mathbf{L},0]. \tag{3.15}$$

The first term in brackets stems from the application of the $b_j(1)$ operator on the phase-factor and the last term from the application of $b_j(1)$ on the momentum trajectory. Since this example contains only two particles, the b-factor only consists of the single term

$$\underline{b}_j(1) = i g_{qp}(t_2,t_1)\vec{k}_2 \cdot \vec{k}_1 \delta_{jk}. \tag{3.16}$$

By causality, pure response field B correlation functions must vanish exactly. This is because the product of b-factors leads to a contradiction in the sequence of times. This can be easily seen from the Heaviside function $\theta(t-t')$ that we omitted in the definition of the scalar Green's functions $g_{ab}(t,t')$. We have to keep the time-ordering in mind that $t > t'$. To clarify this point, we give an example of a 2-point response field correlation function

$$\begin{aligned} B_j(1)B_k(2)Z[\mathbf{J},\mathbf{K}]\big| &= \underline{b}_j(1)\underline{b}_k(2)Z[\mathbf{L},0] \\ &= \left(g_{qp}(t_2,t_1)\vec{k}_1 \cdot \vec{k}_2 \right) \left(g_{qp}(t_1,t_2)\vec{k}_2 \cdot \vec{k}_1 \right) Z[\mathbf{L},0] \end{aligned} \tag{3.17}$$

The first factor implies $t_2 > t_1$ and the second $t_1 > t_2$, and thus, the result vanishes. The same is true for n-point response field cumulants, which lead to the combination of statements $t_j > t_k$ and $t_k > t_j$.
In all following calculations we will only be interested in cross-correlations between the response field B and either/both the density and momentum-density fields, δ and $\vec{\Pi}$, in order to find the corrections due to particle interactions.

3.1.2 *The Free Generating Functional*

In the previous paragraph we have seen that all n-point (cross-)correlation functions of the fields ρ, $\vec{\Pi}$ and B can be written in terms of the free generating functional $Z[\mathbf{L}, 0]$ with shifts $\mathbf{L}$. In this paragraph we perform the integration over initial momentum space and show that the remaining integral can be factorised.
After the application of n one-particle operators we obtain the free generating functional

$$Z_0[\mathbf{L}, 0] = \int d\mathbf{q} d\mathbf{p} P[\mathbf{q}, \mathbf{p}] e^{i\langle \mathbf{L}_q, \mathbf{q}\rangle + i\langle \mathbf{L}_p, \mathbf{p}\rangle}, \tag{3.18}$$

where the initial distribution is given by (2.42) and the shifts are given by (3.7). Here all phase-space coordinates $(\mathbf{q}, \mathbf{p})^T$ denote the initial coordinates.
The integral over momentum space can be carried out if we replace the momenta in the correlation polynomial $\mathcal{C}(\mathbf{p})$ by a partial derivative with respect to the momentum shift $\mathbf{L}_p$. The remaining integral is a Fourier-transform of a multivariate Gaussian function

$$Z_0[\mathbf{L}, 0] = V^{-N} \mathcal{C}\left(\frac{\partial}{i\partial \mathbf{L}_p}\right) \int d\mathbf{q} \exp\left(-\frac{1}{2}\mathbf{L}_p^T C_{pp} \mathbf{L}_p + i\langle \mathbf{L}_q, \mathbf{q}\rangle\right) \tag{3.19}$$

with the momentum correlation matrix C_{pp}. For our cosmological applications we will assume that the correlation polynomial, which is a function of the density and the density-momentum correlations $C_{\delta\delta}$ and $C_{\delta p}$, is unity. This is a safe approximation if correlators are evaluated at sufficiently late times and the Green's function $g_{qp}(t, t')$ is unbounded. The initial conditions for cosmic structure formation are set at the last scattering surface, i. e. the correlations we observe in the CMB. The scale factor of the last scattering surface is $a_i \simeq 10^{-3}$, and the approximation seems to hold for evaluations of correlation functions at $a > 10^{-2}$. Therefore $\mathcal{C}(\mathbf{p}) \simeq 1$ in our calculations.
We will now follow the calculations presented in Bartelmann et al. [5] and show that the position space integral factorises. In this calculation we make use of the fact that in a statistically homogeneous field only coordinate differences $\vec{q}_j - \vec{q}_i$ are relevant and that these differences must be statistically indistinguishable. Therefore we first introduce the coordinate differences of all particles with respect to an arbitrarily chosen particle labeled '1':

$$\vec{q}_{j1} := \vec{q}_j - \vec{q}_1, \tag{3.20}$$

where $j = 2 \dots n$ denotes the labels of the one-particle operators. The scalar product of the positions $\mathbf{q}$ and the spatial shift vectors $\mathbf{L}_q$ is

$$\langle \mathbf{L}_q, \mathbf{q}\rangle = \sum_{j=1}^{n} \vec{L}_{q_j} \cdot \vec{q}_1 + \sum_{j=2}^{n} \vec{L}_{q_j} \cdot \vec{q}_{j1}. \tag{3.21}$$

With this we can evaluate the spatial integral over all $(N - n)$ particles that are not involved in the correlator and the integral over $\vec{q}_1$. The result is

$$Z_0[\mathbf{L}, 0] = V^{-n} (2\pi)^3 \delta_D \left(\sum_{j=1}^{n} \vec{L}_{q_j}\right) \prod_{j=2}^{n} \int_{q_{j1}} \exp\left(-\frac{1}{2}\mathbf{L}_p^T C_{pp} \mathbf{L}_p + i \sum_{j=2}^{n} \vec{L}_{q_j} \cdot \vec{q}_{j1}\right) \tag{3.22}$$

Here we used that the momentum correlation matrix C_{pp} depends only on the absolute value of all pair-wise coordinate differences, by statistical homogeneity and isotropy of

the velocity potential ψ. With this in mind, we want to express $Z_0[\mathbf{L}, 0]$ depending on the coordinate differences

$$\vec{q}_{jk} := \vec{q}_j - \vec{q}_k, \quad \forall k = 2 \dots (n-1), \quad j = (k+1) \dots n \tag{3.23}$$

rather than the differences $\vec{q}_{j1}$ to particle '1' only. To include the remaining coordinate differences in our expression for the generating functional, we introduce appropriate Dirac delta functions and change the integration from $\vec{q}_{j1}$ to $\vec{q}_{jk}$

$$\begin{aligned} Z_0[\mathbf{L}, 0] &= V^{-n}(2\pi)^3 \delta_D \left(\sum_{j=1}^{n} \vec{L}_{q_j} \right) \times \\ &\times \prod_{j>k} \int_{q_{j1}} \exp\left(-\frac{1}{2} \mathbf{L}_p^T C_{pp} \mathbf{L}_p + i \sum_{j=2}^{n} \vec{L}_{q_j} \cdot \vec{q}_{j1} \right) \prod_{a>b} \delta_D(\vec{q}_{ab} - \vec{q}_a + \vec{q}_b), \end{aligned} \tag{3.24}$$

and the indices (a, b) satisfying

$$b = 2 \dots (n-1), \quad a = (b+1) \dots n. \tag{3.25}$$

Next we can use the Fourier-transform to represent the delta distributions and write down the final result

$$Z_0[\mathbf{L}, 0] = V^{-n}(2\pi)^3 \delta_D \left(\sum_{j=1}^{n} \vec{L}_{q_j} \right) e^{Q_D(\vec{k},t)} \prod_{a>b\geqslant 2} \int_{k_{ab}} \prod_{j>k\geqslant 1} I_{jk} \tag{3.26}$$

with several definitions to be completed. The function $Q_D(\vec{k}, t)$ is the damping of the correlations arising from free-streaming of the particles. It is defined as

$$Q_D(\vec{k}, t) := -\frac{1}{2} \vec{L}_{p_j}^T C_{p_j p_j} \vec{L}_{p_j} = -\frac{\sigma_1^2}{6} \sum_{j=1}^{n} \vec{L}_{p_j}^2 \tag{3.27}$$

with the initial velocity dispersion σ_1^2. We define the integrals over coordinate differences as

$$I_{jk} := \int_{q_{jk}} \exp\left(-\vec{L}_{p_j}^T C_{p_j p_k} \vec{L}_{p_k} + i \vec{k}_{jk} \cdot \vec{q}_{jk} \right) \tag{3.28}$$

with the wave-vectors

$$\vec{k}_{jk} := \begin{cases} \vec{L}_{q_j} - \sum_{b=2}^{j-1} \vec{k}'_{jb} + \sum_{a=j+1}^{n} \vec{k}'_{aj}, & \text{for} \quad k = 1, \quad j = 2 \dots n \\ \vec{k}'_{jk}, & \text{for} \quad k = 2 \dots (n-1), \quad j = (k+1) \dots n \end{cases} \tag{3.29}$$

and a, b as in (3.25). Since we pulled the one-particle momentum variance in front, the integral is to be carried out over the coordinate differences. Thus, the generating functional is a convolution of independent factors for all particle pairs over the wave-vectors $\vec{k}'_{ab}$.
In order to evaluate the generic factors I_{jk} we use the definition of the momentum correlation matrix

$$C_{p_j p_k} = \int_k \left(\vec{k} \otimes \vec{k} \right) P_\psi(k) e^{i\vec{k} \cdot \vec{q}_{jk}} = -(\nabla \otimes \nabla) \xi_\psi(q_{jk}) \tag{3.30}$$

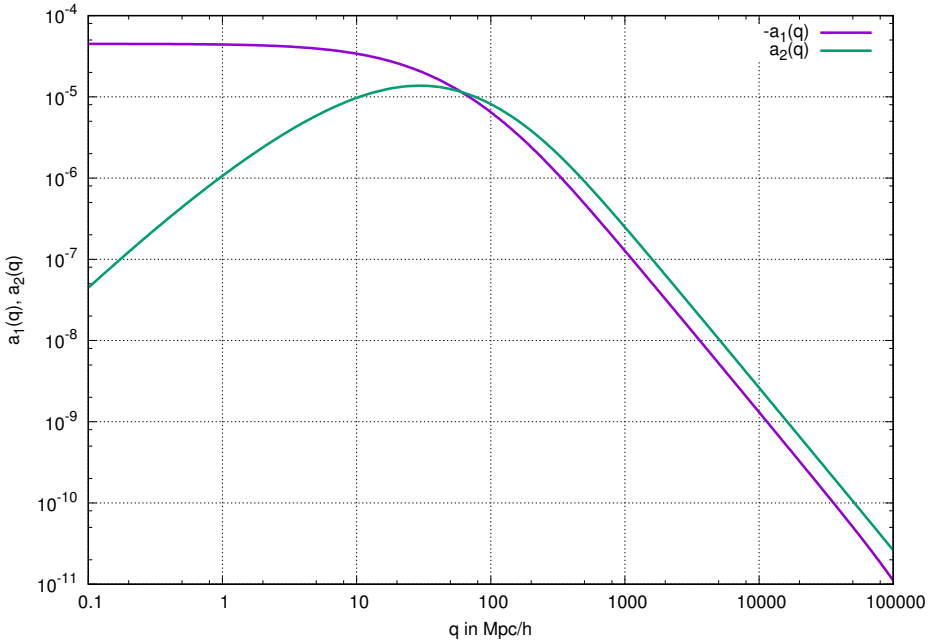

Figure 2: Shown are the functions $a_1(q)$ and $a_2(q)$ of equation (3.33) for a ΛCDM power-spectrum according to Bardeen et al. [2] with cosmological parameters $\Omega_{m0} = 0.3$ and $\Omega_{\Lambda 0} = 0.7$.

with the correlation function ξ_ψ of the velocity potential ψ. By statistical isotropy ξ_ψ can depend on the distance between to points only. Defining the projectors parallel and perpendicular to the direction of the separation of the two points

$$\tilde{\pi}_\parallel = \frac{\vec{q}_{jk} \otimes \vec{q}_{jk}}{q_{jk}^2}, \quad \tilde{\pi}_\perp = I_3 - \tilde{\pi}_\parallel, \tag{3.31}$$

we arrive at

$$C_{p_j p_k} = -\tilde{\pi}_\parallel \xi_\psi''(q_{jk}) - \tilde{\pi}_\perp \frac{\xi_\psi'(q_{jk})}{q_{jk}} \tag{3.32}$$

for the initial momentum correlation matrix. The correlation function and its derivatives are readily constructed from the spherical Bessel functions and their recursion relations

$$\xi_\psi(q) = \frac{1}{2\pi^2} \int dk k^2 P_\psi(k) j_0(kq), \tag{3.33a}$$

$$\xi_\psi'(q) = -\frac{1}{2\pi^2} \int \frac{dk}{k} P_\delta(k) j_1(kq) =: q a_1(q), \tag{3.33b}$$

$$\xi_\psi''(q) - \frac{\xi_\psi'(q)}{q} = \frac{1}{2\pi^2} \int dk P_\delta(k) j_2(kq) =: a_2(q), \tag{3.33c}$$

where we omitted the indices j, k and used the relation $P_\psi = k^{-4} P_\delta$ from the Poisson equation (2.37). We show the functions $a_1(q)$ and $a_2(q)$ in Figure 2.
Since the generic factors involve products of this matrix with the momentum shift vectors $\vec{L}_p$, it is more convenient to express the matrix with projectors with respect to the wave-vector $\vec{k}_{jk}$. These projectors are given by

$$\pi_{jk}^\parallel = \frac{\vec{k}_{jk} \otimes \vec{k}_{jk}}{k_{jk}^2}, \quad \pi_{jk}^\perp = I_3 - \pi_{jk}^\parallel \tag{3.34}$$

and we are looking for the functions $a_{\parallel}(q_{jk})$ and $a_{\perp}(q_{jk})$ such that

$$C_{p_j p_k} = -\pi^{\parallel}_{jk} a_{\parallel}(q_{jk}) - \pi^{\perp}_{jk} a_{\perp}(q_{jk}). \tag{3.35}$$

Using equation (3.32) we arrive at the expressions for the parallel and perpendicular correlation functions

$$a_{\parallel}(q_{jk}) = \mu^2 \xi''_{\psi}(q_{jk}) + (1-\mu^2)\frac{\xi'_{\psi}(q_{jk})}{q_{jk}} \tag{3.36a}$$

$$a_{\perp}(q_{jk}) = (1-\mu^2)\xi''_{\psi}(q_{jk}) + (1+\mu^2)\frac{\xi'_{\psi}(q_{jk})}{q_{jk}} \tag{3.36b}$$

with $\mu = \vec{k}_{jk} \cdot \vec{q}_{jk}$ being the angle cosine between the wave and separation vectors. With those definitions the generic factors become

$$I_{jk} = \int_{q_{jk}} \exp\left(\vec{L}^{\intercal}_{p_j} \pi^{\parallel}_{jk} \vec{L}_{p_k} a_{\parallel}(q_{jk}) + \vec{L}^{\intercal}_{p_j} \pi^{\perp}_{jk} \vec{L}_{p_k} a_{\perp}(q_{jk}) + i\vec{k}_{jk} \cdot \vec{q}_{jk}\right). \tag{3.37}$$

This specifies the free generating functional $Z_0[\mathbf{L}, 0]$ completely.

3.1.3 *Contributions to Momentum-Density Correlators*

Momentum-density correlators are computed from the free generating functional $Z[\mathbf{L}, 0]$ by consecutive application of partial derivatives with respect to the momentum shift vectors $\mathbf{L}_p$. For a free n-point correlation function we write

$$\Pi^{\alpha_1}_{j_1}(1) \dots \Pi^{\alpha_n}_{j_n}(n) Z[\mathbf{J}, \mathbf{K}]\Big|_{\mathbf{J},\mathbf{K}=0} = \left(\prod_{s=1}^{n} g_{pp}(t_s, t_0) \frac{\partial}{i\partial L^{\alpha_s}_{p_{j_s}}}\right) Z_0[\mathbf{L}, 0], \tag{3.38}$$

where $\alpha_s = 1, 2, 3$ are the vector components. The free generating functional contains two functions that are dependent on the momentum shifts

$$f(\mathbf{L}_p) := \exp(Q_D(\vec{k}, t)) = \exp\left(-\frac{\sigma_1^2}{6} \sum_{s=1}^{n} L^2_{p_s}\right), \tag{3.39}$$

$$g(\mathbf{L}_p) := \prod_{j>k} \int_{q_{jk}} \exp\left(\vec{L}_{p_j} \cdot \pi^{\parallel}_{jk} \vec{L}_{p_k} (a_{\parallel} - a_{\perp}) + \vec{L}_{p_j} \cdot \vec{L}_{p_k} a_{\perp} + i\vec{k}_{jk} \cdot \vec{q}_{jk})\right). \tag{3.40}$$

In the second definition we omitted the dependence of $a_{\parallel}$ and $a_{\perp}$ on the spatial separation q_{jk} for brevity.
The next step is to calculate the derivatives of the two functions $f(\mathbf{L}_p)$ and $g(\mathbf{L}_p)$. The first and second derivatives of the damping factor are

$$\frac{\partial}{\partial L^{\alpha}_{p_a}} f(\mathbf{L}_p) = -\frac{\sigma_1^2}{3} L^{\alpha}_{p_a} f(\mathbf{L}_p), \tag{3.41}$$

$$\frac{\partial}{\partial L^{\beta}_{p_b}} \frac{\partial}{\partial L^{\alpha}_{p_a}} f(\mathbf{L}_p) = \left(\frac{\sigma_1^4}{9} L^{\alpha}_{p_a} L^{\beta}_{p_b} - \frac{\sigma_1^2}{3} \delta_{ab} \delta^{\alpha\beta}\right) f(\mathbf{L}_p), \tag{3.42}$$

with the generalisation

$$\begin{aligned}
&\left(\prod_{s=1}^{n} \frac{\partial}{\partial L^{\alpha_s}_{p_s}}\right) f(\mathbf{L}_p) \\
&= f(\mathbf{L}_p) \left[\left(-\frac{\sigma_1^2}{3}\right)^n \prod_{s} L^{\alpha_s}_{p_s} + \left(-\frac{\sigma_1^2}{3}\right)^{n-1} \sum_{(a,b)} \delta_{ab} \delta^{\alpha_a \alpha_b} \prod_{s'} L^{\alpha_s}_{p_s} + \dots\right],
\end{aligned} \tag{3.43}$$

with a sum over the pairs (a, b) and a product over $s' = 1 \dots n$ without a and b. All terms except for the first demand at least two particles to be the same. But in the calculation of n-point correlation functions we connect n different particles with each other. Thus, only the first term contributes to any momentum-density correlator, since terms with lower multiplicity drop out in the limit of $N \to \infty$. So for our purposes we have

$$\left(\prod_{s=1}^{n} \frac{\partial}{\partial L_{p_s}^{\alpha_s}}\right) f(\mathbf{L}_p) = f(\mathbf{L}_p) \left(-\frac{\sigma_1^2}{3}\right)^n \prod_s L_{p_s}^{\alpha_s} \tag{3.44}$$

for the n-th partial derivative of the damping factor $f(\mathbf{L}_p)$ with respect to the momentum shift vectors.
The derivatives of the function $g(\mathbf{L}_p)$, that depends on the initial 2-point momentum correlations, need more work to evaluate. We first work out the derivatives of the quadratic form $Q = \vec{L}_{p_j}^{\mathsf{T}} C_{p_j p_k} \vec{L}_{p_k}$, which are

$$\begin{aligned} \frac{\partial}{\partial L_{p_a}^{\alpha}} Q =& ((\pi_{jk}^{\parallel} L_{p_k})^{\alpha} \delta_{ja} + (L_{p_j} \pi_{jk}^{\parallel})^{\alpha} \delta_{ka})(a_{\parallel}(q_{jk}) - a_{\perp}(q_{jk})) \\ &+ (L_{p_k}^{\alpha} \delta_{ja} + L_{p_j}^{\alpha} \delta_{ka}) a_{\perp}(q_{jk}), \end{aligned} \tag{3.45}$$

$$\frac{\partial}{\partial L_{p_b}^{\beta}} \frac{\partial}{\partial L_{p_a}^{\alpha}} Q = (\delta_{ja}\delta_{kb} + \delta_{ka}\delta_{jb})(\pi_{jk}^{\parallel \alpha\beta}(a_{\parallel}(q_{jk}) - a_{\perp}(q_{jk})) + \delta^{\alpha\beta} a_{\perp}(q_{jk})), \tag{3.46}$$

and higher orders vanish. The generic factors I_{jk} depend exponentially on the quadratic form Q, therefore derivatives of I_{jk} are sums of terms proportional to either the first or second derivatives of Q. For the sake of brevity we define

$$M_a^{\alpha}(q_{jk}) := \frac{\partial}{\partial L_{p_a}^{\alpha}} Q, \quad \text{and} \quad N_{ba}^{\alpha\beta}(q_{jk}) := \frac{\partial}{\partial L_{p_b}^{\beta}} \frac{\partial}{\partial L_{p_a}^{\alpha}} Q, \tag{3.47}$$

which are to be calculated according to (3.45) and (3.46). And we proceed to the calculation of the derivatives of the function $g(L_p)$ that are given by

$$\frac{\partial}{i\partial L_{p_a}^{\alpha}} g(\mathbf{L}_p) = \prod_{j>k\geqslant 1} \int_{q_{jk}} e^{Q(q_{jk}) + i\vec{k}_{jk}\cdot\vec{q}_{jk}} \sum_{x>y\geqslant 1} M_a^{\alpha}(q_{xy}), \tag{3.48}$$

$$\begin{aligned} \frac{\partial}{i\partial L_{p_b}^{\beta}} \frac{\partial}{i\partial L_{p_a}^{\alpha}} g(\mathbf{L}_p) = & \prod_{j>k\geqslant 1} \int_{q_{jk}} e^{Q(q_{jk}) + i\vec{k}_{jk}\cdot\vec{q}_{jk}} \times \\ & \times \left[\sum_{x>y\geqslant 1} N_{ba}^{\alpha\beta}(q_{xy}) + \left(\sum_{x>y\geqslant 1} M_a^{\alpha}(q_{xy}) \right) \left(\sum_{u>v\geqslant 1} M_b^{\beta}(q_{uv}) \right) \right] \end{aligned} \tag{3.49}$$

and obvious extensions to higher order derivatives.

3.2 DIAGRAMMATIC APPROACH

3.2.1 *Perturbation Theory*

The interaction operator is defined as e^{iS_I} with the operator S_I from (2.31) of Section 2.1.4. The non-linearity of the interactions, namely that the trajectory of each particle depends on the interaction with all other particles, makes it impossible to include the

complete interaction described by said operator. In practice, we will expand the exponential in a Taylor series

$$\exp(iS_I) = 1 + iS_I - \frac{1}{2}S_I \cdot S_I + \mathcal{O}(S_I^3), \tag{3.50}$$

such that each order corresponds physically to the number of interactions one particle has along the path. Effectively this is an expansion in the one-particle potential, which becomes small at late times (cf. Bartelmann [3]).
To simplify notations we define the generating functional $Z[\mathbf{J}, \mathbf{K}]$ without the interaction operator as

$$Z_0[\mathbf{J}, \mathbf{K}] = \int d\Gamma \exp\left(i \int_{t_0}^{t} dt' \left\langle \mathbf{J}(t'), \bar{\mathbf{x}}(t') \right\rangle \right). \tag{3.51}$$

We consider a cross-correlation function of $(n-r)$ density and r momentum-density fields

$$\begin{aligned} &\rho_{j_n}(n) \dots \rho_{j_{n-r}}(n-r) \Pi_{j_r}^{\alpha_r}(r) \dots \Pi_{j_1}^{\alpha_1}(1) Z_0[\mathbf{J}, \mathbf{K}] \\ &= \int d\Gamma \left[\prod_{s=1}^{r} \left(g_{pp}(t_s, t_0) p_{j_s}^{\alpha_s} + \int dt' g_{pp}(t_s, t') K_{p_{j_s}}^{\alpha_s}(t') \right) \right] e^{i\langle \mathbf{J}(t) + \mathbf{L}(t), \bar{\mathbf{x}}(t) \rangle}, \end{aligned} \tag{3.52}$$

where the shift $\mathbf{L}$ is due to all n one-particle density operators. If we set the source fields $\mathbf{J}$, $\mathbf{K}$ to zero, we get the free correlation function.
We aim here at a systematic calculation of the corrections due to potential particle interactions up to m-th order to (3.52). Since the function S_I includes one density and one response field, we add two shift vectors to $\mathbf{L}$ at each order. Thus the correction of an n-point correlator at m-th order of particle interactions must be calculated from a $(n+2m)$-point correlator. The number and form of terms contributing to the correction depends on the number r of momentum-density fields. We work this out for some examples and give a diagrammatic representation for the terms below.

ONE MOMENTUM-DENSITY FIELD: We first consider a cross-correlation of $(n-1)$ density and one momentum-density field. The general expression (3.52) reduces to

$$\begin{aligned} &F^{(0),\alpha}_{\Pi\rho\dots\rho}(1 \dots n) := \rho_{j_n}(n) \dots \rho_{j_2}(2) \Pi_{j_1}^{\alpha}(1) Z_0[\mathbf{J}, \mathbf{K}] \\ &= \int d\Gamma \left[\left(g_{pp}(t_1, t_0) p_{j_1}^{\alpha} + \int dt' g_{pp}(t_1, t') K_{p_{j_1}}^{\alpha}(t') \right) \right] e^{i\langle \mathbf{J}(t) + \mathbf{L}(t), \bar{\mathbf{x}}(t) \rangle}. \end{aligned} \tag{3.53}$$

The correction to this function at linear order of interactions is calculated by the correlation

$$\begin{aligned} &B_{l_1}(-1') \rho_{k_1}(1') F^{(0),\alpha}_{\Pi\rho\dots\rho}(1 \dots n) \Big|_{\mathbf{J},\mathbf{K}=0} \\ &= \left[\underline{b}_{l_1}(-1') g_{pp}(t_1, t_0) \frac{\partial}{i\partial L_{p_{j_1}}^{\alpha}} + i g_{pp}(t_1, t_1') k_1'^{\alpha} \delta_{j_1 l_1} \right] Z_0[\mathbf{L}, 0], \end{aligned} \tag{3.54}$$

with the definition of the $\underline{b}_{m_1}(-1')$-factor from (3.14) and the shift tensor having $(n+2)$ entries. The first term corresponds to corrections resulting from deviations in the final particle positions due to particle interactions by means of the b-factor and the second

term corresponds to a change of the momentum due to the potential gradient force. At quadratic order we get again two different types of terms:

$$\begin{aligned}
&B_{l_2}(-2')\rho_{k_2}(2')B_{l_1}(-1')\rho_{k_1}(1')F^{(0),\alpha}_{\rho\ldots\rho\Pi}(1\ldots n)\Big|_{\mathbf{J},\mathbf{K}=0}\\
&= \Bigg[\underline{b}_{l_2}(-2')\underline{b}_{l_1}(-1')g_{pp}(t_1,t_0)\frac{\partial}{i\partial L^{\alpha}_{p_{j_1}}}\\
&+i\underline{b}_{l_2}(-2')g_{pp}(t_1,t_1')k_1'^{\alpha}\delta_{j_1l_1}+i\underline{b}_{l_1}(-1')g_{pp}(t_1,t_2')k_2'^{\alpha}\delta_{j_1l_2}\Big]\,Z_0[\mathbf{L},0]. \qquad (3.55)
\end{aligned}$$

The first term accounts for deviations from the freely-evolved distribution due to two different scattering events along the trajectories of the $(n+m)$ particles and the other two account for the acceleration due to a potential gradient of one particle and the deviation from the free distribution due to a scattering of another particle.

The number of particles for a correction at m-th order is $(n+m)$ since each Kronecker delta in any b-factor identifies two particles. Physically, the meaning of this is simple: assume we calculate the linear correction to the density power-spectrum. The total number of operators (and associated particles) is four, but the b-factor reduces the number of contributing particles to three. In this example two particles (j,k) enter the interaction by the response and density field operators. The terms in the b-factor identify the particle j associated to the response field with either of the two particles (j_1,j_2) contributing to the power-spectrum. Thus, each term in the b-factor accounts for an interaction of either j_1 or j_2 with particle k. We will return to this, when we introduce a diagrammatic representation.

Going to higher orders of S_I we see that the correction of an n-point correlation with one momentum-density field contains two types of terms. The first type is proportional to the product of all b-factors

$$T_1^m = \left[\prod_{s=1}^{m}\underline{b}_{l_s}(-s')\right] g_{pp}(t_1,t_0)\frac{\partial}{i\partial L^{\alpha}_{p_{j_1}}}, \qquad (3.56)$$

and the second type is

$$T_2^m = i\sum_{s=1}^{m}\left(g_{pp}(t_1,t_s')k_s'^{\alpha}\delta_{j_1l_s}\prod_{x\neq s}b_{l_x}(-x')\right). \qquad (3.57)$$

The complete correlation function that contributes to the m-th order correction is

$$F^{(0),\alpha}_{B\rho\Pi\rho\ldots\rho}(-1'1'1\ldots n) = (T_1^m + T_2^m)\,Z_0[\mathbf{L},0]. \qquad (3.58)$$

Then the number of different terms is $N = 1+m$, if we count the product of different b-factors as one.

TWO MOMENTUM-DENSITY FIELDS: If the correlator contains two momentum-density fields, another type of correction term contributes. The new type of term does not contribute to the linear order correction but to all higher orders.

Since the function $F^{(0)}_{\Pi\Pi\rho\ldots\rho}$ contains two momentum trajectories in the kernel, we need to change T_1^m and T_2^m accordingly. That is

$$T_1^m = \left[\prod_{s=1}^{m}\underline{b}_{l_s}(-s')\right] g_{pp}(t_2,t_0)g_{pp}(t_1,t_0)\frac{\partial}{i\partial L^{\beta}_{p_{j_2}}}\frac{\partial}{i\partial L^{\alpha}_{p_{j_1}}}, \qquad (3.59)$$

$$T_2^m = i\sum_{s=1}^{m}\left(\left(\delta_{j_1l_s}g_{pp}(t_1,t_s')k_s'^{\alpha}\frac{\partial}{i\partial L^{\beta}_{p_{j_2}}}+\delta_{j_2l_s}g_{pp}(t_2,t_s')k_s'^{\beta}\frac{\partial}{i\partial L^{\alpha}_{p_{j_1}}}\right)\prod_{x\neq s}b_{l_x}(-x')\right). \qquad (3.60)$$

The third type of terms comes from the correlations between the deviations from the free momentum trajectories due to accelerations along potential gradients and contributes only at $m \geqslant 2$, since the two particles associated with the momentum-density field must have scattered with another particle. At arbitrary order m we can write

$$\begin{aligned} T_3^m = &\Big(\delta_{j_1 l_m}\delta_{j_2 l_{(m-1)}} g_{pp}(t_1,t_m) g_{pp}(t_2,t_{m-1}) k_m'^{\alpha_1} k_{m-1}'^{\alpha_2} \\ &+\delta_{j_2 l_m}\delta_{j_1 l_{(m-1)}} g_{pp}(t_1,t_{m-1}) g_{pp}(t_2,t_m) k_{m-1}'^{\alpha_1} k_m'^{\alpha_2}\Big) \prod_{s\neq(m,m-1)} \underline{b}_{l_s}(-s') \\ &+ \text{different pairs of interacting particles,} \end{aligned} \tag{3.61}$$

where the interacting pairs can be formed from any two particles labeled $l_1 \dots l_m$ and the additional terms have the same form as the first one. The total number of terms is $N = 1 + 2m + 2\frac{m!}{(m-2)!2!}$, if we count permutations of indices.

ARBITRARY NUMBER OF MOMENTUM-DENSITY FIELDS: With the examples above we can deduce the number of terms that contribute to an m-th order correction due to particle interactions to an n-point correlator with r momentum-density fields. We have in total

$$N = \sum_{a=0}^{\min(m,r)} a! \binom{m}{a}\binom{r}{a} \tag{3.62}$$

contributing terms. The sum extends to the minimum of m and r, since some terms do not appear in the linear corrections, for example. The factorial $a!$ results from the product rule and indicates the first order of interaction the term contributes to. The first binomial factor gives the number of permutations available for the response field b_{j_s} to act on either the exponential $\exp(i\langle \mathbf{L}, \bar{\mathbf{x}}(t)\rangle)$ or on the generator field $\vec{K}_p$ in the free momentum solution. The last binomial factor accounts for the number of summands in (3.52) that contain the same number of integrals over the generator field $\vec{K}_p$ which ultimately decides how many qualitatively similar terms contribute. As in the examples, the number of terms does not count the types of terms but the number of permutations in those types.

3.2.2 *Rules*

The previous paragraph showed that the calculation of corrections due to interactions of the form S_I is rather tedious and prone to errors. To calculate the corrections systematically we introduce diagrams as a visual tool representing the contributing terms. We build upon the representation that was developed by Bartelmann et al. [5] for density correlations and extend their framework.
The extension will allow to include momentum-density fields as external wave-vectors, the replacement of one free momentum by the wave-vector of interactions and the identification of particles given by the Kronecker deltas in the previous section. In order to represent those terms we extend rules (i), (iv) and (v) from Section 4.3 in Bartelmann et al. [5] while the others remain unchanged. The rules are the following:

(i) The free generating functional $Z_0[\mathbf{J},\mathbf{K}]$ is represented by a circle. All operators (3.2)-(3.4) include a one-particle density operator ρ_{j_l} causing a phase-shift in Z_0. Thus, each of these operators adds a wave vector to the shift tensor $\mathbf{L}$ as shown in (3.6). According to (3.52), a functional derivative with respect to the source field component $\vec{J}_{p_{j_l}}$ contributes a free one-particle momentum to Z_0.

a. *Attach* $s = n + 2m$ *wave vectors (represented by arrows) to the circle marking the free generating functional* Z_0 *pointing outward, where* s *is the total number of density, momentum-density and response field operators.*

b. *Of these, distinguish* r *by dashed arrows representing the momentum-density operators* $\vec{\Pi}_{j_l}$ *from the* $(s - r)$ *solid arrows representing density fields associated with either* ρ_{j_l} *or* B_{j_l}.

(ii) The operators act at different times which are represented by filled dots on the circumference of Z_0, such that each arrow begins at a filled dot. The internal wave vectors representing interactions are pairwise attached to the same time since the particle interaction S_I is instantaneous. For equal-time cumulants the external wave vectors start at the same filled dot as well.
The time ordering is counter-clockwise and the latest time is at the top. Interactions are represented by two lines attached to Z_0 *at the same point in time. If the correlator is simultaneous, the external wave vectors are also attached to the same point.*

(iii) According to (2.31) the density and the response fields associated with each interaction are connected by an interaction potential v. In the case of a potential depending only on the distance between the particles, the two internal wave vectors of the density and response field operator need to have the same magnitude and opposite directions.
The interaction potential is represented by a circled v *connected to a pair of internal wave vectors, which are marked with a prime. If the potential is translation-invariant, the connected internal wave vectors point in opposite directions and have the same magnitude.*

(iv) Given equations (3.14) and (3.15), each response field identifies two particles at different times, i.e. two different wave vectors at different times are assigned to the same particle. As in the diagrammatic representation for pure density cumulants the response field begins at the negative internal wave vector in the interaction operator S_I.

a. *Each response field is drawn as a circle segment starting at a negative internal wave vector and connecting two different wave vectors. The circle segments always end at a later time.*

b. *Distinguish dashed circle segments representing a deviation of the particle distribution/position from the freely-evolved one given by the response field factor* b_{j_l} *in equation (3.14) from solid circle segments corresponding to a change of the particle momentum by* $g_{pp}(t_s, t_l)k_l^{\alpha_s}\delta_{j_l j_s}$. *These lines can only connect a response field (solid arrow) with a momentum-density (dashed arrow).*

c. *At a dashed wave vector, either no or one solid circle segment must end, but arbitrarily many dashed circle segments may end at the same wave vector, internal or external.*

(v) In density cumulants equivalent diagrams may appear multiple times. This is a consequence of the density being a homogeneous random field, where the external wave vectors are equivalent. For cumulants including at least one momentum-density each diagram appears exactly once and there are no equivalent diagrams.
Each diagram has an assigned multiplicity which is the number of equivalent diagrams.

The application of these rules allows a quick evaluation of the number and kinds of terms that contribute to the desired correlation function. The diagrams explicitly represent all terms that come from products of b-factors in the terms we discussed in the previous paragraph.

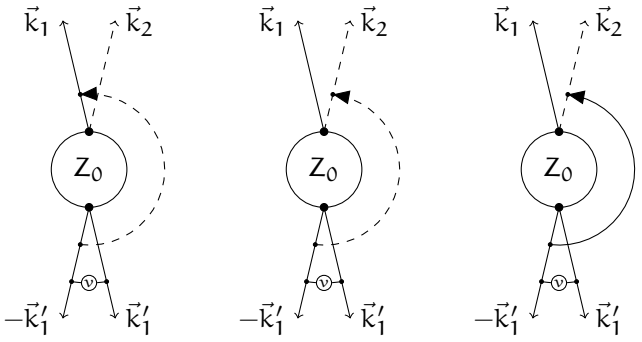

Figure 3: At linear order three terms contribute to the correction of the 2-point cumulant of a density and momentum-density field. The first two come from the b-factor representing a deviation from the final freely-evolved position due to interactions and the last diagram accounts for the deviation from the free momentum trajectory.

3.2.3 *Examples*

To illustrate how the diagrams are constructed we consider a simultaneous 2-point cross-correlation function of a density ρ and a momentum-density field $\vec{\Pi}$.
For the linear correction we apply one additional response field $B(-1')$ and one additional density field $\rho(1')$ to the generating functional, that are linked by a one-particle potential v. The according diagrams are shown in Figure 3. By rule (i) we attached one line for each field to the circle representing the free generating functional. The solid density line and the dashed momentum-density line start at the same point, since we consider a simultaneous correlator, and the internal wave-vectors are connected by the interaction potential. From this configuration we need to construct all particle identifications compatible with rule (iv). There are three possibilities to draw the response field and therefore three terms/diagrams. The first two include a dashed circle segment and come from the b-factor. This accounts for misplacements of a particle from its freely attained position at the time of evaluation. The third diagram accounts for the deviation of the particle's momentum due to the potential gradient. If we enumerate the particles clockwise starting in the upper left from 1 to 4, we can write down the cumulants that the diagrams represent:

$$D_{1a} = \int dt' \int_{k'_1} v(1') g_{qp}(t_1, t') \vec{k}_1 \cdot \vec{k}'_1 \delta_{1,4} g_{pp}(t_1, t_0) \frac{\partial}{i\partial \vec{L}_{p_2}} Z_0[L, 0], \tag{3.63a}$$

$$D_{1b} = \int dt' \int_{k'_1} v(1') g_{qp}(t_1, t') \vec{k}_2 \cdot \vec{k}'_1 \delta_{2,4} g_{pp}(t_1, t_0) \frac{\partial}{i\partial \vec{L}_{p_2}} Z_0[L, 0], \tag{3.63b}$$

$$D_{1c} = \int dt' \int_{k'_1} v(1') g_{pp}(t_1, t') \delta_{2,4} Z_0[L, 0], \tag{3.63c}$$

where the identification of particles changes either $\vec{L}_1$ or $\vec{L}_2$.
At quadratic order we have to consider more terms/diagrams that are readily constructed from our rules (i)-(v). The product of two b-factors is shown in Figure 4. Again we have drawn a circle representing the free generating functional $Z_0[\mathbf{J}, \mathbf{K}]$ and attached four internal and two external lines to it. Next we construct according to rule (iv) the diagrams with dashed circle segments. Respecting time-ordering we can draw eight different diagrams. All of them represent corrections to the 2-point correlator $\langle \rho \vec{\Pi} \rangle$ due to displacements of particles from their freely evolved end-position due to two scatterings along their paths. The diagrams correspond to the terms T_1^m with $m = 2$ in equation

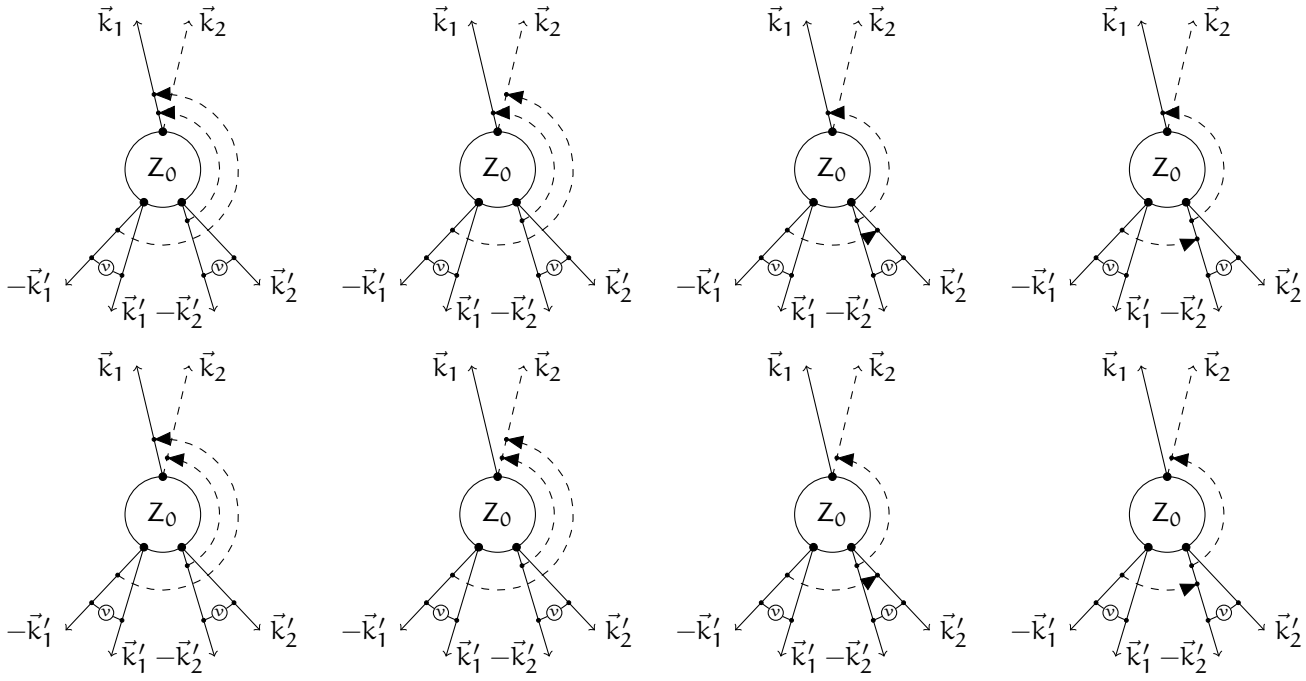

Figure 4: Diagrams representing the correction term T_1^m for an n=2-point cumulant of r=1 momentum-density field and $(n-r)$=1 density field at m=2 order in the particle interactions. The multiplicity of each diagram is one, since there are no equivalent diagrams.

(3.56). Apart from these eight diagrams we can construct six more diagrams as shown in Figure 5 with solid circle segments. These diagrams represent terms of type T_2^m with $m = 2$ from equation (3.57).
As we did for the linear order, we can read off the contributing terms from the diagrams directly. We do so for the first diagram in Figure 4

$$D'_2 = \int dt'_1 dt'_2 \int_{k'_1} \int_{k'_2} \nu(1')\nu(2') g_{qp}(t_1, t'_1)\vec{k}_1 \cdot \vec{k}'_1 g_{qp}(t_1, t'_2)\vec{k}_1 \cdot \vec{k}'_2 \times$$
$$\times \delta_{1,4}\delta_{1,6} g_{pp}(t_1, t_0) \frac{\partial}{i\partial \vec{L}_{p_2}} Z[\mathbf{L}, 0], \tag{3.64}$$

and for the first diagram in Figure 5

$$D''_2 = \int dt'_1 \int dt'_2 \int_{k'_1} \int_{k'_2} \nu(1')\nu(2') g_{qp}(t_1, t'_1)\vec{k}_1 \cdot \vec{k}'_1 \times$$
$$\times g_{pp}(t_1, t'_2)\vec{k}'_2 \delta_{1,6}\delta_{2,4} Z[\mathbf{L}, 0], \tag{3.65}$$

with a clockwise enumeration starting at the top left line. In summary, we can translate diagrams into functions of the form

$$D_m = \left[\prod_{s=1}^{m} \int dt'_s \int_{k'_s} \nu(s')\right] \delta(\vec{k}'_1, \ldots \vec{k}'_m) \left[\prod_{x \in \mathcal{J}} \frac{\partial}{i\partial L_{p_x}^{\alpha_x}}\right] Z_0[L, 0]. \tag{3.66}$$

Here the index set $\mathcal{J} \subseteq (j_1, \ldots, j_r)$ is a subset of the one-particle momentum-density operator labels and depends on the diagram D_m represents. In our example $\mathcal{J}$ is empty for diagrams containing one response field represented by a solid circle segment.

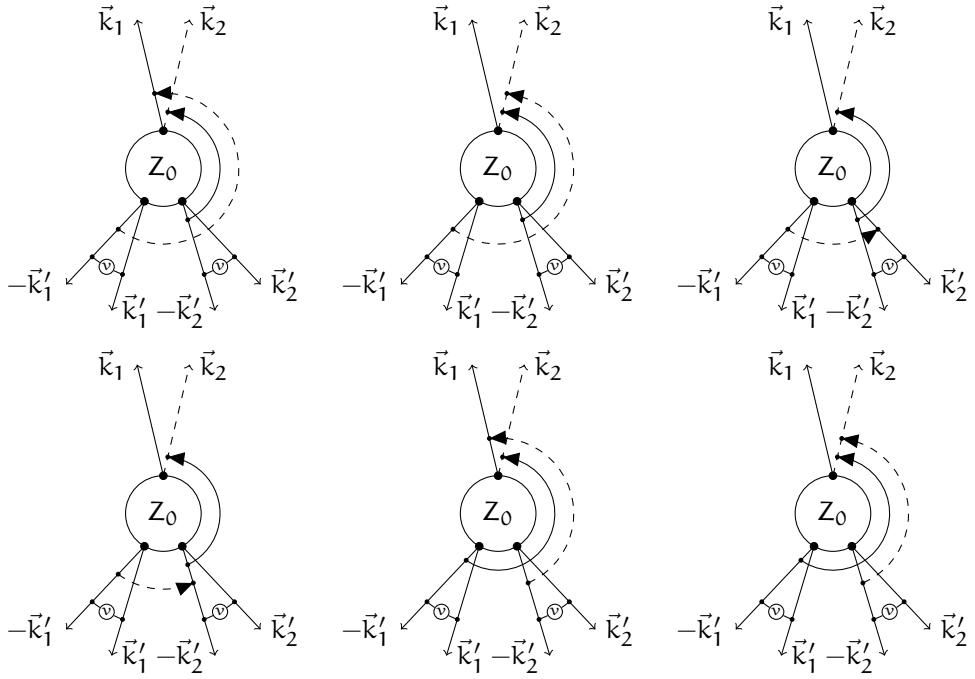

Figure 5: Diagrams representing the correction term T_2^m of an n=2-point cumulant for r=1 momentum-density and $(n-r)$=1 density field at m=2 order in the particle interactions.

Part II

APPLICATIONS

4

2-POINT MOMENTUM-DENSITY CORRELATIONS

In this Chapter we use the tools developed for KFT in the previous Chapters to calculate the 2-point momentum-density correlation tensor. We calculate the free correlator $\langle\vec{\Pi}\otimes\vec{\Pi}\rangle^{(0)}$ and the corrections of linear order $\delta^{(1)}\langle\vec{\Pi}\otimes\vec{\Pi}\rangle$. Our results are given in components and we calculate scalar quantities from them, namely the trace of the correlator and power-spectra for the divergence and the curl of the momentum-density field. We approximate

$$\langle\vec{\Pi}\otimes\vec{\Pi}\rangle(12) = \langle\vec{\Pi}\otimes\vec{\Pi}\rangle^{(0)}(12) + \delta^{(1)}\langle\vec{\Pi}\otimes\vec{\Pi}\rangle(12) \tag{4.1}$$

as the 2-point momentum-density correlation tensor. Statistical homogeneity ensures that $\vec{k}_2 = -\vec{k}_1$. The scalar quantities that we will calculate in this Chapter are

$$\mathrm{Tr}\langle\vec{\Pi}\otimes\vec{\Pi}\rangle = \langle\Pi^\alpha\Pi_\alpha\rangle, \tag{4.2a}$$

$$\langle\Big(\nabla\cdot\vec{\Pi}\Big)\Big(\nabla\cdot\vec{\Pi}\Big)\rangle = \vec{k}_1\cdot\langle\vec{\Pi}\otimes\vec{\Pi}\rangle\vec{k}_1, \tag{4.2b}$$

$$\langle\Big(\nabla\times\vec{\Pi}\Big)\cdot\Big(\nabla\times\vec{\Pi}\Big)\rangle = \|\vec{k}_1\|^2\mathrm{Tr}\langle\vec{\Pi}\otimes\vec{\Pi}\rangle - \langle\Big(\nabla\cdot\vec{\Pi}\Big)\Big(\nabla\cdot\vec{\Pi}\Big)\rangle \tag{4.2c}$$

with the arguments $(12) = (1,-1)$. The last two quantities are also the power-spectra for the projections of $\vec{\Pi}$ on the wave-vector $\vec{k}_1$ multiplied by its absolute value squared.
In the calculations presented here we first include the initial momentum correlations C_{pp} only quadratically in the same way as Bartelmann et al. [6] did for the density fluctuation power-spectrum. Then we use our results from Section 3.1.2 to include the full hierarchy of initial momentum correlations. Since calculations including interactions are numerically challenging, we calculate an average force using Born's approximation. In Section 4.3 we present the calculations of Bartelmann et al. [4] and extend their discussion to the momentum-density correlation tensor. We compare our results with the numerical results of the Millennium-XXL simulation.
As an application we discuss the kinetic Sunyaev-Zel'dovich effect. The CMB is the earliest electro-magnetic signal in the Universe that we can measure. The photons have today a mean temperature of $T = 2.7255\mathrm{K}$ with primordial fluctuations of the order $\delta T/T \sim 10^{-5}$ (Planck Collaboration et al. [32]). The signal was released when the Universe became electrically neutral at a redshift of $z = 1100$, so that the Universe became transparent to photons. In the course of time structures and astrophysical objects (stars, galaxies, etc.) formed. Radiation from those objects reionised the Universe and CMB photons would scatter from electrons. The kinetic Sunyaev-Zel'dovich effect accounts for secondary temperature fluctuations in the CMB from photon scatterings off electrons moving with the bulk of structures. The effect is depends sensitively on the power-spectrum of the momentum-density.

4.1 APPROXIMATED INITIAL CORRELATIONS

In our first calculations we adopt the approximations of Bartelmann et al. [6], i. e. that the initial density and density-momentum correlations are weak and the initial momentum correlations contribute up to quadratic order. Thus, we set the correlation polynomial $\mathcal{C}(\mathbf{p}) = 1$ in the initial phase-space distribution and apply two momentum-density op-

erators to the generating functional. We consider the free contribution first and set all source fields to zero. From (3.52) we can read off

$$\Pi_a^\alpha(1)\Pi_b^\beta(2)Z_0[\mathbf{J},\mathbf{K}]\Big|_{\mathbf{J},\mathbf{K}=0} = \int d\Gamma g_{pp}(t_1,t_0)p_a^\alpha g_{pp}(t_2,t_0)p_b^\beta e^{i\langle \mathbf{L}_q,\mathbf{q}\rangle + i\langle \mathbf{L}_q,\mathbf{q}\rangle}, \tag{4.3}$$

where (a,b) are two different particle labels that without loss of generality can be set to $(1,2)$. Greek indices are the vector components and the shift tensors are

$$\vec{L}_{q_1} = -\vec{k}_1, \quad \vec{L}_{q_2} = -\vec{k}_2, \tag{4.4a}$$

$$\vec{L}_{p_1} = -g_{qp}(t_1,t_0)\vec{k}_1, \quad \vec{L}_{p_2} = -g_{qp}(t_2,t_0)\vec{k}_2. \tag{4.4b}$$

To keep notations short we abbreviate $g_{ij}^{t,t'} := g_{ij}(t,t')$ with i,j being either q or p. The substitution of the momenta by partial derivatives with respect to the momentum shift vectors allows to carry out the momentum integration as in (3.19). Setting $\mathcal{C}(\mathbf{p}) = 1$ and applying the two partial derivatives with respect to $L_{p_1}^\alpha$ and $L_{p_2}^\beta$ we arrive at

$$\begin{aligned} F_{\Pi_1\Pi_2}^{(0)\alpha\beta}(12) = i^2\frac{\partial^2}{\partial L_{p_2}^\beta \partial L_{p_1}^\alpha} Z_0[\mathbf{L},0] = i^2 V^{-N} g_{pp}^{t_1,t_0} g_{pp}^{t_2,t_0} \int d\mathbf{q} e^{Q_D+Q+i\langle \mathbf{L}_q,\mathbf{q}\rangle} \times \\ \times \left[-C_{p_1p_2}^{\alpha\beta} + \left(C_{p_1p_j}\vec{L}_{p_j}\right)^\alpha \left(C_{p_2p_k}\vec{L}_{p_k}\right)^\beta\right], \end{aligned} \tag{4.5}$$

where a sum over the indices j,k is implied, the damping Q_D is taken from (3.27), and the quadratic form $Q := -\vec{L}_{p_x} C_{p_xp_y} \vec{L}_{p_y}$ with $x \neq y$. As we mentioned in the beginning of this Section, we keep initial momentum correlations only up to quadratic order, such that we approximate

$$e^Q \approx 1 + Q + \frac{Q^2}{2} \tag{4.6}$$

for correlations between particles. The damping term suppresses structures by the free-streaming of the particles. We will include this term always one order lower than the 2-point correlations, such that this suppression is not too strong. This is legitimate since we expect gravity to counteract the free-streaming of particles, and therefore less suppression than the full factor e^{Q_D} would suggest.
We write down all terms up to quadratic order in C_{pp} with the appropriate particle labels

$$\begin{aligned} F_{\Pi_1\Pi_2}^{(0)\alpha\beta}(12) = -V^{-2} g_{pp}^{t_1,t_0} g_{pp}^{t_2,t_0} e^{Q_D} \int_{q_1}\int_{q_2} e^{i\langle \mathbf{L}_q,\mathbf{q}\rangle} \times \\ \times \Bigg[-C_{p_1p_2}^{\alpha\beta}\left(1 - \vec{L}_{p_1}^{\intercal} C_{p_1p_2}\vec{L}_{p_2}\right) + \left(\frac{\sigma_1^2}{3}\right)^2 L_{p_1}^\alpha L_{p_2}^\beta \\ + \frac{\sigma_1^2}{3}\left(L_{p_1}^\alpha \left(C_{p_2p_1}\vec{L}_{p_1}\right)^\beta + L_{p_2}^\beta \left(C_{p_1p_2}\vec{L}_{p_2}\right)^\alpha\right) \\ + \left(C_{p_1p_2}\vec{L}_{p_2}\right)^\alpha \left(C_{p_2p_1}\vec{L}_{p_1}\right)^\beta\Bigg]. \end{aligned} \tag{4.7}$$

We use the definition of the momentum correlations $C_{p_1p_2}$ from equation (2.46) to evaluate the spatial integrals and specify to a synchronous correlator ($t_1 = t_2$). The result for the free 2-point momentum-density correlation tensor is given by

$$\langle \Pi^\alpha \Pi^\beta\rangle^{(0)}(12) = \bar{\rho}^2 \delta_D(\vec{k}_1 + \vec{k}_2)(g_{pp}^{t_1,t_0})^2 e^{Q_D}\left(A^{(1)} + A^{(2)} + A_{\text{int}}^{(2)}\right), \tag{4.8}$$

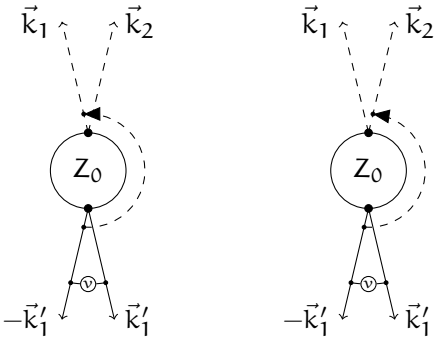

Figure 6: Diagrams contributing at linear order to corrections of the 2-point momentum-density correlator by deviations from the free final particle positions.

where the superscript on the terms A denotes (1) linear and (2) quadratic dependence on C_{pp}. The overall factor $\bar{\rho}^2$ comes from the fact that we need to sum over all pairs of particles giving a factor of $N(N-1)$ and divide the whole expression by V^{-2}. The Dirac delta ensures statistical homogeneity. The terms are

$$A^{(1)} = (2\pi)^3 P_\psi(k_1) k_1^\alpha k_1^\beta, \tag{4.9a}$$

$$A^{(2)} = -\frac{2\sigma_1^2}{3}(g_{qp}^{t_1,t_0})^2 k_1^2 A^{(1)}, \tag{4.9b}$$

$$A^{(2)}_{\text{int}} = (g_{qp}^{t_1,t_0})^2 \int_k P_\psi(k) P_\psi(\Delta)\left(\vec{\Delta}\cdot\vec{k}_1\right)\left[\left(\vec{\Delta}\cdot\vec{k}_1\right)k^\alpha k^\beta + \left(\vec{k}\cdot\vec{k}_1\right)\Delta^\alpha k^\beta\right], \tag{4.9c}$$

where we defined $\vec{\Delta} = \vec{k}_1 - \vec{k}$. By the argument above, we approximate the damping factor $e^{Q_D} \sim 1$ for $A^{(1)}$ and $e^{Q_D} \sim (1-Q_D)^{-1}$ for $A^{(2)}$ and $A^{(2)}_{\text{int}}$ in order to keep the correlation positive-definite, since Q_D is a negative-semidefinite function.
To calculate the corrections in linear order of gravitational interactions we construct the appropriate diagrams as described in Chapter 3. In the following calculation we omit the convolution with the interaction potential and give expressions for the terms represented by the diagrams that contribute to the correlator of one response, one density and two momentum-density fields. We start by the diagrams representing the b-factor. The diagrams are shown in Figure 6. Both of them correspond to the functional form

$$\begin{aligned} B_1(1'12) = -ig_{qp}^{t_1,t'_1}\vec{k}\cdot\vec{k}'_1 V^{-3}(g_{pp}^{t_1,t_0})^2 e^{Q_D}\int_{q_1}\int_{q_2}\int_{q_3} e^{i\langle \mathbf{L}_q,\mathbf{q}\rangle}\times \\ \times\left[-C^{\alpha\beta}_{p_1p_2}\left(\vec{L}^T_{p_x}C_{p_xp_y}\vec{L}_{p_y}\right) + \left(C_{p_1p_j}\vec{L}_{p_j}\right)^\alpha\left(C_{p_2p_k}\vec{L}_{p_k}\right)^\beta\right], \end{aligned} \tag{4.10}$$

where a sum over repeated labels (x,y,j,k) is implied and the vector $\vec{k}$ depends on the diagram. The indices can take the values $(1,2,3)$ labeling the lines in the diagrams clockwise starting with the top left line.
For the left diagram $\vec{k} = \vec{k}_1$ and the shift vectors are

$$\vec{L}_{q_1} = -(\vec{k}_1 - \vec{k}'_1), \quad \vec{L}_{q_2} = -\vec{k}_2, \quad \vec{L}_{q_3} = -\vec{k}'_1, \tag{4.11a}$$

$$\vec{L}_{p_1} = -(g_{qp}^{t_1,t_0}\vec{k}_1 - g_{qp}^{t'_1,t_0}\vec{k}'_1), \quad \vec{L}_{q_2} = -g_{qp}^{t_1,t_0}\vec{k}_2, \quad \vec{L}_{q_3} = -g_{qp}^{t'_1,t_0}\vec{k}'_1, \tag{4.11b}$$

with $t_1 = t_2$, since we calculate a synchronous correlator. For the right diagram $\vec{k} = \vec{k}_2$ and the shift vectors are

$$\vec{L}_{q_1} = -\vec{k}_1, \quad \vec{L}_{q_2} = -(\vec{k}_2 - \vec{k}'_1), \quad \vec{L}_{q_3} = -\vec{k}'_1, \tag{4.12a}$$

$$\vec{L}_{p_1} = -g_{qp}^{t_1,t_0}\vec{k}_1, \quad \vec{L}_{q_2} = -(g_{qp}^{t_1,t_0}\vec{k}_2 - g_{qp}^{t'_1,t_0}\vec{k}'_1), \quad \vec{L}_{q_3} = -g_{qp}^{t'_1,t_0}\vec{k}'_1. \tag{4.12b}$$

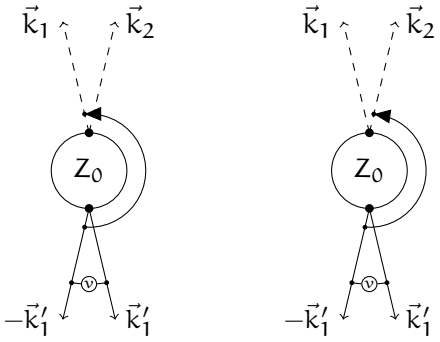

Figure 7: Diagrams contributing at linear order to corrections of the 2-point momentum-density correlator by deviations from the free final particle momenta.

Next we notice that in B_1 at least one label (x, y, j, k) has to be 3 to contribute, since that term would be zero otherwise. After plugging in all definitions for C_{pp} and the shift vectors we get

$$\begin{aligned} B_{\text{total}}(1'12) =& i\bar{\rho}^3 (g_{pp}^{t_1,t_0})^2 g_{qp}^{t_1,t_1'} g_{qp}^{t_1',t_0} \left[(2\pi)^6 \frac{\sigma_1^2}{3} \left(\vec{k}_1 \cdot \vec{k}'_1\right)\left(\vec{k}_2 \cdot \vec{k}'_1\right)(F_1 + F_2) \right. \\ & \left. + (2\pi)^3 \delta_D(\vec{k}_1 + \vec{k}_2) \left(\vec{k}_1 \cdot \vec{k}'_1\right)(F_3 + F_4 + F_5 + F_6 + F_7) \right], \end{aligned} \tag{4.13}$$

with the definitions

$$F_1 := \cdot \left(g_{qp}^{t_1,t_0} \vec{k}_1 - g_{qp}^{t_1',t_0} \vec{k}'_1 \right)^{\alpha} k_2^{\beta} P_\psi(k_2) \delta_D(\vec{k}_1 - \vec{k}'_1) \delta_D(\vec{k}_2 + \vec{k}'_1), \tag{4.14a}$$

$$F_2 := k_1^{\alpha} \cdot \left(g_{qp}^{t_1,t_0} \vec{k}_2 - g_{qp}^{t_1',t_0} \vec{k}'_1 \right)^{\beta} P_\psi(k_1) \delta_D(\vec{k}_1 + \vec{k}'_1) \delta_D(\vec{k}_2 - \vec{k}'_1), \tag{4.14b}$$

$$F_3 := -2\Delta^{\alpha}\Delta^{\beta} g_{qp}^{t_1,t_0} \|\vec{k}'_1\|^2 \left(\vec{k}_1 \cdot \vec{k}'_1\right) P_\psi(\Delta) P_\psi(k'_1), \tag{4.14c}$$

$$F_4 := 2k_1^{\alpha} k_1^{\beta} \|\vec{k}'_1\|^2 \left(\vec{k}'_1 \cdot \left(g_{qp}^{t_1,t_0} \vec{k}_1 - g_{qp}^{t_1',t_0} \vec{k}'_1 \right)\right) P_\psi(k_1) P_\psi(k'_1), \tag{4.14d}$$

$$F_5 := -\left(\Delta^{\alpha} k_1'^{\beta} + k_1'^{\alpha} \Delta^{\beta}\right) g_{qp}^{t_1,t_0} \|\vec{k}'_1\|^2 \left(\vec{k}_1 \cdot \vec{\Delta}\right) P_\psi(\Delta) P_\psi(k'_1), \tag{4.14e}$$

$$F_6 := \left(k_1'^{\alpha} k_1^{\beta} + k_1^{\alpha} k_1'^{\beta}\right) \|\vec{k}'_1\|^2 \left(\vec{k}_1 \cdot \left(g_{qp}^{t_1,t_0} \vec{k}_1 - g_{qp}^{t_1',t_0} \vec{k}'_1 \right)\right) P_\psi(k_1) P_\psi(k'_1), \tag{4.14f}$$

$$F_7 := \left(\Delta^{\alpha} k_1^{\beta} + k_1^{\alpha} \Delta^{\beta}\right) g_{qp}^{t_1',t_0} \left(\vec{k}'_1 \cdot \vec{\Delta}\right)\left(\vec{k}_1 \cdot \vec{k}'_1\right) P_\psi(k_1) P_\psi(\Delta), \tag{4.14g}$$

and the same definition for $\Delta := \vec{k}_1 - \vec{k}'_1$.
Next we construct the diagrams corresponding to deviations from the free final momentum, i. e. diagrams with solid circle segments. The diagrams are shown in Figure 7. The two diagrams represent the terms

$$C_1(1'12) = -i g_{pp}^{t_1,t_0} g_{pp}^{t_1,t_1'} k_1'^{\alpha} e^{Q_D} \int_{q_1}\int_{q_2}\int_{q_3} e^{i\langle \mathbf{L}_q, \mathbf{q}\rangle} \left(C_{p_2 p_k} \vec{L}_{p_k}\right)^{\beta} \left(\vec{L}^{\intercal}_{p_x} C_{p_x p_y} \vec{L}_{p_y}\right), \tag{4.15a}$$

$$C_2(1'12) = -i g_{pp}^{t_1,t_0} g_{pp}^{t_1,t_1'} k_1'^{\beta} e^{Q_D} \int_{q_1}\int_{q_2}\int_{q_3} e^{i\langle \mathbf{L}_q, \mathbf{q}\rangle} \left(C_{p_1 p_k} \vec{L}_{p_k}\right)^{\alpha} \left(\vec{L}^{\intercal}_{p_x} C_{p_x p_y} \vec{L}_{p_y}\right), \tag{4.15b}$$

again, a sum over repeated labels (k, x, y) is implied. The shift vectors are assigned in the same way as for the previous diagrams by the identification of particles through the response field. With the definitions of C_{pp} and the shift tensor we arrive at

$$\begin{aligned} C_1(1'12) =& i\bar{\rho}^3 g_{pp}^{t_1,t_0} g_{pp}^{t_1,t_1'} k_1'^{\alpha} e^{Q_D} \Big[(2\pi) g_{qp}^{t_1',t_0} g_{qp}^{t_1,t_0} \delta_D(\vec{k}_1 - \vec{k}_1') \delta_D(\vec{k}_2 + \vec{k}_1')(G_1 + G_2) \\ &+ (2\pi)^3 g_{qp}^{t_1',t_0} \delta_D(\vec{k}_1 + \vec{k}_2)(G_3 + G_4 + G_5)\Big] \end{aligned} \tag{4.16a}$$

$$\begin{aligned} C_2(1'12) =& i\bar{\rho}^3 g_{pp}^{t_1,t_0} g_{pp}^{t_1,t_1'} k_1'^{\beta} e^{Q_D} \Big[(2\pi) g_{qp}^{t_1',t_0} g_{qp}^{t_1,t_0} \delta_D(\vec{k}_2 - \vec{k}_1') \delta_D(\vec{k}_1 + \vec{k}_1')(G_1' + G_2') \\ &+ (2\pi)^3 g_{qp}^{t_1',t_0} \delta_D(\vec{k}_1 + \vec{k}_2)(G_3' + G_4' + G_5')\Big] \end{aligned} \tag{4.16b}$$

with the functions

$$G_1 := \frac{\sigma_1^2}{3} k_2^{\beta} g_{qp}^{t_1,t_0} k_1'^2 \left(\vec{k}_2 \cdot \vec{k}_1'\right) P_\psi(k_1') \tag{4.17a}$$

$$G_2 := g_{qp}^{t_1',t_0} \int_k k^{\beta} \left(\vec{k} \cdot \vec{k}_1'\right)\left(\vec{k}_1' \cdot \left(\vec{k}_1' - \vec{k}\right)\right)\left(\vec{k}_2 \left(\vec{k}_1' - \vec{k}\right)\right) P_\psi(k) P_\psi(\vec{k}_1' - \vec{k}), \tag{4.17b}$$

$$G_3 := g_{qp}^{t_1',t_0} k_1^{\beta} \left(\vec{k}_1 \cdot \vec{k}_1'\right)\left(\vec{\Delta} \cdot \vec{k}_1'\right)\left(\vec{\Delta} \cdot \left(g_{qp}^{t_1,t_0} \vec{k}_1 - g_{qp}^{t_1',t_0} \vec{k}_1'\right)\right) P_\psi(k_1) P_\psi(\Delta), \tag{4.17c}$$

$$G_4 := k_1^{\beta} k_1'^2 \left(\vec{k}_1' \cdot \left(g_{qp}^{t_1,t_0} \vec{k}_1 - g_{qp}^{t_1',t_0} \vec{k}_1'\right)\right)\left(\vec{k}_1 \cdot \left(g_{qp}^{t_1,t_0} \vec{k}_1 - g_{qp}^{t_1',t_0} \vec{k}_1'\right)\right) P_\psi(k_1) P_\psi(k_1'), \tag{4.17d}$$

$$G_5 := -g_{qp}^{t_1,t_0} \left(\Delta^{\beta} \left(\vec{k}_1 \cdot \vec{k}_1'\right) + k_1'^{\beta} \left(\vec{k}_1 \cdot \Delta\right)\right)\left(\Delta \cdot \left(g_{qp}^{t_1,t_0} \vec{k}_1 - g_{qp}^{t_1',t_0} \vec{k}_1'\right)\right) P_\psi(k_1') P_\psi(\Delta), \tag{4.17e}$$

and

$$G_1' := \frac{\sigma_1^2}{3} k_1^{\alpha} g_{qp}^{t_1,t_0} k_1'^2 \left(\vec{k}_1 \cdot \vec{k}_1'\right) P_\psi(k_1') \tag{4.18a}$$

$$G_2' := g_{qp}^{t_1',t_0} \int_k k^{\alpha} \left(\vec{k} \cdot \vec{k}_1'\right)\left(\vec{k}_1' \cdot \left(\vec{k}_1' - \vec{k}\right)\right)\left(\vec{k}_1 \left(\vec{k}_1' - \vec{k}\right)\right) P_\psi(k) P_\psi(\vec{k}_1' - \vec{k}), \tag{4.18b}$$

$$G_3' := g_{qp}^{t_1',t_0} k_1^{\alpha} \left(\vec{k}_1 \cdot \vec{k}_1'\right)\left(\vec{\Delta} \cdot \vec{k}_1'\right)\left(\vec{\Delta} \cdot \left(g_{qp}^{t_1,t_0} \vec{k}_1 - g_{qp}^{t_1',t_0} \vec{k}_1'\right)\right) P_\psi(k_1) P_\psi(\Delta), \tag{4.18c}$$

$$G_4' := k_1^{\alpha} k_1'^2 \left(\vec{k}_1' \cdot \left(g_{qp}^{t_1,t_0} \vec{k}_1 - g_{qp}^{t_1',t_0} \vec{k}_1'\right)\right)\left(\vec{k}_1 \cdot \left(g_{qp}^{t_1,t_0} \vec{k}_1 - g_{qp}^{t_1',t_0} \vec{k}_1'\right)\right) P_\psi(k_1) P_\psi(k_1'), \tag{4.18d}$$

$$G_5' := -g_{qp}^{t_1,t_0} \left(\Delta^{\alpha} \left(\vec{k}_1 \cdot \vec{k}_1'\right) + k_1'^{\alpha} \left(\vec{k}_1 \cdot \Delta\right)\right)\left(\Delta \cdot \left(g_{qp}^{t_1,t_0} \vec{k}_1 - g_{qp}^{t_1',t_0} \vec{k}_1'\right)\right) P_\psi(k_1') P_\psi(\Delta). \tag{4.18e}$$

In order to get the full correction at first order of particle interactions we need to sum the diagrams and perform the convolution with the interaction potential. Then the full correction is given by

$$\delta^{(1)} \langle \Pi^{\alpha} \Pi^{\beta} \rangle(12) = i \int dt_1' \int_{k_1'} v(1') \left(B_{\text{total}}(1'12) + C_1(1'12) + C_2(1'12)\right). \tag{4.19}$$

The terms of the diagrams are all quadratic in the initial correlation function C_{pp}, therefore we include the damping as $e^{Q_D} \simeq (1 - Q_D)^{-1}$.
The momentum-density correlation tensor including linear corrections due to gravity is given by

$$\langle \Pi^{\alpha} \Pi^{\beta} \rangle(12) = \langle \Pi^{\alpha} \Pi^{\beta} \rangle^{(0)}(12) + \delta^{(1)} \langle \Pi^{\alpha} \Pi^{\beta} \rangle(12) \tag{4.20}$$

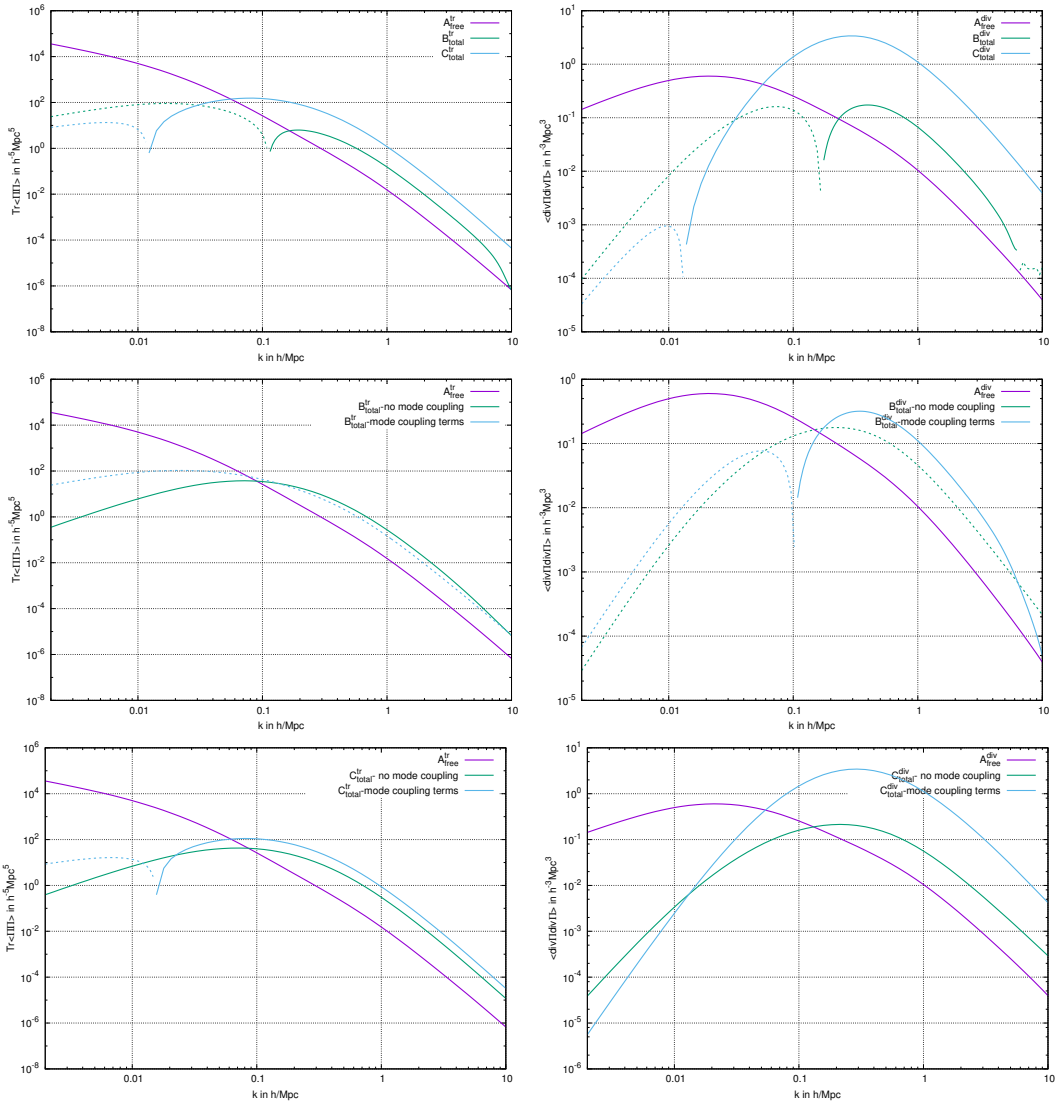

Figure 8: The left column shows the power-spectrum of the trace of the 2-point momentum-density correlator, while the right column shows the power-spectrum of the divergence of the momentum-density. The top panels show the complete expression from Section C.1, the center panels the contribution from diagrams with dashed circle segments, and the bottom panels the contribution from diagrams with solid circle segments. We also separated the terms that couple modes from those terms that do not.

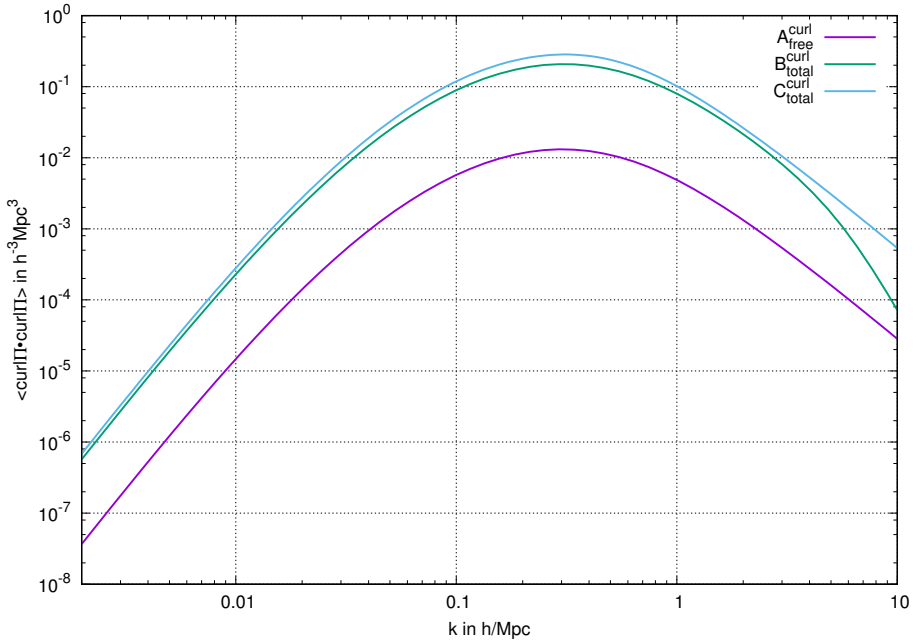

Figure 9: The power-spectrum of $\nabla \times \vec{\Pi}$. It is purely given by convolutions of density fluctuation power-spectra.

which we evaluate at $t_1 = t_2$ and wave-vectors $\vec{k}_1 = -\vec{k}_2$. We omit the functional dependence from now on. From the tensor we calculate the scalar quantities (4.2a)-(4.2c) for which we give explicit expressions in Section C.1. Here we show the the power-spectra for the trace, divergence and curl in the figures and check how large the contribution from the two types of diagrams are.
The Figure 8 shows the terms contributing to the scalar 2-point correlators of the momentum-density today. The left column shows the trace of the correlation tensor, while the right column shows the power-spectrum of the divergence of $\vec{\Pi}$. The top panels show the contributions from the free correlator and from the two types of diagrams shown in Figure 6 and 7. We notice that for a momentum-density correlation the deviation from the inertial momentum trajectories contributes more than the deviation from the particles' final position, i. e. $C_{total} > B_{total}$. The lower panels separate the mode-coupling terms in the corrections of the interaction from terms that are proportional to the velocity variance σ_1^2. The latter have a sub-dominant effect here. The dependence of the power-spectra on the wavenumber is proportional to k^{-1} for the trace and k for the divergence field for large scales. Based on the continuity equation (2.37) this behaviour is reasonable, since the density power-spectrum of the density fluctuations is proportional to k for large scales and $\vec{\Pi} = \rho_b(1+\delta)\vec{p}$, where ρ_b is the background. Therefore we expect the divergence field power-spectrum to behave like the density fluctuation power-spectrum on small scales, but on non-linear scales cross-correlations between δ and $\vec{p}$ become important and the divergence of $\vec{\Pi}$ behaves differently.
In Figure 9 we show the power-spectrum of $\nabla \times \vec{\Pi}$ today, which is completely given by convolutions of two density fluctuation power-spectra weighted by a kernel depending on the wave-vectors (cf. Section C.1). From a hydrodynamical point of view, the velocity is parallel to $\vec{k}$ at any order, as a consequence of the Helmholtz theorem, and therefore the first contributing term to this power-spectrum is the cross-correlation of δ and $\vec{p}$. We also notice from the plot that the most power arises from interactions. Again, the devia-

tion from the final particle positions is on small scales less relevant than the acceleration due to potential gradients.

4.2 FULL INITIAL MOMENTUM CORRELATIONS

We have shown in Chapter 3 that after the application of an arbitrary number of operators (3.2)-(3.4) it is possible to factorise the free generating functional $Z_0[\mathbf{L}, 0]$, which allows the inclusion of the full hierarchy of initial momentum correlations. A momentum-density correlator is calculated by partial derivatives of $Z_0[\mathbf{L}, 0]$ with respect to the momentum shift vectors according to (3.38). Here we repeat the calculation of the previous Section 4.1 using the result (3.26) for the factorised free generating functional.
The free 2-point correlation tensor is by the product rule a sum of four terms

$$\begin{aligned} F^{(0)\alpha\beta}_{\Pi_1\Pi_2}(12) =& i^2 V^{-2}(2\pi)^3\delta_D(\mathbf{L}_q)e^{Q_D(g^{t_1,t_0}_{pp})^2}\left[\left(\frac{\sigma_1^2}{3}\right)^2 L^\alpha_{p_1} L^\beta_{p_2} I_{21}\right. \\ &+\frac{\sigma_1^2}{3}\int_q e^{Q(q)+i\vec{k}_{21}\cdot\vec{q}}\left(L^\alpha_{p_1} M^\beta_2(q) + L^\beta_{p_2} M^\alpha_1(q)\right) \\ &\left.+\int_q e^{Q(q)+i\vec{k}_{21}\cdot\vec{q}}\left(N^{\alpha\beta}_{21}(q) + M^\alpha_1(q) M^\beta_2(q)\right)\right], \end{aligned} \tag{4.21}$$

where we used that only two particles are contributing and the functions $M^\alpha_a(q)$, $N^{\alpha\beta}_{ba}(q)$ defined in equation (3.47). For a synchronous 2-point function we can immediately write down the shift tensor

$$\mathbf{L}_q = -\vec{k}_1 \otimes (\vec{e}_1 - \vec{e}_2), \quad \mathbf{L}_p = -g^{t_1,t_0}_{qp}\vec{k}_1 \otimes (\vec{e}_1 - \vec{e}_2), \tag{4.22}$$

by the Dirac delta function and the auxiliary wave-vector $\vec{k}_{21} = \vec{L}_{q_2} = \vec{k}_1$. Then the free 2-point correlation tensor reduces to

$$\begin{aligned} F^{(0)\alpha\beta}_{\Pi_1\Pi_2}(12) =& V^{-2}(2\pi)^3\delta_D(\mathbf{L}_q)e^{Q_D(g^{t_1,t_0}_{pp})^2}\left[\left(\frac{\sigma_1^2}{3}\right)^2 (g^{t_1,t_0}_{qp})^2 k_1^\alpha k_1^\beta I_{21}\right. \\ &+\frac{2\sigma_1^2}{3}(g^{t_1,t_0}_{qp})^2 k_1^\alpha k_1^\beta \int_q e^{Q(q)+i\vec{k}_{21}\cdot\vec{q}} a_\parallel(q) \\ &+\int_q e^{Q(q)+i\vec{k}_{21}\cdot\vec{q}}\left(\pi^{\parallel\alpha\beta}_{21}(a_\parallel(q) - a_\perp(q)) + \delta^{\alpha\beta} a_\perp(q)\right) \\ &\left.-(g^{t_1,t_0}_{qp})^2 k_1^\alpha k_1^\beta \int_q e^{Q(q)+i\vec{k}_{21}\cdot\vec{q}} a^2_\parallel(q)\right]. \end{aligned} \tag{4.23}$$

The first term comes from the momentum auto-correlations multiplied by the power-spectrum of the density which emphasises the linear relation (2.37). The other terms depend on modified integrals over initial correlations. While for the density the generic integrals have an exponential dependence on the initial momentum correlations, the integrals for the momentum-density power-spectrum include projections parallel and perpendicular to $\vec{k}_1$. Thus, the generic factors must be modified by appropriate factors of the initial parallel and perpendicular correlations. From the above, we can already see that the free power-spectrum of the divergence can only depend on integrals over $a_\parallel$, while for the curl only integrals over $a_\perp$ will remain.
The first order corrections are calculated from the same diagrams as in Figure 6 and Figure 7 as before. For all diagrams we need to evaluate a correlator of two density

and two momentum-density fields with contributions of three particles, because the response field identifies two particles. Thus the difference to the free correlator here is that we include three shift vectors and a prefactor depending on the diagram, which we described in rule (iv)b. The delta distribution relates the shift vectors by $\vec{L}_{q_1} = -(\vec{L}_{q_2} + \vec{L}_{q_3})$ and ensures that $\vec{k}_1 = -\vec{k}_2$ as is true for the free correlator due to statistical homogeneity. The wave-vectors associated to the coordinate pairs $\vec{k}_{jk}$ are in this case

$$\vec{k}_{21} = \vec{L}_{q_2} + \vec{k}'_{32}, \quad \vec{k}_{31} = \vec{L}_{q_2} - \vec{k}'_{32}, \quad \vec{k}_{32} = \vec{k}'_{32}. \tag{4.24}$$

Therefore the diagrams correspond to terms of the form

$$D_1 = -\int dt'_1 \int_{k'_1} \nu(k'_1) S(\vec{k}'_1) F^{(0),\alpha\beta}_{\rho\rho\Pi_1\Pi_2}(-1'1'12) \tag{4.25}$$

with

$$\begin{aligned} F^{(0),\alpha\beta}_{\rho\rho\Pi_1\Pi_2}(-1'1'12) = i^2 V^{-3}(2\pi)^3 \delta_D(\mathbf{L}_q) e^{Q_D(g^{t_1,t_0}_{pp})^2} \int_{k'_{32}} \Bigg[\left(\frac{\sigma_1^2}{3}\right)^2 L^\alpha_{p_1} L^\beta_{p_2} \prod_{j>k\geqslant 1}^{3} I_{jk} \\ + \frac{\sigma_1^2}{3} \prod_{j>k\geqslant 1}^{3} \int_{q_{jk}} e^{Q(q_{jk}) + i\vec{k}_{jk}\cdot\vec{q}} \left(L^\alpha_{p_1} \left(\sum_{x>y\geqslant 1}^{3} M_2^\beta(q_{xy}) \right) + L^\beta_{p_2} \left(\sum_{x>y\geqslant 1}^{3} M_1^\alpha(q_{xy}) \right) \right) \\ + \prod_{j>k\geqslant 1}^{3} \int_{q_{jk}} e^{Q(q_{jk}) + i\vec{k}_{jk}\cdot\vec{q}} \left(\sum_{x>y\geqslant 1}^{3} N_{21}^{\alpha\beta}(q_{xy}) + \left(\sum_{x>y\geqslant 1}^{3} M_1^\alpha(q_{xy}) \right) \left(\sum_{u>v\geqslant 1}^{3} M_2^\beta(q_{uv}) \right) \right) \Bigg] \end{aligned} \tag{4.26}$$

In Section C.2 we show the explicit expressions for the free power-spectra of the trace, the divergence and the curl. We show the results for the three power-spectra today in Figure 10. The power-spectra depend on integrals over the initial correlation functions $a_\parallel$ and $a_\perp$ of equation (3.36). For both the trace and the divergence power-spectrum we find that the leading contribution on large scales comes from the integral over $a_\parallel$, which is the projection of initial momentum correlations parallel to the wave-vector. Based on our previous discussion at the end of the last chapter this is to be expected. On small scales cross-correlations between the density fluctuation and momentum become relevant and for the free power-spectrum only a residual remains. The curl power-spectrum depends only on the integral over $a_\perp$, meaning that initial correlations perpendicular to the wave-vector are enhanced over time. In the limit of small arguments of the exponential in (C.15), i. e. very large scales or short times, the integral vanishes exactly as pointed out by Bartelmann et al. [5]. That means that very early in time the momentum-density does not have any component perpendicular to $\vec{k}$ which is self-consistent with our assumption of an initial gradient field. This also proves that the curl power-spectrum is an effect of cross-correlations between the density fluctuations and the momenta.

The comparison between the free power-spectra involving the full hierarchy of initial momentum correlations with the free power-spectra of the previous Section which consider initial momentum correlations only up to quadratic order we see that the form on small scales $k > 1h/\text{Mpc}$ is strongly affected. If the hierarchy of initial correlations is truncated, interactions are needed to add power to those small scales. This shows that much of the power in the non-linear scales is set by the initial correlations and not by particle interactions.

We did not show first order corrections due to interactions, since the convolution over the auxiliary wave-vector $\vec{k}'_{32}$ makes the corrections (4.26) difficult to handle numerically. In the next Section we work out a way to estimate the effect of the gravitational force by use of the Born approximation and averaging over the freely evolved power-spectrum.

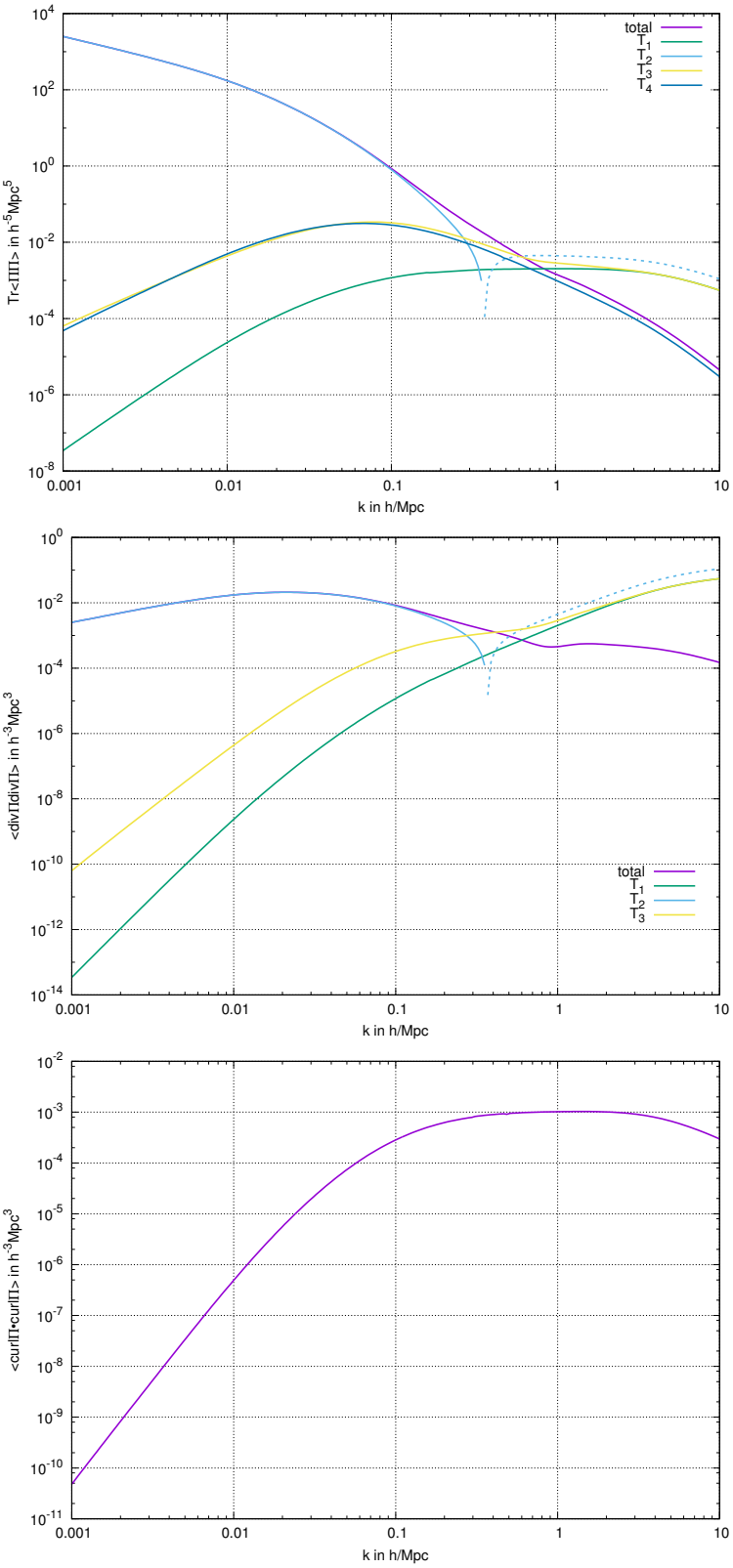

Figure 10: The free power-spectra for the trace, the divergence and the curl are shown. We show the total power-spectrum and the individual terms T_i of (C.13)-(C.15), where the terms are enumerated in the order that they are written in the equations. Negative contributions are represented by dashed lines.

4.3 BORN'S APPROXIMATION

The perturbative ansatz for particle interactions is problematic in practice. Although we have constructed a systematic way to calculate the corrections to free correlators at arbitrary order, the convolutions of the generic factors (and derivatives thereof) make the evaluation numerically challenging.
We suggested in Bartelmann et al. [4] to start from equation (2.8) and include the potential gradient in the classical solution $\mathbf{x}_{cl}(t)$ as an inhomogeneity. The goal of this Section is to review how the Born approximation can be employed to approximate the potential gradient and include the associated corrections in a 2-point correlator. In the end we will apply this to the momentum-density correlation tensor.
First, we apply two one-particle density operators with wave-vectors $\vec{k}_{1,2}$ to the generating functional and set the source field $\mathbf{J}$ to zero

$$Z[\mathbf{L}] = \int d\Gamma \exp\left(i\langle \mathbf{L}_q, \mathbf{q}\rangle + i\langle \mathbf{L}_p, \mathbf{p}\rangle - \mathbf{F}(t)\right), \tag{4.27}$$

with the shifts

$$\mathbf{L}_q = -\vec{k}_1 \otimes (\vec{e}_1 - \vec{e}_2), \quad \mathbf{L}_p = -g_{qp}^{t,t_0}\vec{k}_1 \otimes (\vec{e}_1 - \vec{e}_2), \tag{4.28}$$

since statistical homogeneity enforces $\vec{k}_1 = -\vec{k}_2$. We define the time-integrated interaction term

$$\mathbf{F}(t) := i\int_{t_0}^{t} dt' \langle \mathbf{L}_p(t'), \boldsymbol{\nabla}\mathbf{V}(t')\rangle. \tag{4.29}$$

To evaluate this integral we need to approximate the potential gradient. We express the force between two arbitrary particles 1 and 2 by its Fourier-transform

$$\nabla_1 V_2(t') = i\int_k \vec{k} v(k,t') e^{i\vec{k}\cdot(\vec{q}_1(t') - \vec{q}_2(t'))}, \tag{4.30}$$

with $v(k,t)$ being the one-particle potential in Fourier space. The positions of the particles are given in the Born approximation by

$$\vec{q}(t') = \vec{q} + g_{qp}^{t',t_0}\vec{p}, \tag{4.31}$$

where the phase-space coordinates without an argument denote initial values, i. e. the particles propagate according to their inertial motion.
Next, we calculate an effective force between the particles by averaging the phase-factor. The average is taken over the phase-space distribution of the particles evaluated at the shifts (4.28) corresponding to the density modes involved, and propagated according to their inertial motion. The average is

$$\langle e^{i\vec{k}\cdot(\vec{q}_1(t') - \vec{q}_2(t'))}\rangle = \int d\Gamma e^{i\langle \mathbf{L}_q, \mathbf{q}\rangle + i\langle \mathbf{L}_p, \mathbf{p}\rangle + i\vec{k}\cdot(\vec{q}_1(t') - \vec{q}_2(t'))}, \tag{4.32}$$

which is the free generating functional $Z_0[\mathbf{L}', 0]$ (3.26) at the shifts

$$\mathbf{L}'_q = -\vec{\kappa} \otimes (\vec{e}_1 - \vec{e}_2), \quad \mathbf{L}'_p = -g_{qp}^{t,t_0}\vec{\kappa} \otimes (\vec{e}_1 - \vec{e}_2) \tag{4.33}$$

with $\vec{\kappa} = \vec{k}_1 - \vec{k}$. It was shown in Bartelmann et al. [5] that this is

$$Z_0[\mathbf{L}', 0] = e^{Q_D(\kappa,t')}\left[(2\pi)^3\delta_D(\vec{\kappa}) + \mathcal{P}(\kappa,t')\right], \tag{4.34}$$

with the density fluctuation power-spectrum

$$\mathcal{P}(\kappa, t') = \int_q \left[e^{-(g_{qp}^{t',t_0})^2 \kappa^2 a_{\parallel}(q)} - 1 \right] e^{i\vec{\kappa}\cdot\vec{q}}. \tag{4.35}$$

The angular brackets in (4.34) are the generic factor I_{21} of equation (3.37). The last approximation that we will use is that for sufficiently small arguments of the exponential the function $\mathcal{P}(\kappa, t') \simeq (g_{qp}^{t',t_0})^2 P_\delta(\kappa)$ returns the linearly evolved density fluctuation power-spectrum. Then the force between two arbitrary particles is given by

$$\langle \vec{F}_1 \rangle (t') = i \int_k \vec{k} v(k, t') \left[(2\pi)^3 \delta_D(\vec{\kappa}) + \bar{P}_\delta(\kappa, t') \right], \tag{4.36}$$

where $\bar{P}_\delta(\kappa, t')$ is the damped linearly evolved δ power-spectrum, with the damping factor $e^{Q_D(\kappa,t')}$. For any 2-point function we can use that after the averaging process only the forces on particle 1 and 2 remain, which by Newton's third axiom are opposing $\nabla_1 V_2 = -\nabla_2 V_1$. Thus, the time-integrated interaction term is

$$\mathbf{F}(t') = 2 \int_{t_0}^{t} dt' g_{qp}(t, t') \left[k_1^2 v(k_1, t') + \int_k \left(\vec{k}_1 \cdot \vec{k} \right) v(k, t') \bar{P}_\delta(\kappa, t') \right] \tag{4.37}$$

The first term is purely due to Poisson sampling from a statistically homogeneous field. Therefore this term cannot contribute to any directed quantity, such as the force between particles, and we ignore it in calculations of power-spectra. The second term quantifies the excess from a Poisson sampling due to correlations between particles. This will eventually lead to the enhancement of structures by interaction.
Lastly, we need to specify the one-particle potential $v(k, t')$. The force acting on a particle depends on the choice of the retarded Green's function, which in cosmological applications we choose to be either the Zel'dovich or improved Zel'dovich approximation of Section 2.2. For both trajectories we can write this force as

$$\vec{a} = f(t)\vec{p} - \frac{\nabla v}{g(t)}, \tag{4.38}$$

with $g(t)$ from (2.61). The function $f(t)$ is given by

$$f(t) = \begin{cases} -\frac{\dot{g}}{g} & \text{Zel'dovich} \\ -\frac{\dot{g}}{g}\left(1 - g^{-1}\right) & \text{improved Zel'dovich} \end{cases} \tag{4.39}$$

depending on the chosen Green's function. As Bartelmann et al. [4] point out, the spatial correlations grow like $(g_{qp}^{t,t_0})^2$ while cross-correlations of the velocity and position grow like $g_{pp}^{t,t_0} g_{qp}^{t,t_0}$. Thus, the growth of the velocity dependent force is lowered by a factor of $g_{pp}^{t,t_0}/g_{qp}^{t,t_0}$ compared to the potential-gradient. But the dependence on the wave-vector $\vec{k}$ is the same for both terms $i\frac{\vec{k}}{k^2} P_\delta(k)$ although for different reasons. For the velocity dependent force it is due to the velocity potential gradient, while it is the gradient of the interaction potential for the other. Thus, we can write for the potential in (4.36)

$$v(k, t') = (A_1(t') + A_2(t'))k^{-2}, \tag{4.40}$$

where the time-dependent amplitudes are

$$A_1(t') := f(t) \frac{g_{pp}^{t,t_0}}{g_{qp}^{t,t_0}}, \quad A_2(t') := -\frac{3a}{2g}. \tag{4.41}$$

We have shown in Bartelmann et al. [4] that particle interactions calculated by (4.37) partially compensate the free-streaming of the particles, which is an inevitable consequence of the initial momentum fluctuations in the particle ensemble. On scales $k < 10h/\mathrm{Mpc}$ our results (4.27) reproduce numerical results with an accuracy of $\sim 15\%$. The low discrepancy encourages the use of the Born approximation also in other applications, such as the calculation of the momentum-density correlation tensor or higher order correlations.
We aim at the 2-point correlation tensor of momentum-densities including particle interactions in the Born approximation. The application of two $\vec{\Pi}$-operators returns

$$\Pi_1^\alpha(1)\Pi_2^\beta(2)Z[\mathbf{J}]\Big|_{\mathbf{J}=0} = \int d\Gamma \vec{p}_1^\alpha(t_1)\vec{p}_2^\beta(t_2)\exp\left(i\langle \mathbf{L}_q, \mathbf{q}\rangle + i\langle \mathbf{L}_q, \mathbf{q}\rangle - \mathbf{F}(t)\right), \tag{4.42}$$

with the particle momenta given by

$$p_1^\alpha(t_1) = g_{pp}^{t_1,t_0} p_1^\alpha - \int_{t_0}^{t_1} dt' g_{pp}^{t_1,t'} F_1^\alpha(t'), \tag{4.43}$$

and analogously for the second particle.

4.3.1 *First/Naive Approximation*

In collaboration with Christian Sorgenfrei as part of his Bachelor thesis project we employed the averaged forces between particles given in (4.36) and (4.37). We use the abbreviation

$$\vec{f}_1 := \int_{t_0}^{t_1} dt' g_{pp}^{t_1,t'} \langle \vec{F}_1\rangle(t') \tag{4.44}$$

in order to keep notations shorter. Under this assumption we can write down the synchronous 2-point momentum-density correlation tensor as

$$\begin{aligned}\left\langle \Pi_1^\alpha \Pi_2^\beta \right\rangle = e^{Q_D - \mathbf{F}} \Bigg[&\left((2\pi)^3\delta_D(\vec{k}_1) + \mathcal{P}(k_1)\right)\left(\left(g_{qp}^{t,0} g_{pp}^{t,0}\frac{\sigma_1^2}{3}\right)^2 k_1^\alpha k_1^\beta \right.\\ &\left. - i g_{qp}^{t,0} g_{pp}^{t,0}\frac{\sigma_1^2}{3}\left(f_1^\alpha k_1^\beta + k_1^\alpha f_1^\beta\right) - f_1^\alpha f_1^\beta\right)\\ + &\left[\int_q w(q) a_\parallel(q)\right]\left(\frac{2\sigma_1^2}{3}(g_{qp}^{t,0}g_{pp}^{t,0})^2 k_1^\alpha k_1^\beta - i g_{qp}^{t,0} g_{pp}^{t,0}\left(f_1^\alpha k_1^\beta + k_1^\alpha f_1^\beta\right)\right)\\ -(g_{pp}^{t,0})^2 &\int_q w(q)\left[\pi_{21}^{\parallel\alpha\beta}(a_\parallel(q) - a_\perp(q)) + \delta^{\alpha\beta} a_\perp(q) - a_\parallel^2(q)(g_{qp}^{t,0})^2 k_1^\alpha k_1^\beta\right]\Bigg],\end{aligned} \tag{4.45}$$

where we renamed $t_1 = t$ and introduced the function

$$w(q) := \exp\left(Q(q) + i\vec{k}\cdot\vec{q}\right). \tag{4.46}$$

We give expressions for the trace, divergence and curl power-spectrum in Section C.3.1 and note that those expressions depend on the projections of $\vec{f}_1$ parallel and perpendicular to the wave-vector $\vec{k}_1$. Working out the scalar products with the use of (4.36) and (4.44) we find

$$\vec{k}_1\cdot\vec{f}_1 = i\int_{t_0}^{t} dt' g_{pp}^{t,t'}\left[k_1^2 v(k_1,t') + \int_k \left(\vec{k}_1\cdot\vec{k}\right) v(k,t')\bar{P}_\delta(\kappa,t')\right], \tag{4.47}$$

$$\vec{f}_1\cdot\vec{f}_1 = \frac{\left(\vec{k}_1\cdot\vec{f}_1\right)}{k_1^2}, \tag{4.48}$$

where $\vec{\kappa} = \vec{k}_1 - \vec{k}$. In other words, the perpendicular projection of $\vec{f}_1$ with respect to $\vec{k}_1$ is exactly zero. Therefore, the only effect the averaged force $\langle \vec{F}_1 \rangle(t)$ has on the power-spectrum of the $\vec{\Pi}$-component perpendicular to $\vec{k}_1$ is the compensation of the damping as we saw for the density fluctuation power-spectrum. This is a direct consequence of approximating the momentum trajectory (4.43) with the ensemble-averaged force. Therefore, we deliberately ignored any cross-correlations between the force on one particle and the force acting on the other, and correlations between the forces.
We show the changes of the power-spectra due to the Born approximation evaluated today in Figure 11. The Born approximated force enters in two ways into these plots: (i) it counters the damping factor due to free-streaming on large scales, while momentum-diffusion dominates on small scales, (ii) it adds terms contributing deviations from the free particle momenta. On the large scales we notice no difference between the free results of the previous Section 4.2 and the corrected results discussed here. Power on the small scales is enhanced by as much as two orders of magnitude on $k = 10h/\mathrm{Mpc}$. Since the curl power-spectrum does not contain any additive contributions from the Born approximated force, we can see the same effect as for the density power-spectrum in Bartelmann et al. [4]. The exponential term $\exp(-\mathbf{F})$ counteracts the free-streaming of the particles and results in an enhancement of power on scales $1h/\mathrm{Mpc} < k < 10h/\mathrm{Mpc}$. We will return to this result when we discuss the kSZ effect in Section 4.4. For the trace and the divergence power-spectra we notice that the first additive term, which is proportional to the density fluctuation power-spectrum reduces structure on all scales. This correction can be split in two terms: the first is proportional to the scalar product of the force with the free-streaming motion of the particles, and the second is the scalar product of the force on particle one and on particle two. As the factors act in opposite directions this correction can only remove power. The second correction is proportional to $a_{\parallel}(q)$ and is the product of the ordered/correlated motion of the particle multiplied by the force. This term enhances the power of the momentum-density field on all scales. On the smallest scales the two additive terms are of the same magnitude and only the effect of $\exp(-\mathbf{F})$ remains, which enhances the power on the small scales as for the curl or the density fluctuation power-spectrum. The dependence of the trace and the divergence spectrum is flatter than for the free result of the previous Section 4.2.

4.3.2 *Revised Approximation*

We evaluate the product of the two momentum trajectories in (4.42) and find four terms in total

$$\begin{aligned} p_1^\alpha p_2^\beta = {} & (g_{pp}^{t,0})^2 {p_1}^\alpha {p_2}^\beta + i g_{pp}^{t,0} {p_2}^\beta \int_{t'} g_{pp}^{t,t'} \nabla_1^\alpha V_2(t') \\ & - i g_{pp}^{t,0} {p_1}^\alpha \int_{t'} g_{pp}^{t,t'} \nabla_1^\beta V_2(t') - \int_{t',t''} g_{pp}^{t,t'} g_{pp}^{t,t''} \nabla_1^\alpha V_2(t') \nabla_1^\beta V_2(t'') \end{aligned} \tag{4.49}$$

where we used that $\nabla_1 V_2 = -\nabla_2 V_1$ and only the forces between the two particles will remain after integration over the phase-space distribution. The first term corresponds to the correlator of free momenta. The second and third terms correspond to the correlation between the free momentum of one and the force acting on the other particle. The fourth term is the correlation between the forces on the two particles.

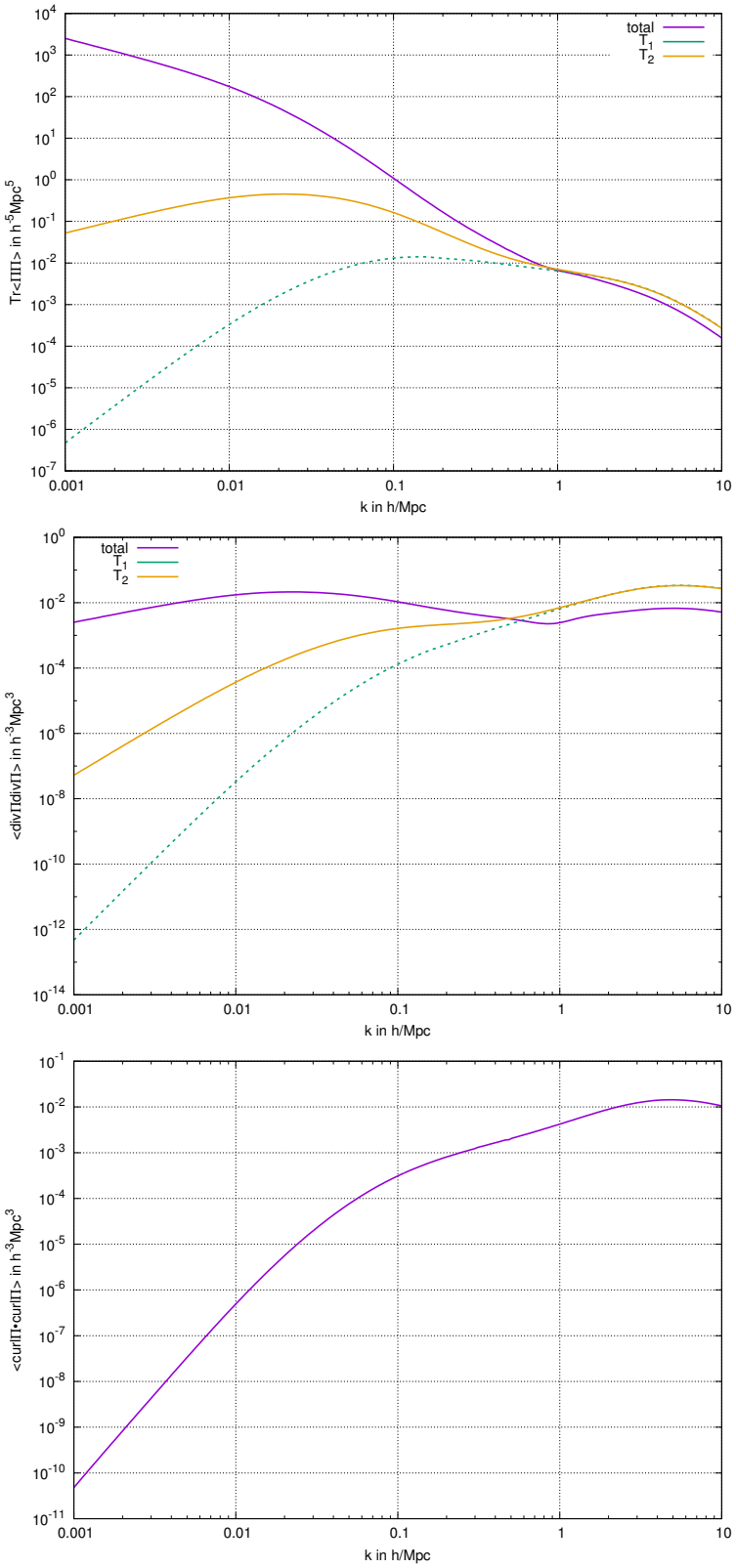

Figure 11: The power-spectra for the trace, the divergence and the curl including corrections due to gravitational interactions evaluated in the Born approximation are shown. We show the total power-spectrum and the corrections T_i due to the gravitational force given by (C.17)-(C.19). The terms are enumerated in the order that they are written in the equations and summarise terms proportional to the same integral over q. Negative contributions are represented by dashed lines.

We wrote down the first term in Section 4.2 and after substituting the momentum by a partial derivative with respect to the shift the second term is

$$T_2 = -g_{pp}^{t,0}\partial_{L_{p_2}}^{\beta}\int d\mathbf{\Gamma}\int dt'\int_k g_{pp}^{t,t'}k^{\alpha}\nu(k,t')\times \\ \times\exp\left(i\langle\mathbf{L}_q,\mathbf{q}\rangle+i\langle\mathbf{L}_p,\mathbf{p}\rangle-\mathbf{F}(t)+i\vec{k}\cdot(\vec{q}_1(t')-\vec{q}_2(t'))\right) \tag{4.50}$$

$$= -g_{pp}^{t,0}\partial_{L_{p_2}}^{\beta}\int d\mathbf{\Gamma}\int dt'\int_k g_{pp}^{t,t'}k^{\alpha}\nu(k,t')\exp\left(i\langle\mathbf{L}'_q,\mathbf{q}\rangle+i\langle\mathbf{L}'_p,\mathbf{p}\rangle-\mathbf{F}(t)\right) \tag{4.51}$$

with the new shifts

$$\mathbf{L}'_q = -\vec{\kappa}\otimes(\vec{e}_1-\vec{e}_2),\quad \mathbf{L}'_p = -(g_{qp}^{t,t_0}\vec{k}_1 - g_{qp}^{t',t_0}\vec{k})\otimes(\vec{e}_1-\vec{e}_2),\quad \hat{\pi}_{21}^{\parallel} = \frac{\vec{\kappa}\otimes\vec{\kappa}}{\kappa^2}, \tag{4.52}$$

with $\vec{\kappa} = \vec{k}_1 - \vec{k}$. Equivalently we can write down the third term.
The fourth term is readily obtained by substituting the Fourier-transforms of the potential gradients

$$T_4 = -\int d\mathbf{\Gamma}\int dt'\int dt''\int_k\int_{k'} g_{pp}^{t,t'}\nu(k,t')g_{pp}^{t,t''}\nu(k',t'')k^{\alpha}k'^{\beta}\times \\ \times\exp\left(i\langle\mathbf{L}'_q,\mathbf{q}\rangle+i\langle\mathbf{L}'_p,\mathbf{p}\rangle-\mathbf{F}(t)\right), \tag{4.53}$$

with the shifts and projector

$$\mathbf{L}'_q = -\vec{\kappa}'\otimes(\vec{e}_1-\vec{e}_2),\quad \mathbf{L}'_p = -(g_{qp}^{t,0}\vec{k}_1 + g_{qp}^{t',0}\vec{k} + g_{qp}^{t'',0}\vec{k}')\otimes(\vec{e}_1-\vec{e}_2), \tag{4.54}$$

$$\hat{\pi}_{21}^{\parallel} = \frac{\vec{\kappa}'\otimes\vec{\kappa}'}{\kappa'^2}, \tag{4.55}$$

and $\vec{\kappa}' = \vec{k}_1 - \vec{k} - \vec{k}'$.

4.4 APPLICATION: KINETIC SUNYAEV-ZEL'DOVICH EFFECT

4.4.1 *Sunyaev-Zeldovich Effect*

The earliest electromagnetic signal that we receive from the Universe is the CMB radiation, which was released at the time of hydrogen recombination. At that time the temperature of the Universe was low enough for electrons and protons to form neutral hydrogen atoms. The removal of free electrons raised the mean free path of photons in the Universe and photons were less likely to scatter off electrons. The time of CMB release is therefore also referred to as the surface of last scattering.
The radiation field is highly isotropic but small anisotropies are present. The mean temperature of the photons today is $T = 2.7255\text{K}$ with anisotropies of the order $\delta T/T \sim 10^{-5}$ (Planck Collaboration et al. [32]). These anisotropies are either primary, i. e. primordial fluctuations seeded during inflation, or secondary, i. e. caused by interactions of photons along their journey from the last scattering surface to the observer.
One example for secondary anisotropies is the Sunyaev-Zel'dovich (SZ) effect (Zeldovich and Sunyaev [36]). As astrophysical objects such as stars formed in the Universe, their radiation reionised the intergalactic medium, thus providing free electrons that could scatter with photons. In fact, the Sunyaev-Zel'dovich effect is the result of inverse Compton scattering off free electrons in the reionised Universe. The scatterings induce a temperature anisotropy by inhomogeneities in the motion of the electrons. We can distinguish the thermal and the kinetic SZ effects, tSZ and the kSZ, respectively. The tSZ is caused by

the random motion of electrons in a hot plasma, while for the kSZ the electrons move with the bulk of structures. The temperature fluctuation induced by bulk motion is given by

$$\frac{\delta T}{T}(\hat{\gamma}) = \int e^{-\tau} \sigma_T n_e \vec{v} \cdot \hat{\gamma} dl, \tag{4.56}$$

where $\hat{\gamma}$ is the unit vector in the line-of-sight direction, n_e is the number density of free electrons, σ_T is the Thomson cross section, τ is the optical depth and $\vec{v}$ the peculiar velocity of structures. The integral is taken along the line-of-sight from the time of emission until today. The electron number density and the peculiar velocity may be combined to the momentum-density that we investigated in Chapter 3. Of course, we have to keep in mind that the electron number density scales with the ionisation fraction χ and the fraction of baryons Ω_b in the Universe.
The 2-dimensional angular power-spectrum of the kSZ temperature fluctuations is obtained from the 3-dimensional power-spectrum of the momentum-density by an integration along the line-of-sight. We note that in this radial projection the contributions from the longitudinal component $\vec{\Pi} \| \vec{k}$ vanish due to cancellations of the contributions from wave peaks and troughs (cf. Vishniac [34], Jaffe and Kamionkowski [17]). Therefore, only the transverse component contributes to the kSZ power-spectrum. In the small-angle approximation the angular power-spectrum is given by a Limber equation (cf. Limber [18])

$$C_l = \frac{\sigma_T^2 \bar{n}_e^2}{H_0^2} \int \frac{dx}{x^2 a^4} e^{-2\tau} P_{\Pi_\perp}\left(\frac{l}{x}, t\right), \tag{4.57}$$

where l is the multipole, $\bar{n}_e$ is the mean electron density and $P_{\Pi_\perp}$ is the power-spectrum of $\vec{\Pi}$ perpendicular to the wave-vector $\vec{k}$ (cf. Ma and Fry [19]). The integral is to be taken over comoving distance $dx = c da/(a^2 H(a))$ from the source to the observer. The small-angle approximation is valid as temperature fluctuations are generated on scales $l \gtrsim 1000$ (cf. Ostriker and Vishniac [25], Jaffe and Kamionkowski [17]).
The observed signal will also depend on the reionisation history. This is encoded in the optical depth τ as well as the ionisation fraction χ. Inhomogeneities during the epoch of reionisation are expected to modulate the kSZ power-spectrum. Park et al. [26] point out that this even boosts the power compared to homogeneous reionisation. In our discussion we focus on the effect of the momentum-density power-spectrum and compare our results for the 3-dimensional power-spectrum to those of other works.

4.4.2 *Results*

The kSZ power-spectrum depends on the transverse component of the momentum-density, i. e. the perpendicular projection of $\vec{\Pi}$ on the wave-vector $\vec{k}$. Comparing to equation (4.2c) we realise that the power-spectrum of the perpendicular component is given by the power-spectrum of the curl-field divided by the wave-number k squared.
For an analytical comparison with previous studies, we focus on the linear regime of perturbations. In Section A.2 we showed that the the velocity components perpendicular to $\vec{k}$ decay inversely proportional to the scale factor at linear order of hydrodynamics. Thus, it is common practice to assume an irrotational velocity field initially. Then, by Helmholtz theorem the velocity field is parallel to $\vec{k}$ at any order and the lowest order contribution to the perpendicular component of the momentum-density comes from

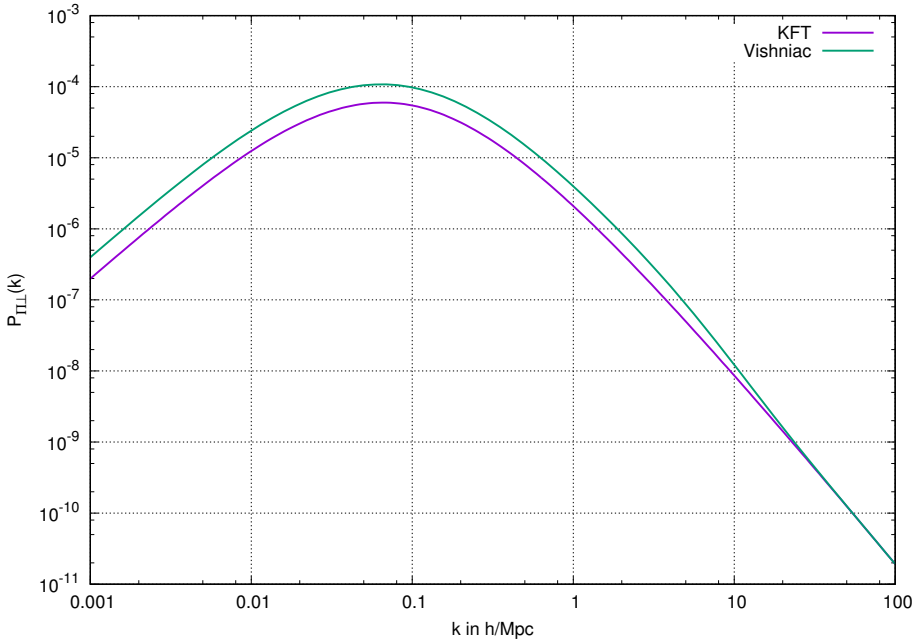

Figure 12: We show the scale dependence of the power-spectrum of the transverse component of $P_{\Pi_\perp}$ from linear theory (4.58), i. e. the result by Vishniac [34], and from KFT (4.59). In the limit of small wavenumbers the results differ by a factor of two, while they are the same for very large wavenumbers.

the cross-correlation of density fluctuations and the momentum. Assuming that both quantities evolve linearly, Vishniac [34] arrived at

$$P^{\rm lin}_{\vec{\Pi}_\perp}(k,t) = \dot{a}^2 f^2 \int_{k'} P_\delta(k',t) P_\delta(\Delta,t) \frac{k^2(k-2k'\mu)^2(1-\mu^2)}{k'^2\Delta^4}, \tag{4.58}$$

where $\Delta = \sqrt{k^2+k'^2-2kk'\mu}$ and μ is the angle cosine between the wave-vectors $\vec{k}$ and $\vec{k}'$. We need to compare this result with our own (C.10). After evaluation of the scalar products and recovering the correct time conversion we arrive at

$$\begin{aligned} P^{\rm KFT}_{\vec{\Pi}_\perp}(k,t) =& \dot{a}^2 f^2 D_+^2 (g_{pp}^{t,t_0})^2 (g_{qp}^{t,t_0})^2 e^{Q_D} \times \\ & \times \int_{k'} P_\delta(k') P_\delta(\Delta) \frac{k^2(k-k'\mu)(k-2k'\mu)(1-\mu^2)}{k'^2\Delta^4}, \end{aligned} \tag{4.59}$$

with the same definitions and after recovering conversion factors due to the transformation of the time coordinate in Section 2.2. We notice that using the Zel'dovich approximation the propagators $g_{qp}^{t,t_0} = D_+$ and $g_{pp}^{t,t_0} = 1$ reproduce the same time-dependence as the Vishniac power-spectrum. The damping is close to unity on linear scales. The kernel of the power-spectrum is different in the Vishniac case $\propto (k-2k'\mu)^2$ and $\propto (k-k'\mu)(k-2k'\mu)$ for KFT. We used for our calculations only the free contributions to the power-spectrum and truncated the dependence on the initial momentum correlations at quadratic order. It is not clear, how the difference in the kernels comes about. We evaluate both integrals numerically and show the results in Figure 12. In the limit $k \to 0$ both power-spectra scale as the wavenumber k^2, which is to be expected due to momentum conservation (Mercolli and Pajer [24]). On the largest scales, where we expect agreement of both calculations, the predictions are off by a factor of two. This

is a direct consequence of the difference in the kernels. We believe that this problem cannot be resolved by truncating the Taylor series in initial momentum correlations at higher orders, since this would involve terms that are cubic in the power-spectrum. We observed previously in Section 4.1 that the contribution from interactions is larger than from the free motion and has the same dependence on k. That suggests that we might not compare the same quantities here, since corrections from interactions at higher orders lead to the same dependence on initial power-spectra.
Park et al. [27] have recently studied the non-linear kSZ and focus on the calculation of the 3-dimensional power-spectrum of the transverse momentum-density component. They point out that in the fluid approach this power-spectrum is a 4-point function which can be split according to Wick's theorem into products of disconnected 2-point functions and the connected 4-point term. The connected term was ignored in all previous studies. We have compared our results of Section 4.3.1 with their results. Their figure Fig. 1 shows simulation results for the power-spectrum of the curl of $\vec{\Pi}$ evaluated today. Comparing the position of bumps and the amplitude with our Figure 11 we find very good agreement. We can also compare to their analytical results in their Fig. 3, where they have included the connected term, and find the same level of agreement. At this point we may note that we arrive at the same result with less effort than in Standard Perturbation Theory (SPT), since our calculation involves the calculation of a 2-point function of the momentum-density from the factorised free generating functional and the inclusion of the Born approximated force, while the SPT calculation involves solving complicated loop integrals (cf. the Appendix of Park et al. [27]).

4.5 COMPARISON WITH MILLENNIUM-XXL

We have planned a comparison of our analytical calculations with simulation data. We have access to data from the Millennium-XXL simulation (Angulo et al. [1]) and had help from Dr. Daniele Sorini for retrieving the power-spectra from the snapshots. The Millennium-XXL simulation contains only dark matter and is an N-body simulation with cosmological parameters $\Omega_{m0} = 0.25$, $\Omega_{\Lambda 0} = 0.75$, $h = 0.73$, the normalisation of the power-spectrum today is fixed by $\sigma_8 = 0.9$, and the spectral index $n = 1$. The boxsize is 3Gpc/h and the particle mass is $6.17 \times 10^9 h^{-1}$ solar masses. The power-spectra at $z = 0$ provided by Dr. Daniele Sorini's codes are shown in Figure 13. We compare this figure with our previous results Figure 8-11. Firstly we notice that the dependence on the wavenumber for the trace and divergence spectra are similar although the curves seem shifted to smaller values of k. Secondly, the curl spectrum is in Figure 13 is very close to the divergence spectrum. We do not expect this behaviour, neither from SPT and simulations (cf. Vishniac [34], Park et al. [27]) nor from KFT. We thus believe that something went wrong in the evaluation of the snapshots, since it may be more difficult to extract a non-linear effect such as this which stems from cross-correlations of the density fluctuations and momentum.

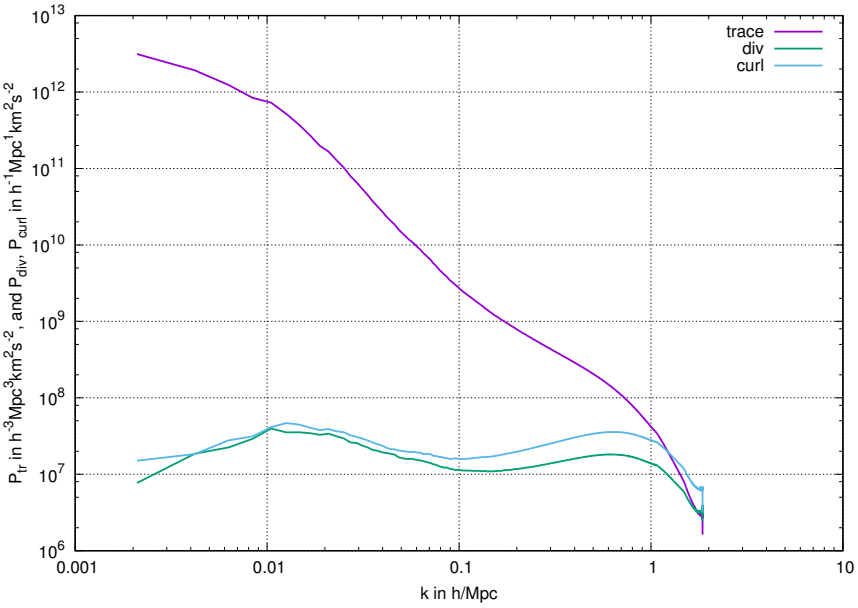

Figure 13: The power-spectra were calculated from the Millennium-XXL simulation with the aid of Dr. Daniele Sorini. Since our comparisons of the curl spectrum divided by k^2 with Vishniac [34] and Park et al. [27] worked out very well, we expect that at least for the curl spectrum the evaluation of the Millennium-XXL snapshots is flawed.

5

INCLUSION OF FUZZY DARK MATTER IN KFT

So far we have treated dark matter as composed of classical microscopic particles that have low initial velocity dispersion and interact gravitationally only. These are the characteristics of CDM. Although CDM models are very successful in explaining the formation of cosmic structure, there are a few conflicts with observations on small-scales, namely the cusp/core problem (e. g. de Blok [37]) and the missing satellites problem (e. g. Bullock [11]). Simulations suggest cuspy dark matter halo density profiles, while observations of galaxy rotation curves favor flat density profiles, and the abundance of low mass halos in simulations is much larger than what is inferred from observations around the Milky Way. Possible solutions to these problems may lie in the currently imperfect treatment of the baryonic gas in simulations (Brooks et al. [10]) or in the nature of dark matter. Here we focus on the second possibility.
While the particle nature of dark matter is unknown, there exists a vast range of particle candidates. Mass bounds for these model particles are provided by observations of the large-scale structure. Warm Dark Matter (WDM) models assume thermally produced particles that suppress small-scale structure due to their velocity dispersion, i. e. the free-streaming out of potential wells. The mass bound for those models is $m_W \geqslant$ few keV$/c^2$. Another suite of models, usually referred to as FDM (Hu, Barkana, and Gruzinov [16]), propose an extremely light non-thermally produced scalar-field particle whose de-Broglie wavelength is relevant on cosmological scales. The most popular class among these models proposes Ultra-Light Axions (ULAs). The mass bound on such particles is $m_a \geqslant 10^{-23}$eV$/c^2$. A recent review is given by Marsh [22].
Here we discuss models of FDM. Hu, Barkana, and Gruzinov [16] point out that the occupation numbers in galactic halos are so large that the dark matter behaves as a classical field if it is composed of ultra-light scalar particles. Then dark matter behaves like a self-gravitating Bose-Einstein Condensate (BEC) with (quartic) self-interactions. In view of structure formation, length scales are much smaller than the horizon and we can work in the Newtonian limit. Then the classical field is described by the Gross-Pitaevskii-Poisson system (Böhmer and Harko [9], and Chavanis [12]). Using the Madelung [20] form of the wave-function the Gross-Pitaevskii (or non-linear Schrödinger) equation turns into a set of hydrodynamic equations, namely a continuity equation for the probability density and an Euler equation with an isotropic pressure due to self-interactions and an anisotropic force due to a quantum potential that stems from Heisenberg's uncertainty principle. On large scales the effects of self-interaction and the quantum potential are irrelevant and FDM behaves like CDM. But on small scales the quantum effects can stabilise halos against gravitational collapse, thereby alleviating small-scale problems of CDM.

5.1 FUZZY DARK MATTER

5.1.1 *Hydrodynamical Treatment*

We assume that dark matter is composed of an extremely light boson, whose de-Broglie wavelength is relevant on cosmological scales. The production of this boson is non-thermal and for ULA due to spontaneous breaking of the Peccei-Quinn symmetry (Peccei and Quinn [28]). Due to the small mass of the boson the occupation numbers must be large and the dynamics are given by the classical field equations of a condensate. As

Marsh [22] pointed out, it is a separate question whether axions actually form a BEC in a cosmological context. For our discussion we assume condensation only to the extent that a classical field captures the dynamics.
For a self-gravitating light bosonic field φ with (quartic) self-interaction the dynamics are given by the Gross-Pitaevskii-Poisson system (Gross [15], Pitaevskii [31])

$$i\hbar\partial_t\varphi = \left(-\frac{\hbar}{2m_a}\nabla^2 + m_a\Phi + gNm_a|\varphi|^2\right)\varphi, \tag{5.1}$$

$$\nabla^2\Phi = 4\pi GNm_a|\varphi|^2, \tag{5.2}$$

with mass m_a of the boson, the gravitational potential Φ and the coupling constant g for the self-interaction. The de-Broglie wavelength for an ULA is

$$\frac{\lambda}{2\pi} = \frac{\hbar}{m_a v} = 1.92\left(\frac{10^{-22}eV/c^2}{m_a}\right)\left(\frac{10km/s}{v}\right)kpc, \tag{5.3}$$

for a typical masses and velocities. The equations (5.1) and (5.2) are valid on sub-horizon but super-Compton scales ($H < k < \frac{\hbar}{m_a c}$). By means of the Madelung [20] transformation of the wave-function

$$\varphi(\vec{r},t) = A(\vec{r},t)\exp\left(i\frac{B(\vec{r},t)}{\hbar}\right), \tag{5.4}$$

and the identifications

$$\rho = Nm_a|\varphi|^2, \quad \vec{u} = \frac{1}{m_a}\nabla B \tag{5.5}$$

for the density and velocity fields we can identify the imaginary and real parts of (5.1) as the continuity and Euler equations of a fluid,

$$\partial_t\rho + \nabla\cdot(\rho\vec{u}) = 0, \tag{5.6}$$

$$\partial_t\vec{u} + (\vec{u}\cdot\nabla)\vec{u} = -\nabla\Phi + \nabla\left(\frac{\hbar^2}{2m_a^2}\frac{\nabla^2\sqrt{\rho}}{\sqrt{\rho}}\right) - g\nabla\rho, \tag{5.7}$$

where we used that the velocity field is irrotational and the vector identity

$$\nabla(\vec{a}\cdot\vec{b}) = (\vec{a}\cdot\nabla)\vec{b} + \left(\vec{b}\cdot\nabla\right)\vec{a} + \vec{a}\times\left(\nabla\times\vec{b}\right) + \vec{b}\times(\nabla\times\vec{a}) \tag{5.8}$$

The continuity equation is to be interpreted as a probability conservation equation. The last term in Euler's equation is solely due to the quartic self-interaction and can be interpreted as an isotropic pressure with a barotropic equation of state (cf. Chavanis [12]).
Apart from self-interactions another interaction enters the Euler equation (5.7) due to the potential

$$V_Q = \frac{\hbar}{2m_a^2}\frac{\nabla^2\sqrt{\rho}}{\sqrt{\rho}} = \frac{\hbar^2}{4m_a^2\rho}\left[\nabla^2\rho - \frac{\nabla\rho\cdot\nabla\rho}{2\rho}\right], \tag{5.9}$$

which in cosmology is often called "quantum pressure". Since the origin of this term is purely connected to Heisenberg's uncertainty principle and has no links to thermodynamics, we will refer to it as quantum potential (Bohm [8]).
Following our discussion of linear structure formation in Section A.2 we can transform

the system of equations (5.2), (5.6) and (5.7) into a single equation for the Fourier modes of the density contrast

$$\ddot{\delta} + 2H\dot{\delta} + \left(-4\pi G\rho_b + \frac{\hbar^2 k^4}{4m_a^2 a^4} + \frac{g\rho_b k^2}{a^2}\right)\delta = 0. \tag{5.10}$$

Here we used the usual definitions for the density contrast $\rho = \rho_b(1+\delta)$, the Hubble function $H = \dot{a}/a$ and used the background solutions (A.22). Since self-interactions are model-dependent and sub-dominant to gravity on linear and non-relativistic scales (Marsh [21]), we ignoring self-interactions ($g = 0$) and do so for the remainder of this chapter, we can define a quantum Jeans scale

$$k_Q = (16\pi G\rho_b m_a^2 a^4/\hbar^2)^{1/4}, \tag{5.11}$$

which defines the length scale on which the quantum potential exactly stabilises structures against gravitational collapse. Thus, growth of structures on small-scales $k > k_Q$ is inhibited by the quantum potential.
Since in general self-interactions are model dependent we ignore them for the rest of the discussion and focus on the effects of the quantum potential V_Q. In fact, equation (5.10) can be solved for $g = 0$ and has a growing and a decaying mode

$$D_+(x) = \left[(3-x^2)\cos x + 3x\sin x\right]/x^2 \tag{5.12}$$

$$D_-(x) = \left[(3-x^2)\sin x - 3x\cos x\right]/x^2, \tag{5.13}$$

with the function $x(k,a) = \sqrt{6}k^2/k_Q^2(a)$. Linear structure growth is therefore scale-dependent for FDM, while it is scale-independent for CDM.

5.1.2 *Initial Conditions*

During inflation the seeds of cosmological structures are believed to be created. If inflation is due to a single inflaton field, the intial conditions are adiabatic. At early times (after inflation) radiation is the dominant energy component and the photons carry the inflationary perturbations. Then the density fluctuations in the photons are related to the density fluctuations of other energy components by

$$\delta_i = \frac{3}{4}(1+w_i)\delta_\gamma, \tag{5.14}$$

where w_i is the equation of state parameter for the component i (cf. equation (A.11)). We repeat the line of argument of Marsh [22]. The equation of state parameter for axions depends on its mass relative to the Hubble function. Early in time, when $H > m_a$, the axion field is overdamped by Hubble friction and $w_a = -1$. When the Hubble function is lower than the mass of the axion ($H < m_a$), the axion field begins oscillating and the equation of state parameter is zero on average, with an oscillation frequency that is much smaller than the expansion rate given by the Hubble function. Then axions/FDM particles behave like ordinary matter and the density perturbations follow the photon perturbations.
As we have seen in the previous paragraph the growth of perturbations on scales smaller than the quantum Jeans scale $k > k_Q$ are suppressed relative to CDM. The dependence of this scale depends on the dominant energy content in the universe: for radiation domination $k_Q = \text{const.}$ and for matter domination $k_Q \propto a^{1/4}$ as can be inferred from

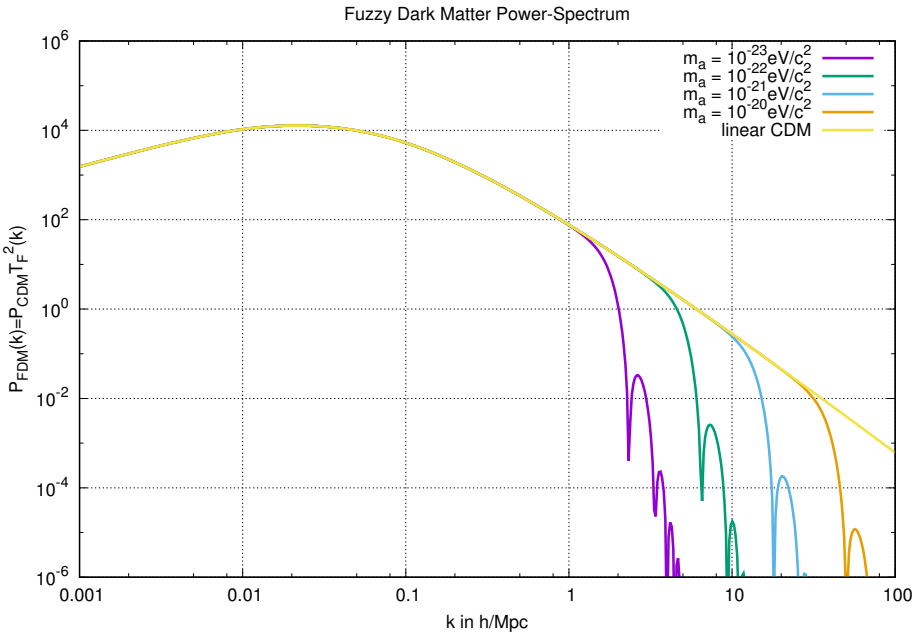

Figure 14: The FDM density fluctuation power-spectrum is shown for particle masses $m_a = 10^{-24} \ldots 10^{-20}\text{eV}/c^2$ in comparison to the CDM density fluctuation power-spectrum. For the CDM power-spectrum $P_{CDM}(k)$ we used the Bardeen et al. [2] power-spectrum and evolved it with the scale-independent linear growth factor $D_+(a)$. The power on small scales is suppressed for FDM particles due to the quantum potential.

(5.11). To account for the suppression of structure below this scale one can introduce a transfer function $T_F(k)$, such that

$$P_{FDM}(k) = T_F^2(k) P_{CDM}(k). \tag{5.15}$$

Here $P_i(k)$ are the power-spectra of density fluctuations at the last scattering surface, i. e. the time of CMB release. Numerically, the transfer function is found to be

$$T_F(k) = \frac{\cos x^3}{1+x^8} \quad \text{with} \quad x = 1.61 \left(\frac{m_a}{10^{-22}\text{eV}/c^2} \right)^{1/18} \frac{k}{k_{V_Q,eq}} \tag{5.16}$$

with the quantum Jeans scale at matter-radiation equality

$$k_{V_Q,eq} = 9 \left(\frac{m_a}{10^{-22}\text{eV}/c^2} \right)^{1/2} \text{Mpc}^{-1}. \tag{5.17}$$

Since k_Q depends only mildly on the scale factor, the quantum Jeans scale today is similar to the scale at matter-radiation equality. We show the initial power spectrum of FDM for masses $m_a = 10^{-23} \ldots 10^{-20}\text{eV}/c^2$ in Figure 14. The normalisation is chosen such that today $\sigma_8 = 0.8$ for the CDM power-spectrum. The initial power-spectrum of FDM falls off rapidly near the quantum Jeans scale and is proportional to a squared cosine. This behaviour is due to the harmonic equation (5.10), where a transition from exponential growth for large scales to harmonic oscillations on small scales occurs. For larger masses of the bosonic particle k_Q is larger and therefore less structure relative to CDM is suppressed.

5.2 EXTENSION OF KFT

5.2.1 *Dynamics*

In the previous Section we found that the dynamics of FDM is that of an effective fluid. This fluid is subject to gravity and the quantum potential arising from Heisenberg's uncertainty principle (cf. equation (5.7)). In order to treat dark matter as a light bosonic field in terms of KFT, we need to find a way to include the quantum potential into the dynamics of the microscopic particles. There are two solutions we want to discuss: a perturbative treatment as in Section 2.1.4 and an effective potential along the lines of the Born approximation in Section 4.3.
Before we discuss the two options we repeat the Euler equation in an expanding spacetime (ignoring self-interactions)

$$\partial_t \vec{v} + H\vec{v} + (\vec{v}\cdot\nabla)\,\vec{v} = -\frac{\nabla V}{a} + \nabla V_Q, \tag{5.18}$$

where we define the quantum potential V_Q as

$$V_Q = \frac{\hbar^2}{2m_a^2 a^3}\left[\frac{\nabla^2\sqrt{\rho}}{\sqrt{\rho}}\right] = \frac{\hbar^2}{2m_a^2 a^3}\left[\frac{\nabla^2\rho}{2\rho} - \frac{\nabla\rho\cdot\nabla\rho}{4\rho^2}\right]. \tag{5.19}$$

The mass of the bosonic particle is m_a and a is the scale factor. Since it is a potential interaction, we can adopt ideas from our treatment of gravity.

PERTURBATIVE DYNAMICS: Here we aim at an operator expression that in analogy to (2.30) can be used to perturbatively include the effects of the quantum potential V_Q. From the Euler equation we realise that particles are accelerated by another potential, which counteracts gravitational collapse. Therefore we can write for the j-th particle

$$\dot{\vec{p}}_j(\vec{q},t) = \nabla_{q_j} V_Q = \int_q \delta_D(\vec{q}-\vec{q}_j)\nabla V_Q(\vec{q},t) = -\int_q \left[\nabla\delta_D(\vec{q}-\vec{q}_j)\right] V_Q(\vec{q},t). \tag{5.20}$$

This is the same form as for the gravitational potential. Hence, the action associated with the quantum potential interaction is

$$S_Q = -\int dt \int_q \left(\sum_{j=1}^{N} \frac{\delta}{i\delta\vec{K}_{p_j}(t')}\cdot\left[\nabla_q\delta_D(\vec{q}-\vec{q}_j(t))\right]\right) V_Q(\vec{q},t), \tag{5.21}$$

where the term in brackets represents the response field again.
The tricky part here is to evaluate the quantum potential V_Q from one-particle contributions, since it involves inverse densities. Since the density is a distribution-valued function, its inverse cannot be expressed by an operator involving functional derivatives. In order to avoid complications we expand the inverse density in a Taylor series around the background value and as a first approximation we use the background value for now. Then the quantum potential is

$$V_Q(\vec{q},t) \simeq \frac{\hbar^2}{2m_a^2 a^3}\left[\frac{\nabla^2\rho}{2\rho_b} - \frac{\nabla\rho\cdot\nabla\rho}{4\rho_b^2}\right] \tag{5.22}$$

with the background density ρ_b independent of position.
The last step is to transform the quantum potential into Fourier-space and express the densities by operators. By use of the convolution theorem we get

$$\tilde{V_Q}(\vec{k},t) = \frac{\hbar^2}{2m_a^2 a^3}\left[\frac{-k^2\rho(\vec{k},t)}{2\rho_b} + \frac{1}{4\rho_b^2}\int_{k'} \vec{k}'\cdot\left(\vec{k}-\vec{k}'\right)\rho(\vec{k}',t)\rho(\vec{k}-\vec{k}',t)\right]. \tag{5.23}$$

With this expression we can account for the quantum potential in the perturbative expansion that we described in Chapter 3.

EFFECTIVE DYNAMICS: Since the calculation of each contribution in the perturbative scheme is a tedious task, we tried to incorporate the effects of the quantum potential V_Q by assuming an effective quantum potential of each particle. In a next step we evaluated the quantum force applying the Born approximation and averaging over the correlated particle ensemble in the same way as Bartelmann et al. [4]. The calculations presented in this paragraph were done by Leander Fischer as part of a student research project under our co-supervision.
To find an effective quantum potential we need to assume an underlying density profile. We choose

$$\rho(q) = \rho_b \left[c + \exp\left(-\frac{q^2}{(2\sigma^2)} \right) \right] \tag{5.24}$$

which may be seen as an effective size of the particles. The parameters c and σ are free. In the case of the width σ of the Gaussian profile a sensible choice may be the Compton wavelength of the FDM particle, $\lambda_{\text{Compton}} = \frac{\hbar_{\text{Planck}}}{m_a c} \simeq 0.5\text{pc}$ for a typical mass of $m_a = 10^{-22}\text{eV}/c^2$, or the de-Broglie wavelength with typical cluster velocities.
Beginning with the density profile (5.24) we arrive at an effective potential of the form

$$V_{Q,\text{eff}}(q,t) = \frac{\hbar^2}{4m_a^2\sigma^2 a^3}\chi\left(-3 + \frac{q^2}{2\sigma^2}(2-\chi)\right) \tag{5.25}$$

with the definition

$$\chi := \left(1 + c e^{\frac{q^2}{2\sigma^2}}\right). \tag{5.26}$$

The naive choice for the particle size is a Gaussian profile without any offset. This choice leads to a different quantum potential and in particular non-physical behaviour at infinite distances. For $\rho = \exp(-\frac{x^2}{2\sigma^2})$ we get $V_Q \propto x^2$ and therefore diverging. Thus, particles at large distances would feel large accelerations, which is unphysical. The constant off-set $c\rho_b$ prevents the divergent behaviour. We show the effective quantum potential in Figure 15 with the choice of parameters being $c = 1$ and $\sigma = 1\text{Mpc}/h$. While in the application we will choose smaller values for the width σ, we aim here for a proof of concept. The plot shows that for short distances from the center the quantum potential is repulsive and becomes attractive in a small range of distances, before its effect becomes negligible.
In the end we want to calculate the resulting force in the same way as we did for gravity in Section 4.3. The correction to the density fluctuation power-spectrum due to a potential gradient is determined by

$$\mathbf{F}(t) = -i\int dt' \langle \mathbf{L}_p(t'), \boldsymbol{\nabla} \mathbf{V_Q}(t') \rangle \tag{5.27}$$

where $\langle . \rangle$ denotes an average and $\langle ., . \rangle$ a scalar product. With the effective quantum potential $V_{Q,\text{eff}}(q,t)$ the scalar product evaluates to

$$\langle \mathbf{L}_p(t'), \boldsymbol{\nabla} \mathbf{V_Q}(t') \rangle = 2 g_{qp}(t,t') \left[k_1^2 \tilde{V}_{Q,\text{eff}}(k_1,t') + \vec{k}_1 \int_k \vec{k} \tilde{V}_{Q,\text{eff}}(k,t') \bar{P}_\delta(\vec{k}_1 - \vec{k}, t') \right], \tag{5.28}$$

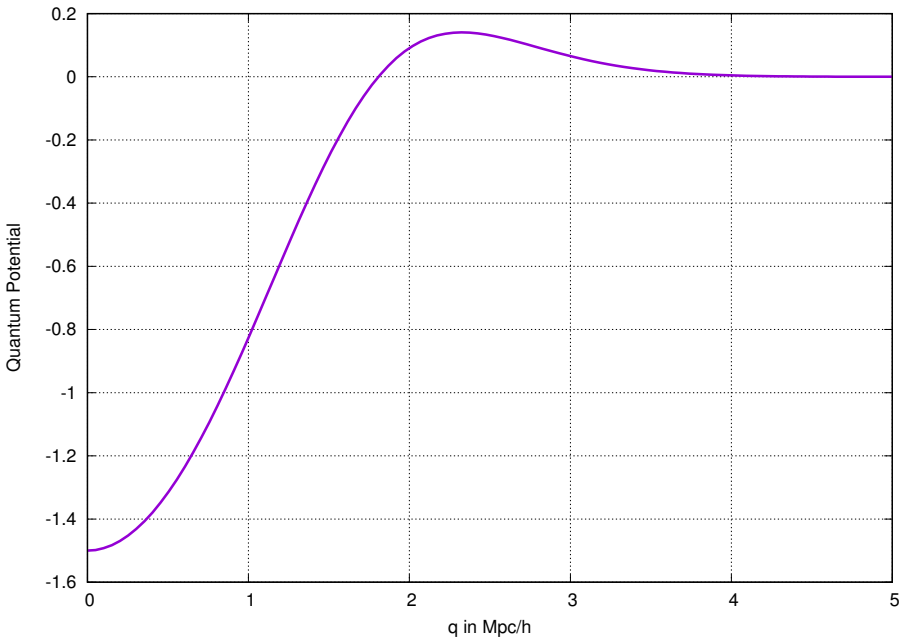

Figure 15: Shown is the effective quantum potential $V_{Q,\mathrm{eff}}(q,t)$ of (5.25) divided by the overall amplitude. The free parameters were chosen to be $c = \sigma = 1$, where σ is measured in Mpc/h.

where $\tilde{V}_{Q,\mathrm{eff}}(k,t')$ denotes the Fourier-transform of (5.25) and $\bar{P}_\delta(\vec{k}_1 - \vec{k}, t')$ is the linearly evolved density fluctuation power-spectrum. The first term is an uncorrelated force, i. e. this term does not contribute a directed force as it corresponds to a homogeneous Poisson process. Thus, we may ignore the first term in the effective dynamics. The second term on the other hand is the correlated contribution to the force and will therefore lead to a directed net force which in this context is repulsive.
Since the effective quantum potential depends on distance only, its Fourier-transform is readily given by an integral over a spherical Bessel function

$$\tilde{V}_{Q,\mathrm{eff}}(k,t) = 4\pi \int dq q^2 V_Q(q,t) j_0(kq). \tag{5.29}$$

As in Bartelmann et al. [4] we introduce the relative wave-vector $\vec{\kappa} = \vec{k}_1 - \vec{k}$ and the dimensionless parameter $y = \kappa/k_1$ so that the Born-approximated force due to the quantum potential becomes

$$\mathbf{F}(t) = -\int_{t_0}^{t} dt' A(t,t') \frac{k_1^5}{2\pi^2} \int_0^\infty dy \int_{-1}^{1} d\mu y^2 (1 - y\mu) \tilde{V}_{Q,\mathrm{eff}}(k(\mu),t) \bar{P}_\delta(k_1 y, t') \tag{5.30}$$

with the time-dependent amplitude

$$A(t') = \frac{\hbar^2}{4 m_a^2 \sigma^2 a^3} g_{qp}(t,t'). \tag{5.31}$$

We show the result of this integral in Figure 16 evaluated using a Monte-Carlo integration routine with 128 and 1024 points at two different times. We notice that the chosen integration method is not stable enough to apply the result to the density fluctuation power-spectrum. The main problem in the evaluation lies in the Fourier integral of the

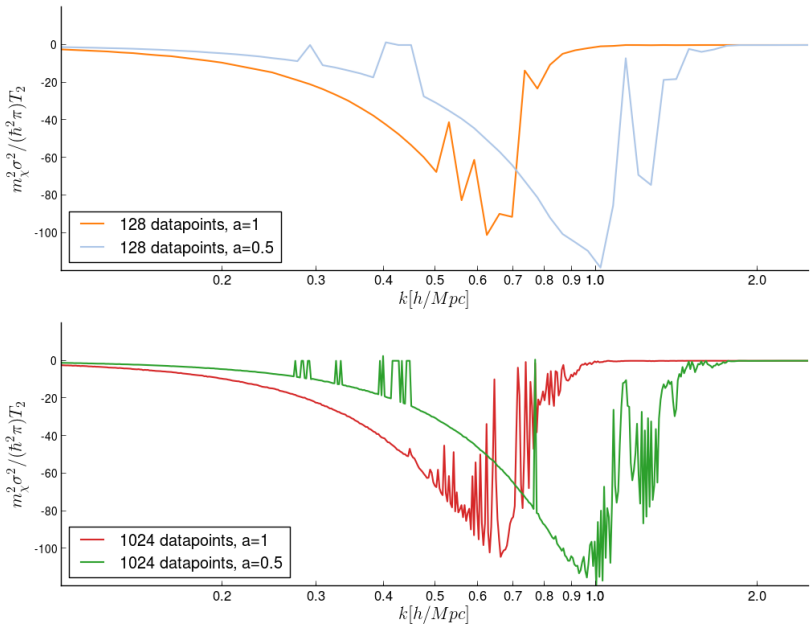

Figure 16: Shown is the Born-approximated force term resulting from the effective quantum potential (5.25) for $c = 1$ and $\sigma = 1\text{Mpc/h}$ at different times $a = 0.5$ and $a = 1$. We evaluated the integral (5.30) using a Monte-Carlo integration routine with 128 and 1024 points. The evaluation has yet to be improved to apply this correction to the density fluctuation power-spectrum. We infer at this point that $V_{Q,\text{eff}}$ has a repulsive effect, as we expected. Courtesy of Leander Fischer.

effective quantum potential, but this problem may be solved employing other integration methods such as a Levin collocation. Although the results are not stable, we can infer that the force is repulsive. Although we expected the repulsive nature of the quantum potential, we did not expect the scale on which the effect is the strongest. The effect is the strongest on scales where structures start to deviate from linear growth.
Since the effective quantum potential involves two free parameters, we checked the influence of those parameters on the effective correction. In Figure 17 the effects are shown. As we might expect, c changes the amplitude and the width σ changes both the amplitude and the scale on which the effect is the strongest by changing the curvature of the potential.
In this paragraph we have shown that we can incorporate the additional dynamics of FDM by assuming an effective potential for the particles assuming a Gaussian density profile. The aim was a proof of concept and more work is to be done in solving the integral (5.30). Also we have to find reasonable choices for the parameters c and σ of the underlying density profile. The results of this part thus far suggest that the effect of the quantum potential is most relevant on scales at the onset of non-linear structure formation.

5.2.2 *Probability Distribution*

In Figure 14 we showed the effect of the quantum potential V_Q on the initial power-spectrum of density fluctuations for various masses of the FDM particle: fluctuations on scales smaller than the quantum Jeans scale ($k > k_Q$) oscillate rather than collapse. On those scales fluctuations are stable and the power-spectrum is suppressed. In order to

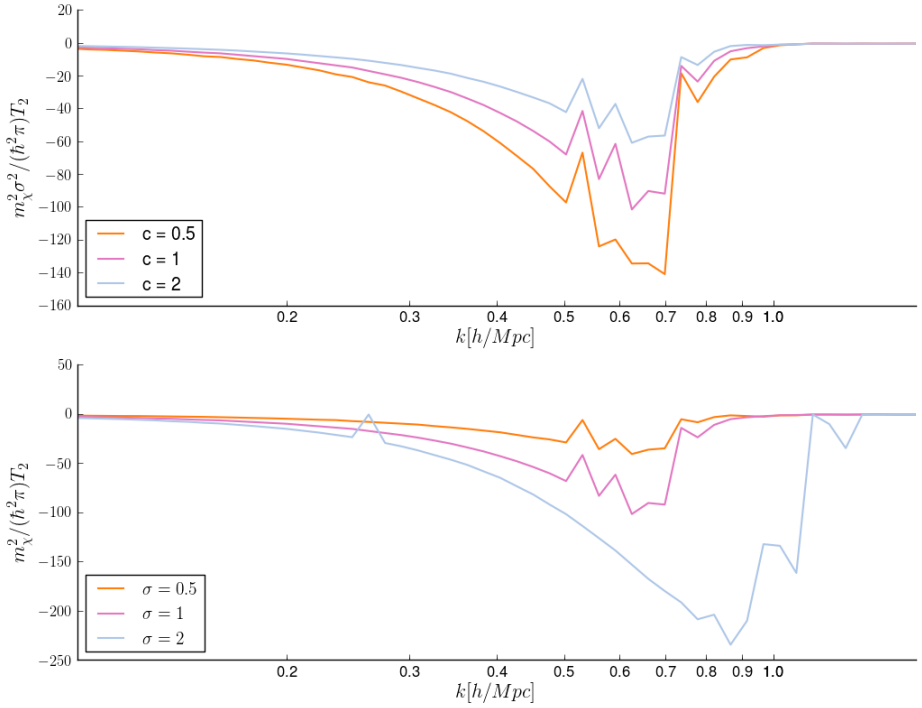

Figure 17: Shown is the Born-approximated force term resulting from the effective quantum potential (5.25) for different values of the parameters c and σ. Courtesy of Leander Fischer

incorporate this effect in KFT we need to adjust the initial distribution of microscopic particles in phase-space, namely $P[\mathbf{q}, \mathbf{p}]$ of (2.42).
The suppression of power on small scales does not change the nature of the perturbations: the density fluctuation δ and the velocity potential ψ are homogeneous and isotropic Gaussian random fields fully specified by their respective power-spectra. In particular, their relation by continuity does not change.
Then the analytic expressions of Chapter 2 for the initial probability distribution (2.42) and the initial density $C_{\delta\delta}$, density-momentum $C_{\delta p}$ and momentum C_{pp} correlations (2.44)-(2.46) are valid for FDM as well. But in this application the initial power-spectrum $P_\delta(k)$ entering the expressions has to be adjusted using the transfer function $T_F(k)$ (5.16) of the previous section.
We have shown in Chapter 3 that after the application of n density operators the generating functional factorises, if initial density and density-momentum correlations are weak. Then an n-point correlation of the density or momentum-density fields only depends on the initial momentum correlation matrix and is given by the correlation function $\xi_\psi(q)$ of the velocity potential and its first and second derivatives. We repeat the definitions of the functions

$$a_1(q) := \frac{\xi'_\psi(q)}{q}, \quad a_2(q) := \xi''_\psi(q) - \frac{\xi'_\psi(q)}{q}, \tag{5.32}$$

that we introduced previously (cf. 3.1.2) and compare these functions for the suppressed FDM power-spectrum with the CDM power-spectrum of Bardeen et al. [2] in Figures 18 and 19.
We observe the following properties of the functions $a_1(q)$ and $a_2(q)$: (i) asymptotically the functional dependence on the distance q is the same independent of the dark matter

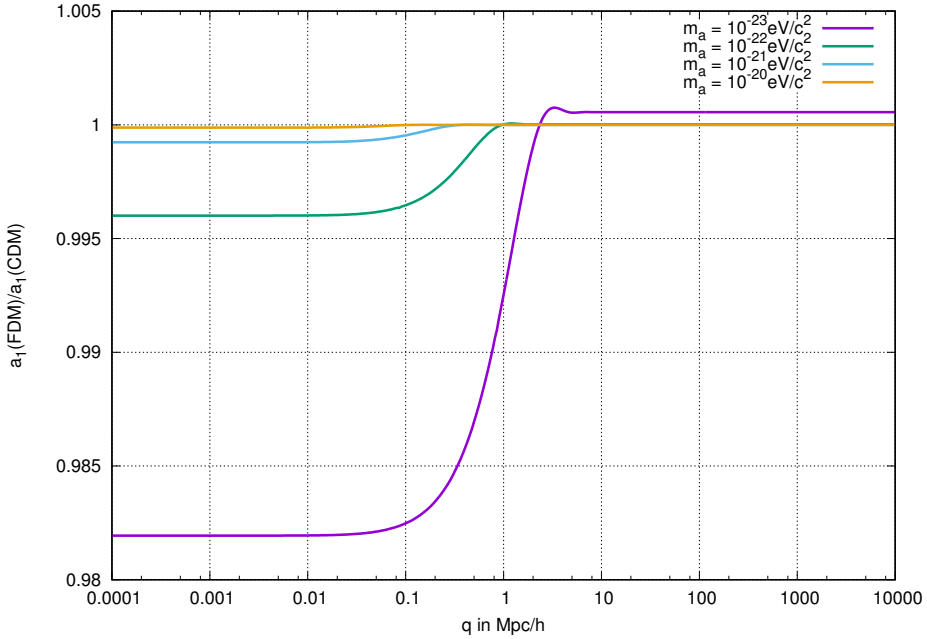

Figure 18: Shown is the ratio of the correlation function $a_1(q)$ for FDM and CDM. While the dependence on distance is asymptotically the same for either mass m_a of the boson and CDM, the amplitude is reduced on small scales due to the quantum potential. The smaller the mass m_a, the stronger is the suppression, since k_Q decreases.

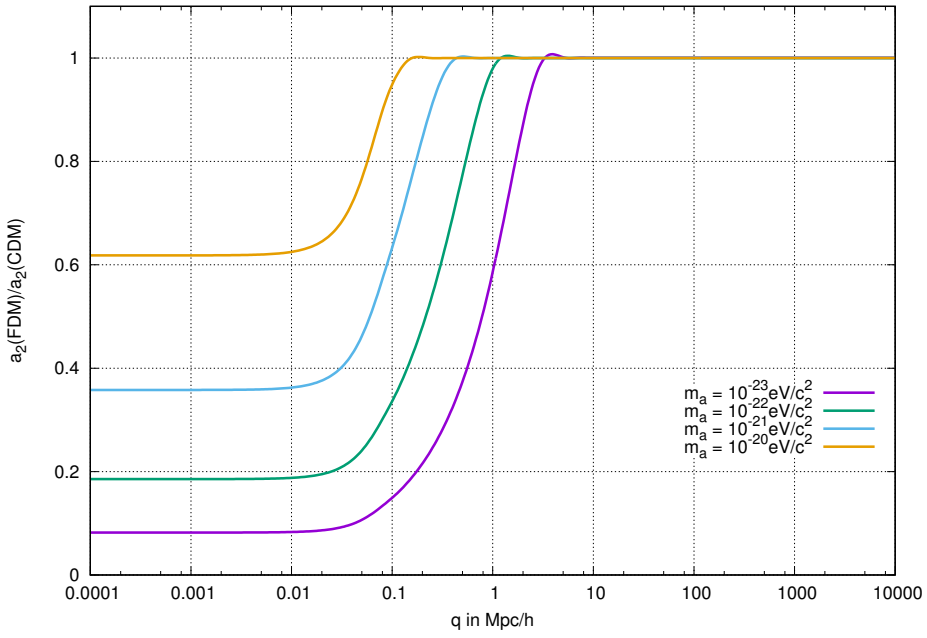

Figure 19: Shown is the ratio of the correlation function $a_2(q)$ for FDM and CDM. As for $a_1(q)$ we notice that the dependence on distance is asymptotically the same for either mass m_a of the boson and CDM, the amplitude is reduced on small scales due to the quantum potential. The smaller the mass m_a, the stronger is the suppression, since k_Q decreases.

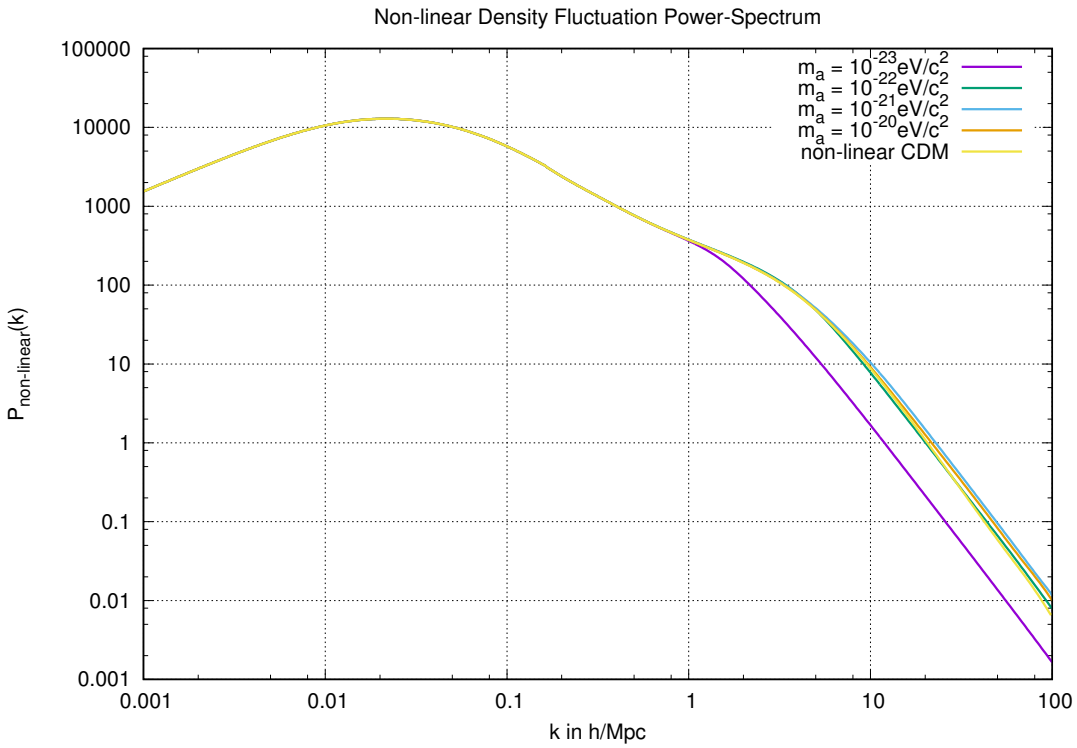

Figure 20: We show the non-linearly evolved density fluctuation power-spectrum using Newtonian dynamics and the suppressed initial power-spectrum of FDM. On linear scales Fuzzy and Cold Dark Matter show the same behaviour. While power on the scales that are non-linear today are suppressed in the initial conditions, gravity can restore power on those scales. For the lowest mass $m_a = 10^{-23}eV/c^2$ the restoring effect is the weakest.

model and the mass m_a of the light bosonic particle, (ii) the amplitude of both functions is reduced for small distances relative to CDM. The second effect is stronger for lighter particles. This effect is readily understood, when we look at (5.10) and the corresponding quantum Jeans scale. The wavenumber k_Q, i. e. the smallest inverse length scale on which perturbations are stable, is proportional to the square-root of the particle mass. Therefore, lower-mass particles suppress initial correlations on larger scales than heavier particles.

5.2.3 *CDM Dynamics for FDM*

In this paragraph we apply the formalism of KFT with Newtonian dynamics to the initial conditions of Fuzzy Dark Matter. We ignore the quantum potential in the dynamics completely but include its effects on the initial power-spectrum of density fluctuations. Using the Born approximation (cf. Section 4.3) we calculate the non-linear density fluctuation power-spectrum today from the initial conditions given by the FDM power-spectrum from equation (5.15). The non-linear power-spectrum is given by

$$P(k,t) = e^{Q_D(k,t) - \mathbf{F}_N(t)} \int_q \left[e^{-g_{qp}^2(t,t_0)a_{\parallel}(q)k^2} - 1 \right] e^{i\vec{k}\cdot\vec{q}}, \tag{5.33}$$

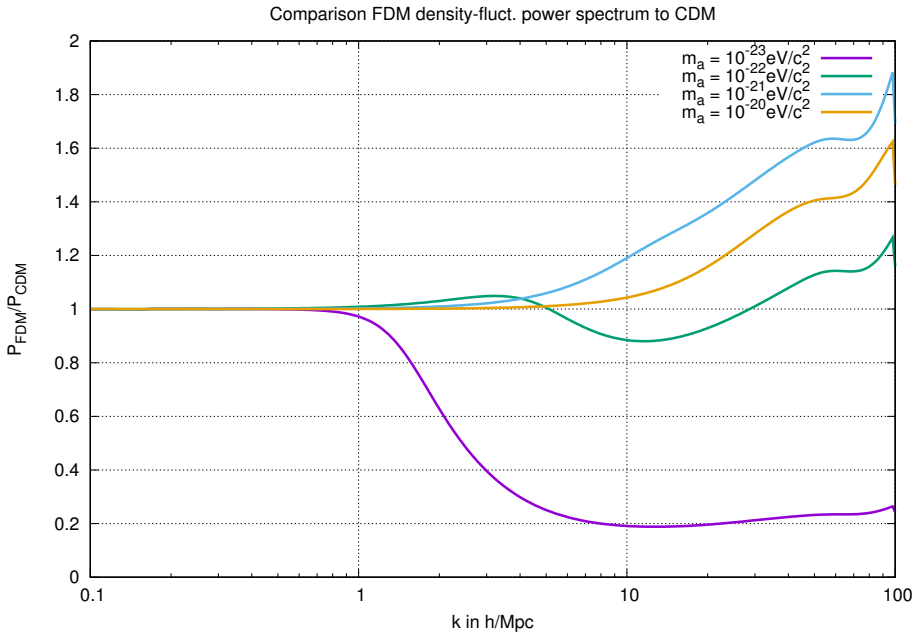

Figure 21: The ratio of the non-linear density fluctuation power-spectrum for a bosonic particle of mass m_a and the power-spectrum of Cold Dark Matter. For the smallest mass considered (purple) gravity is not enough to get a power-spectrum similar to CDM. For a boson of the fiducial mass or heavier the power-spectra are very similiar up to $k \simeq 5h/\text{Mpc}$, while for very small scales the FDM power-spectrum is larger than the CDM power-spectrum.

where $a_{\parallel}(q) = a_1(q) + \mu^2 a_2(q)$ defined in (3.33) and μ is the angle cosine between $\vec{k}$ and $\vec{q}$. The negative quadratic form $Q_D(k,t)$ accounts for the free-streaming of the particle ensemble and damps structure on small scales. $\mathbf{F}_N(t)$ is the average gravitational force calculated with the Born approximation as in Bartelmann et al. [4]. They showed that the analytic result (5.33) is on average $\simeq 15\%$ off typical numerical results up to wave numbers $k \leqslant 10h/\text{Mpc}$. A calculation for the average gravitational force is also given in Section 4.3 above.

In Figure 20 we show the non-linear power-spectrum. The evolution of the linear scales is unaffected by any modifications of the initial correlation functions, since the quantum pressure is negligible. For smaller scales we observe that gravity has enough restoring power to raise the correlations of FDM to about the same level as CDM, except for the smallest boson mass $m_a = 10^{-23}eV/c^2$ considered. This is counterintuitive since the average gravitational force $\mathbf{F}_N(t)$ depends on the linearly evolved density correlations in the ensemble and connects particles on all scales by a convolution integral. Therefore suppression of power on small scales also decreases the average force on those scales. We show this in Figure 22.

In order to see the difference between the non-linear power-spectra more clearly we plotted in Figure 21 the ratio of the power-spectra. On scales $k \leqslant 10h/\text{Mpc}$ we find relative deviations of up to 20% for masses $m_a = 10^{-22}eV/c^2$ and higher. For those masses of the bosonic field the gravitational interaction between the particles leads to similar non-linear structure as Cold Dark Matter. For the lowest mass that we have considered the quantum potential has suppressed too much structure prior to CMB release that, even though gravity forms structure, it is much less than is expected from numerical simulations and observations. Comparing with our results of the previous

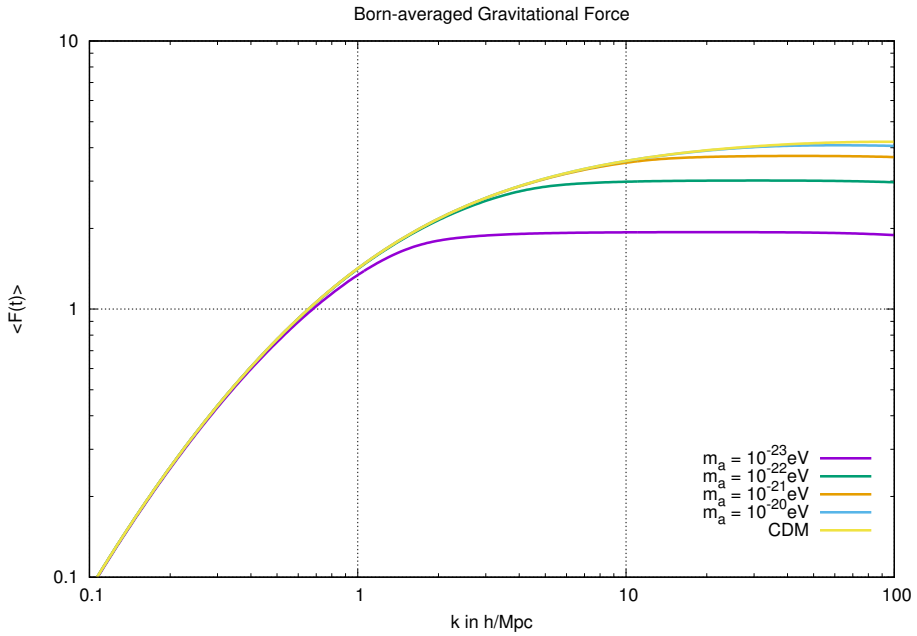

Figure 22: The averaged gravitational force $\mathbf{F}_N(t)$ in the Born approximation is shown for Cold Dark Matter and different boson masses $m_a = 10^{-23} \ldots 10^{-20} \mathrm{eV}/c^2$.

paragraph we find that the truncated initial power also mainly affects those scales near the onset of non-linear structure evolution. The power-spectrum of the boson with the largest mass follows the Cold Dark Matter power-spectrum the closest since the initial conditions are also closest to the fiducial CDM case. The plot shows a puzzling trend on the non-linear scales ($k > 0.3h/\mathrm{Mpc}$): relative to the CDM power-spectrum the fiducial mass boson ($m_a = 10^{-22}\mathrm{eV}/c^2$) has more power on scales $1h/\mathrm{Mpc} < k < 5h/\mathrm{Mpc}$ and less power on scales $5h/\mathrm{Mpc} < k < 30h/\mathrm{Mpc}$ and rising for smaller scales, while the boson with $m_a = 10^{-21}\mathrm{eV}/c^2$ has everywhere more power and the amplitude of the power-spectrum for the most massive boson $m_a = 10^{-20}\mathrm{eV}/c^2$ falls between the amplitude for the two lighter bosons. This trend could result from the fact that we normalised the power-spectrum $P_{CDM}(k)$ with the value $\sigma_8 = 0.8$ rather than the power-spectrum $P_{FDM}(k)$.
On highly non-linear scales $k > 10h/\mathrm{Mpc}$ the amplitude of the Fuzzy Dark Matter power-spectrum grows relative to the Cold Dark Matter power-spectrum. The reason for this deviation lies in the suppression of initial correlations on small scales and influences the damping $Q_D(k,t)$. The amplitude of the damping function Q_D depends on the initial velocity dispersion

$$\sigma_1^2 = \int_k k^{-2} P_\delta(k). \tag{5.34}$$

The suppression of power on small scales due to the quantum potential effectively reduces free-streaming as the velocity dispersion is lowered. Effectively Figure 21 shows that the damping due to free-streaming for CDM is stronger than in the FDM case.
In this paragraph we assumed the dynamics of FDM to be the same as of CDM, i. e. classical microscopic particles under the influence of gravity in an expanding space-time, and calculated the non-linear density fluctuation power-spectrum. For the calculation we used the initial momentum correlations given by the FDM power-spectrum $P_{FDM}(k) = T_F^2(k) P_{CDM}$ given the transfer function (5.16). On the linear scales we did not find any

difference between the different dark matter models. On non-linear scales we found that the gravitational interaction between the particles can restore structure that was suppressed by the quantum potential interaction before the time of last scattering. The smallest scales $k > 10h/\mathrm{Mpc}$ are plagued by the large damping factor due to free-streaming, which dominates all other effects that may be relevant on those scales.
At this point we can think of two improvements of this calculation in order to compare better with numerical results (e. g. Schive et al. [33]): (i) normalisation of $P_{FDM}(k)$ via σ_8. In our calculation we fixed the amount of power enclosed by a radius of $8\mathrm{Mpc}/h$ for the CDM power-spectrum to emphasise the effect of the transfer function $T_F(k)$ on the small scales. For a proper treatment the amplitude of P_{FDM} should be fixed by σ_8. (ii) inclusion of scale-dependent growth in the averaged gravitational force. The calculation of $\mathbf{F}(t)$ involves an integral over the linearly evolved density fluctuation power-spectrum. This is intuitively clear as for an uncorrelated homogeneous and isotropic density field the average force equals zero. Here we used the power-spectrum linearly evolved with the growth factor of CDM that is scale-independent. With a change of the growth factor $D_+(a) \mapsto D_+(k, a)$ of equation (5.12) we might improve the calculations presented here.

5.2.4 *Modifications by the Quantum Potential*

In this section we derived how KFT, which is a non-equilibrium statistical field theory for classical particles, needs to be extended in order to model Fuzzy Dark Matter such as axions rather than Cold Dark Matter. We ignored self-interactions in our discussion, which would be accounted for by an isotropic pressure gradient force with a barotropic equation of state (cf. Chavanis [12]). The main dynamical difference between CDM and FDM is the relevance of the particle's de-Broglie wavelength on cosmological scales. Then the wave nature of the particles introduces a quantum potential that acts repulsively on small scales, which stabilises density perturbations against collapse. This leads to a truncation of the initial power-spectrum and a scale-dependent linear growth of structures. In order to incorporate the effects of the quantum potential we need to modify both, the dynamics and the initial probability distribution.
For the dynamics we can introduce a new potential interaction as we did for gravity and treat it perturbatively (cf. 2.1.4). Another possibility is to introduce an effective potential, evaluating the resulting force in the Born approximation and averaging over the correlated particle ensemble. Our early results for an underlying Gaussian density distribution suggest that the repulsive quantum force is strongest on scales near the onset of non-linear structures ($1h/\mathrm{Mpc} \geqslant k \geqslant 0.3h/\mathrm{Mpc}$). On those scales growth of structure deviates from the linear solution and higher orders become important. Intuitively this makes sense, since on larger scales FDM acts like CDM and on smaller scales structures have already collapsed by non-linear interactions. We emphasise that the presented calculations are a proof of concept only. We have to work out a stable integration scheme for the Fourier-transform of the effective quantum potential, and sensible parameter values for c and σ need to be included.
The only modification to the initial probability distribution is the form of the power-spectrum. The quantum potential leads to a truncation of power on scales smaller than the quantum Jeans scale k_Q of (5.11). The truncation can be captured by a transfer function that is a cosine function with a rapidly decreasing envelope. We explored the effect of the modified initial power-spectrum by assuming gravitational interactions only, i. e. we used FDM initial conditions and CDM dynamics. For all particle masses considered we observed the formation of non-linear structures compatible with the non-linear

scales of CDM, but for the lowest mass considered ($m_a = 10^{-23}\mathrm{eV}/c^2$) the amplitude of non-linear structure was up to 80% lower than for standard CDM. For the typical Ultra-Light Axion mass $m_a = 10^{-22}\mathrm{eV}/c^2$ and heavier we found that the truncated initial power-spectrum affects the density fluctuation power-spectrum scales near the onset of non-linear structure as well. While this effect is slightly shifted to smaller scales $3h/\mathrm{Mpc} \geqslant k \geqslant 0.5h/\mathrm{Mpc}$ compared to the effect of FDM dynamics, it is peculiar that only scales close to the onset of non-linear behaviour are affected.
Ultimately we aim at the combination of FDM initial conditions and particle dynamics given by Newtonian gravity, the quantum potential and possible self-interactions. While the actual calculations are beyond the scope of this thesis, we have discussed the relevant modifications to the formulation of KFT to incorporate the classical equations for a condensate.

6

CONCLUDING REMARKS

This thesis is based on the recently developed KFT for cosmic structure formation of Bartelmann et al. [6]. KFT is a non-equilibrium statistical field theory for initially correlated particles obeying the Hamiltonian equations of motion. The ensemble of particles is described by a generating functional that contains all information about the initial distribution of particles in phase-space and their dynamics described by a retarded Green's function. In analogy to QFT, correlation functions of macroscopic quantities can be extracted by application of appropriate functional derivatives. Interactions between particles can be included perturbatively as in QFT or by an effective force calculated in the Born approximation (cf. Bartelmann et al. [4]).

In the first part of this thesis we developed a systematic way to calculate n-point correlation functions of the momentum-density field $\vec{\Pi}$. In order to do so we employ recent developments in the calculation of density correlators by Bartelmann et al. [5]. They showed that the statistical homogeneity and isotropy of the initial correlations allows the factorisation of the generating functional, i. e. it becomes a convolution of structurally equivalent factors. Here we show that the same calculation can be carried out for $\vec{\Pi}$ correlators, since each momentum can be substituted by a partial derivative with respect to the corresponding momentum shift.

Corrections to a correlator due to particle interactions are treated perturbatively. Every order of the particle interaction corresponds to one scattering event along the path of a particle contributing to the correlator. As a visual aid for the calculation of corrections we extend the diagrams originally suggested by Bartelmann et al. [5] in order to represent corrections to n-point correlation functions of density and momentum-density fields.

In the second part, we calculate the 2-point $\langle\vec{\Pi}\otimes\vec{\Pi}\rangle$ correlation tensor and scalar quantities thereof, namely the trace, the divergence and the curl power-spectrum. The divergence and the curl power-spectra are the power-spectra of the projections of $\vec{\Pi}$ parallel or perpendicular to the wave-vector $\vec{k}$ multiplied by k^2. In the first calculation we considered initial momentum correlations only up to quadratic order as Bartelmann et al. [6] in their first calculations of the density fluctuation power-spectrum. In that approximation, power on small scales is a consequence of particle interactions. In the subsequent calculations we employ the framework of the first part and use the factorised generating functional. This calculation considers the full hierarchy of initial momentum correlations. Plotting the free power-spectra we see enhanced power on small scales differing from the linearly evolved power. Thus, more than particle interactions, initial correlations are responsible for the deformation of the power-spectrum on non-linear/small scales. Instead of perturbative corrections by interactions we employed together with the BSc student Christian Sorgenfrei the Born approximation for the gradient of the interaction potential and averaged over the correlated particle distribution.

In view of the kSZ effect, which is a secondary temperature anisotropy in the CMB radiation induced by inverse Compton scattering of photons with free electrons following the bulk motion of structures, we compared our results for the power-spectrum of the transverse component $\vec{\Pi}\perp\vec{k}$ with the literature. The first comparison is between our free result quadratic in the initial conditions and the linear result by Vishniac [34]. Our results agree save for a factor of 2. In the second comparison we find that our result using the full hierarchy of initial momentum correlations and interactions within the Born ap-

proximation matches the analytic and simulation results of Park et al. [27] very well.
In the last Chapter of this thesis we aim at a description of FDM in the framework of KFT. Fuzzy Dark Matter is a term for non-thermally produced extremely light bosons whose de-Broglie wavelength is relevant on cosmological scales. The difference from CDM is the quantum potential in the equations of motion for FDM particles, which is repulsive on small scales. We have shown how the quantum potential can be treated perturbatively in the same way as the gravitational potential. In collaboration with Leander Fischer as part of his student research project we tried to describe the quantum potential by an effective potential and evaluate the force within the Born approximation. Our early results show that this force has the strongest effect on scales close to the onset of non-linear structures and counteracts the gravitational force. This suggests a suppression of power on the intermediate scales compared to standard CDM. Apart from the dynamics, the repulsive nature of the quantum potential stabilises density fluctuations on small scales. This leads to a suppression of power in the initial power-spectrum compared to CDM. The suppression scale depends on the particle mass. We investigated the effect on the non-linear density fluctuation power-spectrum today assuming an initial FDM power-spectrum in the phase-space probability distribution and ignoring the quantum potential in the dynamics. Our results show that the different initial conditions also affect scales near the onset of non-linear structure formation.

Part III

APPENDIX

A

COSMOLOGY

A.1 FRIEDMANN EQUATIONS

The dynamics of space-time is described in the framework of General Relativity. Here, space-time is a four dimensional manifold with a metric tensor $g_{\mu\nu}$ being the dynamical field of the theory. The metric defines the line element, i. e. the differential arc length of world lines, and a scalar product by

$$ds^2 = g_{\mu\nu} dx^\mu dx^\nu \tag{A.1}$$

$$a_\mu b^\mu = g_{\mu\nu} a^\nu b^\mu. \tag{A.2}$$

We adopt conventions that index pairs on different levels are to be summed over and greek indices enumerate all four space-time coordinates ($0 \leqslant \mu \leqslant 3$) while latin indices enumerate three dimensional space ($1 \leqslant i \leqslant 3$). The metric tensor $g_{\mu\nu}$ is symmetric, which implies it has 10 independent components. The geometric degrees of freedom, i. e. the metric components, are coupled to the energy content of space-time by Einstein's field equations (Einstein [13])

$$G_{\mu\nu} = \frac{8\pi G}{c^4} T_{\mu\nu} + \Lambda g_{\mu\nu}. \tag{A.3}$$

The right-hand side is the energy content expressed by the energy-momentum tensor $T_{\mu\nu}$ augmented by a 'cosmological constant' Λ term. The left-hand side is the Einstein tensor

$$G_{\mu\nu} = R_{\mu\nu} - \frac{1}{2} R g_{\mu\nu}, \tag{A.4}$$

which is given by the Ricci (curvature) tensor $R_{\mu\nu}$ and its trace. The Ricci tensor is a function of the first and second order derivatives of the metric and thus Einstein's field equations are second order differential equations for the metric components. It is important to note that this theory is inherently non-linear, since the geometry of space-time is determined by its energy content and the motion of matter and energy is determined by the geometry of space-time.
In cosmology two simplifying assumptions about space-time are being made:

- spatial isotropy,
- spatial homogeneity.

These assumptions can only hold for averages over sufficiently large scales. Observations of galaxies show that their distribution is anisotropic but the CMB is highly isotropic. The CMB is the signal from the last scattering surface, when the Universe became electrically neutral and transparent (to photons). Before, the mean free path of photons was very short due to the large Thomson cross-section of the free electrons. Homogeneity follows from the fact that no position in the Universe is preferred to any other.
This allows considerable simplifications for the metric tensor. Considering a fundamental observer, whose comoving coordinates are fixed ($dx^i = 0$), his proper time must be the coordinate time and therefore $g_{00} = -c^2$. It must be possible to choose coordinates such that the space-time components of the metric g_{0i} are zero, since $g_{0i} \neq 0$ would

specify a direction, violating isotropy. Then the metric permits a foliation of space-time into spatial slices of constant time, since the line element takes on the form

$$ds^2 = -c^2dt^2 + g_{ij}dx^i dx^j. \tag{A.5}$$

Homogeneity allows the spatial hypersurfaces to be scaled by a function $a(t)$ that depends on time only, and isotropy demands spherical symmetry. Introducing polar coordinates $(\chi, \vartheta, \varphi)$ the line element can be written in the form

$$ds^2 = -c^2dt^2 + a^2(t)\left[d\chi^2 + f^2(\chi)\left(d\vartheta^2 + \sin^2\vartheta d\varphi^2\right)\right]. \tag{A.6}$$

The radial function $f(\chi)$ depends on the curvature of space, which by homogeneity must be the same everywhere on the same hypersurface and must be trigonometric, linear or hyperbolic in χ:

$$f(\chi) = \begin{cases} K^{-1/2}\sin(K^{1/2}\chi), & K > 0 \\ \chi, & K = 0 \\ \|K\|^{-1/2}\sinh(\|K\|^{1/2}\chi), & K < 0 \end{cases}, \tag{A.7}$$

Here K parameterises the spatial curvature. The metric can therefore describe a spatially closed ($K > 0$), flat ($K = 0$) or open ($K < 0$) space-time. The metric defining the line element described by equation (A.6) is called Robertson-Walker metric.
The dynamics of space-time given by Einstein's field equations (A.3) now reduces to differential equations for the scale-factor $a(t)$. In order to retrieve equations for $a(t)$ we need to specify the energy-momentum tensor, which will be that of a perfect fluid as seen by a fundamental observer:

$$T_{\mu\nu} = \left(\rho c^2 + p\right)u_\mu u_\nu + p g_{\mu\nu}. \tag{A.8}$$

Due to homogeneity the energy density ρ and the pressure p may be functions of time only. The differential equations governing the evolution of the scale-factor are

$$\left(\frac{\dot{a}}{a}\right)^2 = \frac{8\pi G}{3}\rho + \frac{\Lambda c^2}{3} - \frac{Kc^2}{a^2} \tag{A.9a}$$

$$\frac{\ddot{a}}{a} = -\frac{4\pi G}{3}\left(\rho + \frac{3p}{c^2}\right) + \frac{\Lambda c^2}{3}. \tag{A.9b}$$

These are *Friedmann's equations* [14]. The overdot refers to a derivative with respect to time. If the scale-factor in the Robertson-Walker metric satisfies these two equations, (A.6) is called Friedmann-Lemaître-Robertson-Walker metric. The scale-factor is uniquely determined once its value is set for a specific point in time. A common choice is $a(t_0) = a_0 = 1$ today.
Friedmann's equations can be combined to yield an equation for the evolution of the energy density

$$\dot{\rho} + 3\frac{\dot{a}}{a}\left(\rho + \frac{p}{c^2}\right) = 0 \tag{A.10}$$

This equation expresses energy conservation and is equivalent to the first law of thermodynamics in absence of heat flows which would violate isotropy.
Pressure and energy density of a species, e. g. (non-)relativistic matter, are related by the equation of state parameter w in the following way

$$p = w\rho c^2. \tag{A.11}$$

For non-relativistic matter $w = 0$ and the energy density is proportional to a^{-3}, i. e. the energy density is diluted due to the expansion of space. Relativistic matter has $w = {}^1/_3$ and the energy density falls like a^{-4}, i. e. in addition to the dilution the energy is redshifted.
Next we introduce parameters and rewrite equation (A.9a) in terms of those. The first parameter is the Hubble function

$$H(t) = \frac{\dot{a}(t)}{a(t)}, \tag{A.12}$$

which is the expansion rate of the Universe. Its value today is called the Hubble constant and is usually expressed in terms of the dimensionless parameter h

$$H_0 = 100h\frac{\mathrm{km/s}}{\mathrm{Mpc}}. \tag{A.13}$$

with $h = 0.6727 \pm 0.0066$ (Planck Collaboration et al. [32]). A length scale of the Universe is given by the Hubble length $l_H = {}^c/_{H(t)}$, i. e. the speed of light divided by the Hubble function. The total energy density in a spatially flat Universe with $K = 0$ is the critical density

$$\rho_c = \frac{3H^2}{8\pi G} \tag{A.14}$$

with a value today of

$$\rho_{c0} = 1.86 \times 10^{-29} h^2 \frac{g}{cm^3}. \tag{A.15}$$

It is customary to express the energy densities of non-relativistic matter, radiation (relativistic matter), the cosmological constant and curvature as dimensionless quantities in the following way:

$$\Omega_m = \frac{\rho_m(t)}{\rho_c}, \quad \Omega_r = \frac{\rho_r(t)}{\rho_c}, \quad \Omega_\Lambda = \frac{\Lambda c^2}{3H^2}, \quad \Omega_K = -\frac{Kc^2}{a^2H^2}. \tag{A.16}$$

With these parameters the first Friedmann equation (A.9a) becomes

$$H^2(t) = H_0^2 \left(\Omega_{m0} a^{-3} + \Omega_{r0} a^{-4} + \Omega_{\Lambda 0} + \Omega_{K0} a^{-2}\right), \tag{A.17}$$

where the curvature parameter today equals $\Omega_{K0} = 1 - \sum \Omega_{i0}$ and is close to zero.

A.2 LINEAR STRUCTURE FORMATION

While on the largest scales the Universe is homogeneous and isotropic, it contains structures such as galaxies and galaxy clusters. The growth of these structures should be worked out in terms of General Relativity but, since their size is much smaller than the scale of the Universe, i. e. the Hubble length $l_H = {}^c/_H$, and velocities are non-relativistic, any effects of curvature and propagation of information at a finite speed can be neglected. Then it is sufficient to work with Newtonian dynamics.
A perfect fluid under the influence of gravity obeys the hydrodynamic equations together with the Poisson equation for the gravitational potential Φ:

$$\partial_t \rho + \nabla \cdot (\rho \vec{u}) = 0, \tag{A.18}$$

$$\partial_t \vec{u} + (\vec{u} \cdot \nabla)\, \vec{u} = -\frac{\nabla p}{\rho} - \nabla \Phi, \tag{A.19}$$

$$\nabla^2 \Phi = 4\pi G \rho. \tag{A.20}$$

The first is the continuity equation stating the conservation of mass in a given volume: the change of a fluid element's density in time is given by the difference of in- and out-flow of mass. The second is the Euler equation which is a momentum conservation equation. The acceleration of a fluid element is given by the forces, i. e. pressure gradient and gravity, acting on it. The last is the Poisson equation meaning that the curvature of the gravitational potential is sourced by the mass density.
The density ρ, velocity $\vec{u}$, pressure P and gravitational potential Φ are functions of time t and position $\vec{x}$ since we are now considering the formation of inhomogeneous structures. We will decompose these quantities in a homogeneous and isotropic background and a small perturbation. For any quantity $Q(t,\vec{x})$ we write:

$$Q(t,\vec{x}) = Q_b(t) + \delta Q(t,\vec{x}), \tag{A.21}$$

where the subscript b indicates the background solution. The background quantities solve equations (A.18)-(A.20) exactly and have the form

$$\rho_b = \rho_0 a^{-3}, \quad \vec{u}_b = \frac{\dot{a}}{a}\vec{r} = H(t)\vec{r}, \quad \Phi_b = \frac{2\pi G}{3}\rho_b r^2, \tag{A.22}$$

and the scale-factor obeys Friedmann's equations. The subscript 0 refers to the value today, when $a_0 = 1$.
We can now plug in the perturbed quantities into (A.18)-(A.20), use the fact that the background solves the equations separately and keep only terms linear in the perturbations. We then arrive at

$$\begin{aligned} \partial_t\delta\rho + 3H\delta\rho + H\vec{r}\cdot\nabla\delta\rho + \rho\nabla\cdot\delta\vec{u} &= 0 && \text{(A.23)}\\ \partial_t\delta\vec{u} + 3H\delta\vec{u} + H\vec{r}\cdot\nabla\delta\vec{u} &= -\frac{\nabla\delta P}{\rho} - \nabla\delta\Phi && \text{(A.24)}\\ \nabla^2\delta\Phi &= 4\pi G\delta\rho. && \text{(A.25)} \end{aligned}$$

Usually the equations are expressed in terms of the density contrast $\delta = \delta\rho/\bar{\rho}$ and comoving coordinates $\vec{x} = \vec{r}/a$ are introduced. Spatial derivatives must be changed accordingly $\nabla_x = a\nabla_r$, and from the total differential of an arbitrary function $f(t,\vec{r})$

$$df = \partial_t f dt + \nabla_r f d\vec{r} = (\partial_t + H\vec{x}\cdot\nabla_x) f dt + \nabla_x f d\vec{x} \tag{A.26}$$

the partial time derivative in physical coordinates must be augmented by the advective derivative with the cosmic flow. Then the linearised hydrodynamical equations are

$$\begin{aligned} \partial_t\delta + \nabla\cdot\vec{v} &= 0 && \text{(A.27)}\\ \partial_t\vec{v} + 2H\vec{v} &= -\frac{\nabla\delta P}{a^2\bar{\rho}} - \frac{\nabla\delta\Phi}{a^2} && \text{(A.28)}\\ \nabla^2\Phi &= 4\pi G\bar{\rho}a^2\delta, && \text{(A.29)} \end{aligned}$$

where we introduced the comoving peculiar velocity $\vec{v} = {}^{\delta\vec{u}}/_{a}$ and omitted the reference to the comoving coordinate $\vec{x}$ in the gradient terms. In addition to these equations we need an equation of state relating the density and pressure perturbations

$$\delta P = c_s^2\delta\rho, \tag{A.30}$$

with the speed of sound c_s.

A.2.1 *Density Perturbations*

The linearised equations can be combined to yield a second order equation for the density contrast

$$\ddot{\delta} + 2H\dot{\delta} - \left(\frac{c_s^2 \nabla\delta}{a^2} + 4\pi G\rho\delta\right) = 0, \tag{A.31}$$

which is usually transformed into Fourier-space, i. e. the density contrast is decomposed into plane-waves (cf. B.2.1). In Fourier space the evolution equation for each mode $\vec{k}$ reads

$$\ddot{\delta}_k + 2H\dot{\delta}_k + \left(\frac{k^2 c_s^2}{a^2} - 4\pi G\rho\right)\delta_k = 0. \tag{A.32}$$

From this equation it becomes apparent that pressure gradients will counteract the gravitational contraction on small scales and lead to oscillations. The scale where gravitational and pressure forces are in equilibrium is called the comoving Jeans scale

$$k_J = \frac{2a\sqrt{\pi G\rho}}{c_s}. \tag{A.33}$$

Any perturbations on scales smaller than the Jeans scale ($k > k_J$) will oscillate and on larger scales ($k < k_J$) either grow or decay.
On scales much larger than the Jeans scale or in pressureless fluids, i. e. dark matter, pressure gradients can be neglected and the density contrast has a growing and decaying solution

$$\delta_k(a) = C_1 D_+(a) + C_2 D_-(a) \simeq \delta_0 D_+(a), \tag{A.34}$$

that depend on the energy content of the Universe. Only the growing solution will be of interest and is

$$D_+(a) = \frac{5a}{2}\Omega_m(a)\left(\Omega_m^{4/7}(a) - \Omega_\Lambda(a) + \left(1 + \frac{\Omega_m}{2}\right)\left(1 + \frac{\Omega_\Lambda(a)}{70}\right)\right)^{-1}, \tag{A.35}$$

as given by Bernardeau et al. [7]. We give two examples:

- in the matter-dominated era with $\Omega_{m0} = 1$ density perturbations grow as the scale factor a
- in the radiation-dominated era density perturbations grow proportional to a^2.

A.2.2 *Velocity Perturbations*

The peculiar velocity $\delta\vec{u}$ of structures can also be read off the linearised equations. The continuity equation (A.27) yields for the velocity divergence

$$\nabla \cdot \delta\vec{u} = -a\dot{a}\frac{d\delta}{da} = -\dot{a}\frac{d\ln D_+}{d\ln a}\delta. \tag{A.36}$$

Commonly the logarithmic derivative of the growth factor is abbreviated as $f = \frac{d\ln D_+}{d\ln a}$ which is the growth rate. Then the peculiar velocity in linear theory is given by

$$\delta\vec{u} = i\frac{\vec{k}}{k^2}\dot{a}f(a)\delta. \tag{A.37}$$

For a pressureless fluid, Euler's equation in its linearised form (A.28) suggests that the peculiar velocity is proportional to the gradient of the potential perturbation. Employing the ansatz $\delta\vec{u} = u(t)\nabla\delta\Phi$ we arrive at

$$u(t) = -\frac{2f(a)}{3aH\Omega}, \tag{A.38}$$

where $H(t)$ the Hubble function and $\Omega = \sum_i \Omega_i$ is the sum over the energy density parameters as defined in (A.16).
By taking the solenoidal part, i. e. the velocity components perpendicular to the wave-vector $\vec{k}$, of Euler's equation (A.28) we find

$$\delta\vec{u}_\perp \propto a^{-1}. \tag{A.39}$$

Thus, the curl of the peculiar velocity in linear theory decays inversely proportional to the scale factor from whatever initial value it had. Therefore it is safe to assume, that the peculiar velocity field is sourced by a scalar potential initially.

B

MATHEMATICAL BACKGROUND

B.1 NOTATION AND ABBREVIATIONS

B.1.1 *Tensor Notation*

In KFT the dynamical fields are the microscopic degrees of freedom of a canonical ensemble of N classical particles. Each particle may be labeled by a latin letter $j, k, l, \dots = 1 \dots N$ and therefore its position in 6-dimensional phase-space is

$$\vec{x}_j(t) = \begin{pmatrix} \vec{q}_j(t) \\ \vec{p}_j(t) \end{pmatrix}, \tag{B.1}$$

where $\vec{q}_j$ is the position and $\vec{p}_j$ the canonical momentum. In order to keep notations short and simple, we adopt the tensor notation of Bartelmann et al. [6] and organise the phase-space coordinates of all particles in tensors

$$\mathbf{x}(t) = \vec{x}_j(t) \otimes \vec{e}_j = \begin{pmatrix} \vec{q}_j(t) \\ \vec{p}_j(t) \end{pmatrix} \otimes \vec{e}_j, \tag{B.2}$$

where summation over repeated indices is implied. The N-dimensional vectors $\vec{e}_j$ label the particles with only the j-th component being non-vanishing and unity, i. e. $(\vec{e}_j)_i = \delta_{ij}$. We will also bundle the positions $\mathbf{q}(t)$ and momenta $\mathbf{p}(t)$ in the same way

$$\mathbf{q}(t) = \vec{q}_j(t) \otimes \vec{e}_j, \qquad \mathbf{p}(t) = \vec{p}_j(t) \otimes \vec{e}_j \tag{B.3}$$

for convenience. The properties of the tensor product are

$$(a \otimes b)(c \otimes d) = (ac) \otimes (cd) \tag{B.4}$$

$$(a \otimes b)^\intercal = a^\intercal \otimes b^\intercal \tag{B.5}$$

$$\mathrm{Tr}(a \otimes b) = \mathrm{Tr}a \cdot \mathrm{Tr}b, \tag{B.6}$$

and we define the scalar product of two tensors of type (B.2) by

$$\langle \mathbf{a}, \mathbf{b} \rangle \equiv (\vec{a}_j \otimes \vec{e}_j) \cdot \left(\vec{b}_k \otimes \vec{e}_k\right) = \vec{a}_j \cdot \vec{b}_k \delta_{jk} = \vec{a}_j \cdot \vec{b}_j, \tag{B.7}$$

with an implied summation over repeated indices. In this notation the 6-dimensional phase-space gradient for the j-th particle takes the form

$$\nabla_j = \begin{pmatrix} \nabla_{q_j} \\ \nabla_{p_j} \end{pmatrix}, \tag{B.8}$$

where the gradient ∇_{q_j} acts on the position and ∇_{p_j} acts on the momentum of the j-th particle. We can extend this along the lines of (B.2) to all N particles.
Apart from the particles' respective phase-space coordinates we attribute source fields $\mathbf{J}(t)$ and $\mathbf{K}(t)$ to particles

$$\mathbf{J}(t) = \begin{pmatrix} \vec{J}_{q_j}(t) \\ \vec{J}_{p_j}(t) \end{pmatrix} \otimes \vec{e}_j, \quad \mathbf{K}(t) = \begin{pmatrix} \vec{K}_{q_j}(t) \\ \vec{K}_{p_j}(t) \end{pmatrix} \otimes \vec{e}_j, \tag{B.9}$$

with the obvious reduction to the position and momentum subspaces.

B.1.2 *Abbreviations*

Aside from the tensorial notation we introduce additional abbreviations. Integrals over 6N-dimensional phase-space are written as

$$\int d\mathbf{x} = \int d\mathbf{q} \int d\mathbf{p} = \left(\prod_j^N \int d^3 q_j \right) \left(\prod_j^N \int d^3 p_j \right), \tag{B.10}$$

with the obvious reduction to position and momentum subspaces. Since we will encounter various Fourier transformations (cf. B.2.1), we introduce the following shorthand notations

$$\int_q = \int d^3 q, \quad \int_k = \int \frac{d^3 k}{(2\pi)^3}, \tag{B.11}$$

where $\vec{q}$ is the real-space and $\vec{k}$ the Fourier-space position vector.
The macroscopic fields that we calculate from the generating functional (2.8) in the body of this work depend on both time t and position in Fourier-space $\vec{k}$, which we abbreviate as $1 = \left(\vec{k}_1, t_1\right)$ and $-1 = \left(-\vec{k}_1, t_1\right)$ for notational convenience.
We will also abbreviate parial derivatives with respect to time with either of the following

$$\frac{\partial}{\partial t} f(t) = \partial_t f(t) = \dot{f}(t). \tag{B.12}$$

B.2 MATHEMATICAL CONCEPTS

B.2.1 *Fourier Transform*

The Fourier transform of a function $f(\vec{q})$ in real space represents a decomposition into plane waves with wave number $\vec{k}$. It is defined by the integral

$$\tilde{f}(\vec{k}) = \mathcal{F}[f(\vec{q})] = \int_q f(\vec{q}) e^{-i\vec{k}\cdot\vec{q}}, \tag{B.13}$$

and its inverse is given by

$$f(\vec{q}) = \mathcal{F}^{-1}[\tilde{f}(\vec{k})] = \int_k \tilde{f}(\vec{k}) e^{i\vec{k}\cdot\vec{q}} \tag{B.14}$$

with the abbreviations introduced in (B.11).
In this work we will frequently make use of two particular Fourier-transforms, namely for the Dirac delta distribution

$$\mathcal{F}[1] = \int_q e^{-i\vec{k}\cdot\vec{q}} = (2\pi)^3 \delta_D(\vec{k}), \tag{B.15}$$

and for a Gaussian distribution

$$\mathcal{F}\left[\frac{1}{\sqrt{(2\pi)^3}\sigma} \exp\left(-\frac{q^2}{2\sigma^2} \right) \right] = \exp\left(-\frac{\sigma^2 k^2}{2} \right), \tag{B.16}$$

which is again a Gaussian distribution but with inverse width.
An important property of Fourier transforms is expressed by the convolution theorem,

i. e. the Fourier transform of a convolution in real space turns into a multiplication in Fourier space:

$$\mathcal{F}[f * g] = \mathcal{F}\left[\int_x f(\vec{x})g(\vec{q}-\vec{x})\right] = \tilde{f}(\vec{k})\tilde{g}(\vec{k}), \tag{B.17}$$

which also applies to a convolution in Fourier space and the inverse transform.
Another property we will frequently make use of is the relation between the derivative of a function in real space and its Fourier transform:

$$\mathcal{F}[\nabla_q f(\vec{q})] = i\vec{k}\tilde{f}(\vec{k}), \tag{B.18}$$

which is readily proven by a partial integration and assuming the function vanishes at infinity. Of course this relation can be easily extended to higher order derivatives.

B.2.2 *Functional Derivative*

The main object of KFT is the generating functional $Z[\mathbf{J}, \mathbf{K}]$, which is an integral over phase-space weighted by a conditional probability. Information about macroscopic fields are obtained by appropriate functional derivatives acting on the generating functional.
In general a functional is a map from the set of continuous and differentiable functions into the set of real or complex numbers:

$$F : C^\infty \mapsto \mathbb{R} \quad \text{or} \quad F : C^\infty \mapsto \mathbb{C}. \tag{B.19}$$

An easy example is the integral of a function

$$F[\varphi] = \int_a^b dx\varphi(x) \tag{B.20}$$

over an interval (a, b). The functional derivative $\frac{\delta F}{\delta \varphi(x)}$ quantifies the change of the functional F when varying the function φ. Say the variation of the function by a small amount can be written as $\delta\varphi(x) = \epsilon\phi(x)$ with ϵ being an infinitesimal number and some function $\phi(x)$. Then the functional derivative is defined by

$$\int dx \frac{\delta F[\varphi]}{\delta\varphi(x)}\phi(x) = \frac{d}{d\epsilon}F[\varphi + \epsilon\phi]\Big|_{\epsilon=0}. \tag{B.21}$$

Analogous to the usual derivative, the functional derivative is linear, obeys the product and the chain rules, and the order of mixed functional derivatives can be chosen arbitrarily.
While (B.21) is the formal definition of the functional derivative and closely related to the principle of least action, we will give the reader a few relations that will be used frequently in the calculations of this work. The functional derivative of a function $\varphi(x)$ with respect to itself is

$$\frac{\delta}{\delta\varphi(y)}\varphi(x) = \delta_D(x-y), \tag{B.22}$$

where $x, y \in \mathbb{R}^d$ with arbitrary dimension d. If the dimension is different from one, we understand that the difference $(x-y)$ is zero in every component.

We will often apply the functional derivative to an exponential of an integral over a product of functions. The result reads

$$\begin{aligned}\frac{\delta}{\delta\varphi(y)}\exp\left(\int dx\varphi(x)\xi(x)\right)&\\ &= \exp\left(\int dx\varphi(x)\xi(x)\right)\int dx\delta_D(x-y)\xi(x)\\ &= \xi(y)\exp\left(\int dx\varphi(x)\xi(x)\right).\end{aligned} \tag{B.23}$$

Since the source fields (B.9) are 6-dimensional vectors for each particle, we encounter the functional derivative with respect to vector-valued functions. We interpret this as a functional gradient

$$\frac{\delta}{\delta\vec{\varphi}(\vec{x})} = \left(\frac{\delta}{\delta\varphi_1(\vec{x})},\dots,\frac{\delta}{\delta\varphi_n(\vec{x})}\right)^T \tag{B.24}$$

for an n-component function.

B.2.3 *Green's Function*

In Chapter 2 we will discuss the trajectories of particles through phase-space by means of Green's functions, which are the solutions to the homogeneous (free) equations of motion. A homogeneous equation of the form

$$(\partial_t + a(t))\,f(t) = 0 \tag{B.25}$$

is solved by

$$f_R(t) = f_0\exp\left(-\int_{t_0}^{t} dt' a(t')\right) \tag{B.26a}$$

$$f_A(t) = f_0\exp\left(\int_{t}^{t_0} dt' a(t')\right), \tag{B.26b}$$

where the indices denote the retarded f_R and advanced f_A solutions and f_0 denoting the initial value. Since we are only interested in the retarded solution of this problem, we discard the advanced solution for now.
Knowing the solution of (B.25) allows solving the inhomogeneous equation

$$(\partial_t + a(t))\,f(t) = g(t) \tag{B.27}$$

by variation of constants. The retarded solution is given by

$$f_R(t) = \int^{t} dt' g(t')\exp\left(-\int_{t'}^{t} dt'' a(t'')\right)\theta(t-t'). \tag{B.28}$$

Therefore the retarded Green's function to the problem is

$$G_R(t,t') = \exp\left(-\int_{t'}^{t} dt'' a(t'')\right)\theta(t-t'). \tag{B.29}$$

The complete solution is given by a superposition of the homogeneous and particular solutions

$$f(t) = G_R(t,t_0)f_0 + \int_{t_0}^{t} dt' G_R(t,t')g(t') \tag{B.30}$$

with appropriate boundary conditions and $t > t_0$.
We give here a simple example from classical mechanics and leave the discussion of motion in expanding space to the body of this work. Imagine a particle moving under the influence of an interaction potential through phase-space with initial position $\vec{x}^{(i)} = \left(\vec{q}^{(i)}, \vec{p}^{(i)}\right)^T$. Its equation of motion is given by the Hamiltonian equations

$$\partial_t \vec{q} = \nabla_p H(\vec{q}, \vec{p}, t), \quad \partial_t \vec{p} = -\nabla_q H(\vec{q}, \vec{p}, t), \tag{B.31}$$

where $H(\vec{q}, \vec{p}, t)$ is the Hamiltonian of the motion

$$H(\vec{q}, \vec{p}, t) = \frac{p^2}{2m} + V(\vec{q}, t). \tag{B.32}$$

Rewriting the equations of motion for the phase-space vector $\vec{x}$ they read

$$\partial_t x = \mathcal{I} \nabla H(\vec{q}, \vec{p}, t) = \begin{pmatrix} \nabla_p \\ -\nabla_q \end{pmatrix} H(\vec{q}, \vec{p}, t) = \begin{pmatrix} \vec{p}/m \\ -\nabla_q V \end{pmatrix}, \tag{B.33}$$

where we used the form of the symplectic matrix $\mathcal{I}$ and the form of the Hamiltonian. We can now split the motion into the ballistic free motion of the particle due to its initial momentum $\vec{p}^{(i)}$ and treat the interaction due to the potential $V(\vec{q}, t)$ as the inhomogeneity. Then the Green's function for this problem reads

$$G_R(t, t') = \begin{pmatrix} I_3 & \frac{t-t'}{m} I_3 \\ 0 & I_3 \end{pmatrix} \theta(t - t'), \tag{B.34}$$

such that the trajectory of this particle through phase-space is given by

$$\vec{x}(t) = G_R(t, t^{(i)}) \vec{x}^{(i)} - \int_{t^{(i)}}^{t} dt' G_R(t, t') \begin{pmatrix} 0 \\ \nabla_q V(\vec{q}, t') \end{pmatrix}, \tag{B.35}$$

that is a sum of the free motion and the correction due to a potential interaction, e. g. gravity.

C

SCALARS OF THE 2-POINT MOMENTUM-DENSITY CORRELATION TENSOR

C.1 APPROXIMATED INITIAL CORRELATIONS

Here we give expressions for the power-spectrum of the momentum-density, divergence and curl of this field based on our calculations of Section 4.1.

$$\mathrm{Tr}\langle\vec{\Pi}\otimes\vec{\Pi}\rangle = \bar{\rho}^2\delta_D(\vec{k}_1+\vec{k}_2)(2\pi)^3\left(A^{tr}_{free}+B^{tr}_{total}+C^{tr}_{total}\right), \tag{C.1}$$

$$\langle\nabla\cdot\vec{\Pi}\nabla\cdot\vec{\Pi}\rangle = \bar{\rho}^2\delta_D(\vec{k}_1+\vec{k}_2)(2\pi)^3\left(A^{div}_{free}+B^{div}_{total}+C^{div}_{total}\right), \tag{C.2}$$

$$\langle\left(\nabla\times\vec{\Pi}\right)\cdot\left(\nabla\times\vec{\Pi}\right)\rangle = \bar{\rho}^2\delta_D(\vec{k}_1+\vec{k}_2)(2\pi)^3\left(A^{curl}_{free}+B^{curl}_{total}+C^{curl}_{total}\right), \tag{C.3}$$

where the functions A^i_{free} denotes the free contributions, B^i_{total} denotes the corrections from the diagrams in Figure 6, and C^i_{total} denotes the corrections from the diagrams in Figure 7, with $i = (tr, div, curl)$. The explicit form of the terms is after renaming $\vec{k}_1 = -\vec{k}_2 = \vec{k}$:

$$\begin{aligned}
A^{tr}_{free} =& (g^{t,t_0}_{pp})^2 e^{Q_D}\left[P_\psi(k)k^2\left(1-\frac{2\sigma_1^2}{3}(g^{t,t_0}_{qp})^2k^2\right)\right.\\
&\left.+(g^{t,t_0}_{qp})^2\int_{k'}P_\psi(k')P_\psi(\Delta)\left(\vec{\Delta}\cdot\vec{k}\right)\left(\left(\vec{\Delta}\cdot\vec{k}\right)k'^2+\left(\vec{k}\cdot\vec{k}'\right)\left(\vec{\Delta}\cdot\vec{k}'\right)\right)\right],
\end{aligned} \tag{C.4}$$

$$\begin{aligned}
B^{tr}_{total} =& 2(g^{t,t_0}_{pp})^2\int dt' g^{t,t'}_{qp}g^{t',t_0}_{qp}\left[e^{Q_D}\nu(k,t')\frac{\sigma_1^2}{3}(g^{t,t_0}_{qp}-g^{t',t_0}_{qp})k^6P_\psi(k)\right.\\
&+\int_{k'}e^{Q_D}\nu(k',t')\left(\vec{k}\cdot\vec{k}'\right)\times\\
&\times\left[-g^{t,t_0}_{qp}k'^2P_\psi(\Delta)P_\psi(k')\left(\Delta^2\left(\vec{k}\cdot\vec{k}'\right)+\left(\vec{\Delta}\cdot\vec{k}'\right)\left(\vec{\Delta}\cdot\vec{k}\right)\right)\right.\\
&+k'^2P_\psi(k)P_\psi(k')\left(g^{t,t_0}_{qp}\vec{k}-g^{t',t_0}_{qp}\vec{k}'\right)\cdot\left(\vec{k}'k^2+\vec{k}\left(\vec{k}\cdot\vec{k}'\right)\right)\\
&\left.\left.+g^{t',t_0}_{qp}\left(\vec{\Delta}\cdot\vec{k}\right)\left(\vec{\Delta}\cdot\vec{k}'\right)\left(\vec{k}\cdot\vec{k}'\right)P_\psi(k)P_\psi(\Delta)\right]\right],
\end{aligned} \tag{C.5}$$

$$\begin{aligned}
C^{tr}_{total} =& 2g^{t,t_0}_{pp}\int dt' g^{t,t'}_{pp}g^{t',t_0}_{qp}\left[e^{Q_D}\left(\nu(k,t')(g^{t,t_0}_{qp})^2\frac{\sigma_1^2}{3}k^6P_\psi(k)\right.\right.\\
&\left.-g^{t',t_0}_{qp}g^{t,t_0}_{qp}\int_{k'}\left(\vec{k}\cdot\vec{k}'\right)^2\left(\vec{\Delta}\cdot\vec{k}\right)^2P_\psi(k')P_\psi(\Delta)\right)\\
&+\int_{k'}e^{Q_D}\nu(k',t')\left[\left(\vec{k}\cdot\vec{k}'\right)P_\psi(k)\left(g^{t,t_0}_{qp}\vec{k}-g^{t',t_0}_{qp}\vec{k}'\right)\right.\\
&\cdot\left(\vec{\Delta}g^{t',t_0}_{qp}\left(\vec{k}\cdot\vec{k}'\right)\left(\vec{\Delta}\cdot\vec{k}'\right)P_\psi(\Delta)+\vec{k}k'^2\left(\vec{k}'\cdot\left(g^{t,t_0}_{qp}\vec{k}-g^{t',t_0}_{qp}\vec{k}'\right)\right)P_\psi(k')\right)\\
&-g^{t,t_0}_{qp}k'^2\left(\vec{\Delta}\cdot\left(g^{t,t_0}_{qp}\vec{k}-g^{t',t_0}_{qp}\vec{k}'\right)\right)P_\psi(\Delta)P_\psi(k')\times\\
&\left.\left.\times\left(\left(\vec{\Delta}\cdot\vec{k}'\right)\left(\vec{k}\cdot\vec{k}'\right)+k'^2\left(\vec{\Delta}\cdot\vec{k}\right)\right)\right]\right],
\end{aligned} \tag{C.6}$$

with the definition $\vec{\Delta} := \vec{k} - \vec{k}'$. For the divergence spectrum the explicit expressions are

$$\begin{aligned}
A^{\text{div}}_{\text{free}} =& (g^{t,t_0}_{pp})^2 e^{Q_D} \left[P_\psi(k) k^4 \left(1 - \frac{2\sigma_1^2}{3} (g^{t,t_0}_{qp})^2 k^2 \right) \right. \\
& \left. + 2 (g^{t,t_0}_{qp})^2 \int_{k'} P_\psi(k') P_\psi(\Delta) \left(\vec{\Delta} \cdot \vec{k} \right)^2 \left(\vec{k} \cdot \vec{k}' \right)^2 \right], \qquad \text{(C.7)} \\
B^{\text{div}}_{\text{total}} =& 2 (g^{t,t_0}_{pp})^2 \int dt' g^{t,t'}_{qp} g^{t',t_0}_{qp} \left[e^{Q_D} \nu(k,t') \frac{\sigma_1^2}{3} (g^{t,t_0}_{qp} - g^{t',t_0}_{qp}) k^8 P_\psi(k) \right. \\
& + \int_{k'} e^{Q_D} \nu(k',t') \left(\vec{k} \cdot \vec{k}' \right) \times \\
& \times \left[-2 g^{t,t_0}_{qp} k'^2 P_\psi(\Delta) P_\psi(k') \left(\vec{\Delta} \cdot \vec{k} \right)^2 \left(\vec{k} \cdot \vec{k}' \right) \right. \\
& + k^2 k'^2 P_\psi(k) P_\psi(k') \left(g^{t,t_0}_{qp} \vec{k} - g^{t',t_0}_{qp} \vec{k}' \right) \cdot \left(\vec{k}' k^2 + \vec{k} \left(\vec{k} \cdot \vec{k}' \right) \right) \\
& \left. \left. + g^{t',t_0}_{qp} \left(\vec{\Delta} \cdot \vec{k} \right) \left(\vec{\Delta} \cdot \vec{k}' \right) \left(\vec{k} \cdot \vec{k}' \right) k^2 P_\psi(k) P_\psi(\Delta) \right] \right], \qquad \text{(C.8)} \\
C^{\text{div}}_{\text{total}} =& 2 g^{t,t_0}_{pp} \int dt' g^{t,t'}_{pp} g^{t',t_0}_{qp} \left[e^{Q_D} \left(\nu(k,t') (g^{t,t_0}_{qp})^2 \frac{\sigma_1^2}{3} k^8 P_\psi(k) \right. \right. \\
& \left. - g^{t',t_0}_{qp} g^{t,t_0}_{qp} k^2 \int_{k'} \left(\vec{k} \cdot \vec{k}' \right)^2 \left(\vec{\Delta} \cdot \vec{k} \right)^2 P_\psi(k') P_\psi(\Delta) \right) \\
& + \int_{k'} e^{Q_D} \nu(k',t') \left(\vec{k} \cdot \vec{k}' \right) \left[k^2 P_\psi(k) \left(g^{t,t_0}_{qp} \vec{k} - g^{t',t_0}_{qp} \vec{k}' \right) \right. \\
& \left. \cdot \left(\vec{\Delta} g^{t',t_0}_{qp} \left(\vec{k} \cdot \vec{k}' \right) \left(\vec{\Delta} \cdot \vec{k}' \right) P_\psi(\Delta) + \vec{k} k'^2 \left(\vec{k}' \cdot \left(g^{t,t_0}_{qp} \vec{k} - g^{t',t_0}_{qp} \vec{k}' \right) \right) P_\psi(k') \right) \\
& \left. \left. - 2 g^{t,t_0}_{qp} k'^2 \left(\vec{\Delta} \cdot \left(g^{t,t_0}_{qp} \vec{k} - g^{t',t_0}_{qp} \vec{k}' \right) \right) P_\psi(\Delta) P_\psi(k') \left(\vec{\Delta} \cdot \vec{k} \right) \left(\vec{k} \cdot \vec{k}' \right) \right] \right]. \qquad \text{(C.9)}
\end{aligned}$$

For the curl spectrum we multiply the terms of the trace with k^2 and subtract the divergence terms

$$\begin{aligned}
A^{\text{curl}}_{\text{free}} =& (g^{t,t_0}_{pp} g^{t,t_0}_{qp})^2 e^{Q_D} \int_{k'} P_\psi(k') P_\psi(\Delta) \left(\vec{\Delta} \cdot \vec{k} \right) \times \\
& \times \left[k^2 k'^2 \left(\vec{\Delta} \cdot \vec{k} \right) + k^2 \left(\vec{k} \cdot \vec{k}' \right) \left(\vec{\Delta} \cdot \vec{k}' \right) - 2 \left(\vec{k} \cdot \vec{k}' \right)^2 \left(\vec{\Delta} \cdot \vec{k} \right) \right], \qquad \text{(C.10)} \\
B^{\text{curl}}_{\text{total}} =& 2 (g^{t,t_0}_{pp})^2 \int dt' g^{t,t'}_{qp} g^{t',t_0}_{qp} g^{t,t_0}_{qp} \int_{k'} e^{Q_D} \nu(k',t') P_\psi(k') P_\psi(\Delta) k'^2 \left(\vec{k} \cdot \vec{k}' \right) \times \\
& \times \left[2 \left(\vec{k} \cdot \vec{k}' \right) \left(\vec{\Delta} \cdot \vec{k} \right)^2 - k^2 \Delta^2 \left(\vec{k} \cdot \vec{k}' \right) - k^2 \left(\vec{\Delta} \cdot \vec{k} \right) \left(\vec{\Delta} \cdot \vec{k}' \right) \right], \qquad \text{(C.11)} \\
C^{\text{curl}}_{\text{total}} =& 2 g^{t,t_0}_{pp} \int dt' g^{t,t'}_{pp} g^{t',t_0}_{qp} g^{t,t_0}_{qp} \int_{k'} e^{Q_D} \nu(k',t') P_\psi(k') P_\psi(\Delta) k'^2 \left(\vec{\Delta} \cdot \left(g^{t,t_0}_{qp} \vec{k} - g^{t',t_0}_{qp} \vec{k} \right) \right) \times \\
& \times \left[2 \left(\vec{k} \cdot \vec{k}' \right)^2 \left(\vec{\Delta} \cdot \vec{k} \right) - k^2 \left(\vec{\Delta} \cdot \vec{k}' \right) \left(\vec{k} \cdot \vec{k}' \right) - k^2 k'^2 \left(\vec{\Delta} \cdot \vec{k} \right) \right]. \qquad \text{(C.12)}
\end{aligned}$$

It is important to note at this point that the power-spectrum of $\nabla \otimes \vec{\Pi}$ is completely determined by mode-coupling terms. And is therefore a non-linear effect.

C.2 FULL INITIAL MOMENTUM CORRELATIONS

In this section we give only the free contributions since the explicit expressions including the first order interactions do not provide any more insight than the expressions given in Section 4.2.

$$\begin{aligned}\mathrm{Tr}\left\langle \vec{\Pi}\otimes\vec{\Pi}\right\rangle =&\bar{\rho}^2\delta_D(\vec{k}+\vec{k}')(2\pi)^3e^{Q_D}\left[\left\{\int_q \exp(Q(q)+i\vec{k}\cdot\vec{q})\right\}\left(g^{t,0}_{qp}g^{t,0}_{pp}\frac{\sigma_I^2}{3}\right)^2k^2\right.\\&+\left\{\int_q \exp(Q(q)+i\vec{k}\cdot\vec{q})a_{\parallel}(q)\right\}\left[(g^{t,0}_{pp})^2\left(\frac{2\sigma_I^2}{3}(g^{t,0}_{qp}\vec{k})^2-1\right)\right]\\&+\left\{\int_q \exp(Q(q)+i\vec{k}\cdot\vec{q})a^2_{\parallel}(q)\right\}(g^{t,0}_{qp}g^{t,0}_{pp})^2k^2\\&\left.-\left\{\int_q \exp(Q(q)+i\vec{k}\cdot\vec{q})a_{\perp}(q)\right\}2(g^{t,0}_{pp})^2\right],\end{aligned}\tag{C.13}$$

$$\begin{aligned}\vec{k}\cdot\left\langle \vec{\Pi}\otimes\vec{\Pi}\right\rangle\vec{k} =&\bar{\rho}^2\delta_D(\vec{k}+\vec{k}')(2\pi)^3e^{Q_D}\left[\left\{\int_q \exp(Q(q)+i\vec{k}\cdot\vec{q})\right\}\left(g^{t,0}_{qp}g^{t,0}_{pp}\frac{\sigma_I^2}{3}\right)^2k^4\right.\\&+\left\{\int_q \exp(Q(q)+i\vec{k}\cdot\vec{q})a_{\parallel}(q)\right\}\left[(g^{t,0}_{pp}\vec{k})^2\left(\frac{2\sigma_I^2}{3}(g^{t,0}_{qp}\vec{k})^2-1\right)\right]\\&\left.+\left\{\int_q \exp(Q(q)+i\vec{k}\cdot\vec{q})a^2_{\parallel}(q)\right\}(g^{t,0}_{qp}g^{t,0}_{pp})^2k^4\right],\end{aligned}\tag{C.14}$$

$$\begin{aligned}\langle\left(\nabla\times\vec{\Pi}\right)\cdot\left(\nabla\times\vec{\Pi}\right)\rangle =&\bar{\rho}^2\delta_D(\vec{k}+\vec{k}')(2\pi)^3e^{Q_D}\times\\&\times\left[-2(g^{t,0}_{pp}k)^2\int_q \exp(Q(q)+i\vec{k}\cdot\vec{q})a_{\perp}(q)\right].\end{aligned}\tag{C.15}$$

The quadratic form $Q(q)$ is defined by

$$Q(q) := -(g^{t,t_0}_{qp})^2k^2a_{\parallel}(q),\tag{C.16}$$

for a 2-point function. We omit at this point the explicit expressions for the corrections of the linear interaction order, since their form does not provide any insight. The terms are readily written down from (4.26).

C.3 BORN'S APPROXIMATION

C.3.1 *First/Naive Approximation*

In the following we make use of the fact that the force on particle one is opposite to the force on particle two but of the same magnitude:

$$\begin{aligned}
&\mathrm{Tr}\left\langle \vec{\Pi}\otimes\vec{\Pi}\right\rangle \\
&= e^{Q_D-\mathbf{F}}\left[\left\{\int_q w(q)\right\}\left(\left(g_{qp}^{t,0}g_{pp}^{t,0}\frac{\sigma_1^2}{3}\right)^2 k^2 - 2ig_{qp}^{t,0}g_{pp}^{t,0}\frac{\sigma_1^2}{3}\vec{k}\cdot\vec{f}_1 - (\vec{f}_1)^2\right)\right. \\
&+\left\{\int_q w(q)a_{\parallel}(q)\right\}\left[(g_{pp}^{t,0})^2\left(\frac{2\sigma_1^2}{3}(g_{qp}^{t,0}\vec{k})^2-1\right) - 2ig_{qp}^{t,0}g_{pp}^{t,0}\vec{k}\cdot\vec{f}_1\right] \\
&\left.+\left\{\int_q w(q)a_{\parallel}^2(q)\right\}(g_{qp}^{t,0}g_{pp}^{t,0})^2k^2 - \left\{\int_q w(q)a_{\perp}(q)\right\}2(g_{pp}^{t,0})^2\right],
\end{aligned} \tag{C.17}$$

$$\begin{aligned}
&\vec{k}\cdot\left\langle \vec{\Pi}\otimes\vec{\Pi}\right\rangle\vec{k} \\
&= e^{Q_D-\mathbf{F}}\left[\left\{\int_q w(q)\right\}\left(\left(g_{qp}^{t,0}g_{pp}^{t,0}\frac{\sigma_1^2}{3}\right)^2 k^4 - 2ig_{qp}^{t,0}g_{pp}^{t,0}\frac{\sigma_1^2}{3}k^2\vec{k}\cdot\vec{f}_1 - (\vec{k}\cdot\vec{f}_1)^2\right)\right. \\
&+\left\{\int_q w(q)a_{\parallel}(q)\right\}\left[(g_{pp}^{t,0}\vec{k})^2\left(\frac{2\sigma_1^2}{3}(g_{qp}^{t,0}\vec{k})^2-1\right) - 2ig_{qp}^{t,0}g_{pp}^{t,0}k^2\vec{k}\cdot\vec{f}_1\right] \\
&\left.+\left\{\int_q w(q)a_{\parallel}^2(q)\right\}(g_{qp}^{t,0}g_{pp}^{t,0})^2k^4\right],
\end{aligned} \tag{C.18}$$

$$\begin{aligned}
&\left\langle \nabla\times\vec{\Pi}\cdot\nabla\times\vec{\Pi}\right\rangle = k^2\mathrm{Tr}\left\langle\vec{\Pi}\otimes\vec{\Pi}\right\rangle - \vec{k}\cdot\left\langle\vec{\Pi}\otimes\vec{\Pi}\right\rangle\vec{k} \\
&= e^{Q_D-\mathbf{F}}\left[\left\{\int_q w(q)\right\}\left((\vec{k}\cdot\vec{f}_1)^2-(\vec{f}_1)^2k^2\right) - 2(g_{pp}^{t,0}k)^2\int_q w(q)a_{\perp}(q)\right] \\
&= -2e^{Q_D-\mathbf{F}}(g_{pp}^{t,0}k)^2\int_q \exp(Q(q)+i\vec{k}\cdot\vec{q})a_{\perp}(q),
\end{aligned} \tag{C.19}$$

with $w(q) = \exp(Q(q)+i\vec{k}\cdot\vec{q})$

C.3.2 *Revised Approximation*

We showed the form of terms T_2 and T_3 in (4.51). Due to statistical homogeneity is the contribution of those terms the same and we may write

$$\begin{aligned}
2T_2 =& 2(2\pi)^3\bar{\rho}^2\delta_D(\mathbf{L}_q)g_{pp}^{t,0}e^{-\mathbf{F}}\int_{\vec{\kappa},t'} g_{pp}^{t,t'}\nu(\vec{k}-\vec{\kappa},t')e^{Q_D}\times \\
&\times\left[\frac{\sigma_1^2}{3}B^i\int_q e^{A(\vec{\kappa},\vec{q},t,t')} + \int_q (K_1^i+K_2^i)e^{A(\vec{\kappa},\vec{q},t,t')}\right],
\end{aligned} \tag{C.20}$$

with $\vec{\kappa} = \vec{k}-\vec{k}'$ and $i = (\mathrm{tr},\mathrm{div},\mathrm{curl})$. With the definition of the shift tensors and the projector

$$\mathbf{L}_q' = -\vec{\kappa}\otimes(\vec{e}_1-\vec{e}_2), \quad \mathbf{L}_p' = -(g_{qp}^{t,t_0}\vec{k}-g_{qp}^{t',t_0}\vec{k}')\otimes(\vec{e}_1-\vec{e}_2), \quad \hat{\pi}_{21}^{\parallel} = \frac{\vec{\kappa}\otimes\vec{\kappa}}{\kappa^2}, \tag{C.21}$$

we can write down the function

$$A(\vec{\kappa},\vec{q},t,t') = L'_{p_2}\hat{\pi}^{\parallel}_{21}L'_{p_1}\left(a_{\parallel}(q)-a_{\perp}(q)\right)+L'_{p_2}\cdot L'_{p_1}a_{\perp}(q)+i\vec{\kappa}\cdot\vec{q}$$
$$= -(g^{t,0}_{qp})^2\left[(1-\chi)k\mu-\chi\kappa\right]^2 a_{\parallel}(q)-(g^{t,0}_{qp})^2(1-\chi)^2(1-\mu^2)k^2a_{\perp}(q)+i\vec{\kappa}\cdot\vec{q}. \quad (C.22)$$

Here μ is the angle cosine between $\vec{k}$ and $\vec{\kappa}$, and $\chi := g^{t',t_0}_{qp}/g^{t,t_0}_{qp}$. The other functions B^i and $K^i_{1,2}$ are defined by scalar products

$$B^{tr} := \left(\vec{k}-\vec{\kappa}\right)\cdot L'_{p_2} = g^{t,0}_{qp}\left((1-\chi)k(k-\kappa\mu)-\chi\kappa(k\mu-\kappa)\right), \quad (C.23)$$

$$B^{div} := \vec{k}\cdot\left(\vec{k}-\vec{\kappa}\right)\vec{k}\cdot L'_{p_2} = g^{t,t_0}_{qp}k^2(k-\kappa\mu)((1-\chi)k-\chi\kappa\mu), \quad (C.24)$$

$$B^{curl} := k^2\left(\vec{k}-\vec{\kappa}\right)\cdot L'_{p_2}-\vec{k}\cdot\left(\vec{k}-\vec{\kappa}\right)\vec{k}\cdot L'_{p_2} = g^{t,0}_{qp}\chi\kappa^2k^2(1-\mu^2), \quad (C.25)$$

and the other kernels have the form

$$K^{tr}_1 = \left(\vec{k}-\vec{\kappa}\right)\cdot(\hat{\pi}^{\parallel}L'_{p_2})a_{\parallel}(q)$$
$$= g^{t,0}_{qp}\left(k\mu-\kappa\right)\left((1-\chi)k\mu-\chi\kappa\right)a_{\parallel}(q) \quad (C.26)$$
$$K^{tr}_2 = \left(\vec{k}-\vec{\kappa}\right)\cdot L'_{p_2}-\left(\vec{k}-\vec{\kappa}\right)\cdot(\hat{\pi}^{\parallel}L'_{p_2})a_{\perp}(q)$$
$$= g^{t,0}_{qp}(1-\chi)k^2(1-\mu^2)a_{\perp}(q) \quad (C.27)$$

for the trace, and

$$K^{div}_1 = \vec{k}\cdot\left(\vec{k}-\vec{\kappa}\right)\vec{k}\cdot(\hat{\pi}^{\parallel}L'_{p_2})a_{\parallel}(q)$$
$$= g^{t,0}_{qp}k^2\mu(k-\kappa\mu)\left((1-\chi)k\mu-\chi\kappa\right)a_{\parallel}(q) \quad (C.28)$$
$$K^{div}_2 = \vec{k}\cdot\left(\vec{k}-\vec{\kappa}\right)\left(\vec{k}\cdot L'_{p_2}-\vec{k}\cdot(\hat{\pi}^{\parallel}L'_{p_2})\right)a_{\perp}(q)$$
$$= g^{t,0}_{qp}(1-\chi)k^3(k-\kappa\mu)(1-\mu^2)a_{\perp}(q) \quad (C.29)$$

for the divergence, and

$$K^{curl}_1 = k^2K_1-K^{div}_1$$
$$= -g^{t,0}_{qp}(1-\mu^2)k^2\kappa\left((1-\chi)k\mu-\chi\kappa\right)a_{\parallel}(q) \quad (C.30)$$
$$K^{curl}_2 = k^2K_2-K^{div}_2$$
$$= g^{t,0}_{qp}(1-\chi)k^3\kappa(1-\mu^2)\mu a_{\perp}(q) \quad (C.31)$$

for the curl power-spectrum.
The fourth correction term can be written as

$$T_4 = -(2\pi)^3\bar{\rho}^2\delta_D(\mathbf{L}_q)e^{-\mathbf{F}}\int dt'\int dt''\int_{k',\kappa'} g^{t,t'}_{pp}g^{t,t''}_{pp}e^{Q_D}C^i\int_q e^{A'(\vec{\kappa}',\vec{q},t',t'')}, \quad (C.32)$$

with the shifts and projector

$$\mathbf{L}'_q = -\vec{\kappa}'\otimes(\vec{e}_1-\vec{e}_2), \quad \mathbf{L}'_p = -(g^{t,0}_{qp}\vec{k}-g^{t',0}_{qp}\vec{k}'-g^{t'',0}_{qp}\vec{k}'')\otimes(\vec{e}_1-\vec{e}_2), \quad (C.33)$$

$$\hat{\pi}^{\parallel}_{21} = \frac{\vec{\kappa}'\otimes\vec{\kappa}'}{\kappa'^2}, \quad (C.34)$$

and $\vec{\kappa}' = \vec{k}-\vec{k}'-\vec{k}''$. The kernels are

$$C^{tr} = \vec{k}\cdot\vec{k}' = k(k_1\mu\mu'-k-\kappa\mu'), \quad (C.35)$$

$$C^{div} = (\vec{k}_1\cdot\vec{k})(\vec{k}_1\cdot\vec{k}') = k_1^2k\mu\mu'(k_1-k\mu\mu'-\kappa\mu), \quad (C.36)$$

$$C^{curl} = k_1^2C^{tr}-C^{div} = k_1^2k(k(\mu^2\mu'^2-1)+\kappa\mu'(\mu^2-1)). \quad (C.37)$$

BIBLIOGRAPHY

[1] R. E. Angulo, V. Springel, S. D. M. White, A. Jenkins, C. M. Baugh, and C. S. Frenk. "Scaling relations for galaxy clusters in the Millennium-XXL simulation." In: *Monthly Notices of the Royal Astronomical Society* 426.3 (2012), pp. 2046–2062. DOI: 10.1111/j.1365-2966.2012.21830.x. eprint: /oup/backfile/content_public/journal/mnras/426/3/10.1111/j.1365-2966.2012.21830.x/2/426-3-2046.pdf. URL: http://dx.doi.org/10.1111/j.1365-2966.2012.21830.x.

[2] J. M. Bardeen, J. R. Bond, N. Kaiser, and A. S. Szalay. "The statistics of peaks of Gaussian random fields." In: ApJ 304 (May 1986), pp. 15–61. DOI: 10.1086/164143.

[3] M. Bartelmann. "Trajectories of point particles in cosmology and the Zel'dovich approximation." In: Phys. Rev. D 91.8, 083524 (Apr. 2015), p. 083524. DOI: 10.1103/PhysRevD.91.083524. arXiv: 1411.0805 [gr-qc].

[4] M. Bartelmann, F. Fabis, S. Konrad, E. Kozlikin, R. Lilow, C. Littek, and J. Dombrowski. "Analytic calculation of the non-linear cosmic density-fluctuation power spectrum in the Born approximation." In: *ArXiv e-prints* (Oct. 2017). arXiv: 1710.07522.

[5] M. Bartelmann, F. Fabis, E. Kozlikin, R. Lilow, J. Dombrowski, and J. Mildenberger. "Kinetic field theory: effects of momentum correlations on the cosmic density-fluctuation power spectrum." In: *New Journal of Physics* 19.8, 083001 (Aug. 2017), p. 083001. DOI: 10.1088/1367-2630/aa7e6f. arXiv: 1611.09503.

[6] Matthias Bartelmann, Felix Fabis, Daniel Berg, Elena Kozlikin, Robert Lilow, and Celia Viermann. "A microscopic, non-equilibrium, statistical field theory for cosmic structure formation." In: *New Journal of Physics* 18.4 (2016), p. 043020. URL: http://stacks.iop.org/1367-2630/18/i=4/a=043020.

[7] F. Bernardeau, S. Colombi, E. Gaztañaga, and R. Scoccimarro. "Large-scale structure of the Universe and cosmological perturbation theory." In: *Physics Reports* 367.1 (2002), pp. 1 –248. ISSN: 0370-1573. DOI: https://doi.org/10.1016/S0370-1573(02)00135-7. URL: http://www.sciencedirect.com/science/article/pii/S0370157302001357.

[8] David Bohm. "A Suggested Interpretation of the Quantum Theory in Terms of "Hidden" Variables. I." In: *Phys. Rev.* 85 (2 1952), pp. 166–179. DOI: 10.1103/PhysRev.85.166. URL: https://link.aps.org/doi/10.1103/PhysRev.85.166.

[9] C. G. Böhmer and T. Harko. "Can dark matter be a Bose Einstein condensate?" In: J. Cosmology Astropart. Phys. 6, 025 (June 2007), p. 025. DOI: 10.1088/1475-7516/2007/06/025. arXiv: 0705.4158.

[10] A. M. Brooks, M. Kuhlen, A. Zolotov, and D. Hooper. "A Baryonic Solution to the Missing Satellites Problem." In: ApJ 765, 22 (Mar. 2013), p. 22. DOI: 10.1088/0004-637X/765/1/22. arXiv: 1209.5394.

[11] J. S. Bullock. "Notes on the Missing Satellites Problem." In: *ArXiv e-prints* (Sept. 2010). arXiv: 1009.4505 [astro-ph.CO].

[12] P. H. Chavanis. "Growth of perturbations in an expanding universe with Bose-Einstein condensate dark matter." In: A&A 537, A127 (Jan. 2012), A127. DOI: 10.1051/0004-6361/201116905. arXiv: 1103.2698.

[13] A. Einstein. "Die Feldgleichungen der Gravitation." In: *Sitzungsberichte der Königlich Preußischen Akademie der Wissenschaften (Berlin), Seite 844-847.* (1915).

[14] A. Friedmann. "Über die Krümmung des Raumes." In: *Zeitschrift fur Physik* 10 (1922), pp. 377–386. DOI: 10.1007/BF01332580.

[15] E. P. Gross. "Structure of a quantized vortex in boson systems." In: *Il Nuovo Cimento (1955-1965)* 20.3 (1961), pp. 454–477. ISSN: 1827-6121. DOI: 10.1007/BF02731494. URL: https://doi.org/10.1007/BF02731494.

[16] W. Hu, R. Barkana, and A. Gruzinov. "Fuzzy Cold Dark Matter: The Wave Properties of Ultralight Particles." In: *Physical Review Letters* 85 (Aug. 2000), pp. 1158–1161. DOI: 10.1103/PhysRevLett.85.1158. eprint: astro-ph/0003365.

[17] A. H. Jaffe and M. Kamionkowski. "Calculation of the Ostriker-Vishniac effect in cold dark matter models." In: Phys. Rev. D 58.4, 043001 (Aug. 1998), p. 043001. DOI: 10.1103/PhysRevD.58.043001. eprint: astro-ph/9801022.

[18] D. N. Limber. "The Analysis of Counts of the Extragalactic Nebulae in Terms of a Fluctuating Density Field." In: ApJ 117 (Jan. 1953), p. 134. DOI: 10.1086/145672.

[19] C.-P. Ma and J. N. Fry. "Nonlinear Kinetic Sunyaev-Zeldovich Effect." In: *Physical Review Letters* 88.21, 211301 (May 2002), p. 211301. DOI: 10.1103/PhysRevLett.88.211301. eprint: astro-ph/0106342.

[20] E. Madelung. "Quantentheorie in hydrodynamischer Form." In: *Zeitschrift für Physik* 40.3 (1927), pp. 322–326. ISSN: 0044-3328. DOI: 10.1007/BF01400372. URL: https://doi.org/10.1007/BF01400372.

[21] D. J. E. Marsh. "Nonlinear hydrodynamics of axion dark matter: Relative velocity effects and quantum forces." In: Phys. Rev. D 91.12, 123520 (June 2015), p. 123520. DOI: 10.1103/PhysRevD.91.123520. arXiv: 1504.00308.

[22] D. J. E. Marsh. "Axion cosmology." In: Phys. Rep. 643 (July 2016), pp. 1–79. DOI: 10.1016/j.physrep.2016.06.005. arXiv: 1510.07633.

[23] P. C. Martin, E. D. Siggia, and H. A. Rose. "Statistical Dynamics of Classical Systems." In: *Phys. Rev. A* 8 (1 1973), pp. 423–437. DOI: 10.1103/PhysRevA.8.423. URL: https://link.aps.org/doi/10.1103/PhysRevA.8.423.

[24] L. Mercolli and E. Pajer. "On the velocity in the Effective Field Theory of Large Scale Structures." In: J. Cosmology Astropart. Phys. 3, 006 (Mar. 2014), p. 006. DOI: 10.1088/1475-7516/2014/03/006. arXiv: 1307.3220.

[25] J. P. Ostriker and E. T. Vishniac. "Generation of microwave background fluctuations from nonlinear perturbations at the ERA of galaxy formation." In: ApJ 306 (July 1986), pp. L51–L54. DOI: 10.1086/184704.

[26] H. Park, P. R. Shapiro, E. Komatsu, I. T. Iliev, K. Ahn, and G. Mellema. "The Kinetic Sunyaev-Zel'dovich Effect as a Probe of the Physics of Cosmic Reionization: The Effect of Self-regulated Reionization." In: ApJ 769, 93 (June 2013), p. 93. DOI: 10.1088/0004-637X/769/2/93. arXiv: 1301.3607.

[27] H. Park, E. Komatsu, P. R. Shapiro, J. Koda, and Y. Mao. "The Impact of Nonlinear Structure Formation on the Power Spectrum of Transverse Momentum Fluctuations and the Kinetic Sunyaev-Zel'dovich Effect." In: ApJ 818, 37 (Feb. 2016), p. 37. DOI: 10.3847/0004-637X/818/1/37. arXiv: 1506.05177.

[28] R. D. Peccei and H. R. Quinn. "CP conservation in the presence of pseudoparticles." In: *Physical Review Letters* 38 (June 1977), pp. 1440–1443. DOI: 10.1103/PhysRevLett.38.1440.

[29] P. J. E. Peebles. *The large-scale structure of the universe*. 1980.

[30] Michael E. Peskin and Daniel V. Schroeder. *An Introduction to quantum field theory*. Reading, USA: Addison-Wesley, 1995. ISBN: 9780201503975, 0201503972. URL: http://www.slac.stanford.edu/~mpeskin/QFT.html.

[31] L. P. Pitaevskii. "Vortex Lines in an Imperfect Bose Gas." In: *JETP* 40.2 (Aug. 1961).

[32] Planck Collaboration et al. "Planck 2015 results. XIII. Cosmological parameters." In: A&A 594, A13 (Sept. 2016), A13. DOI: 10.1051/0004-6361/201525830. arXiv: 1502.01589.

[33] H.-Y. Schive, T. Chiueh, T. Broadhurst, and K.-W. Huang. "Contrasting Galaxy Formation from Quantum Wave Dark Matter, ψDM, with ΛCDM, using Planck and Hubble Data." In: ApJ 818, 89 (Feb. 2016), p. 89. DOI: 10.3847/0004-637X/818/1/89. arXiv: 1508.04621.

[34] E. T. Vishniac. "Reionization and small-scale fluctuations in the microwave background." In: ApJ 322 (Nov. 1987), pp. 597–604. DOI: 10.1086/165755.

[35] Y. B. Zel'dovich. "Gravitational instability: An approximate theory for large density perturbations." In: A&A 5 (Mar. 1970), pp. 84–89.

[36] Y. B. Zeldovich and R. A. Sunyaev. "The Interaction of Matter and Radiation in a Hot-Model Universe." In: Ap&SS 4 (July 1969), pp. 301–316. DOI: 10.1007/BF00661821.

[37] W. J. G. de Blok. "The Core-Cusp Problem." In: *Advances in Astronomy* 2010, 789293 (2010), p. 789293. DOI: 10.1155/2010/789293. arXiv: 0910.3538.

COLOPHON

This document was typeset using the typographical look-and-feel `classicthesis` developed by André Miede. The style was inspired by Robert Bringhurst's seminal book on typography "*The Elements of Typographic Style*". `classicthesis` is available for both LaTeX and LyX:

https://bitbucket.org/amiede/classicthesis/

Happy users of `classicthesis` usually send a real postcard to the author, a collection of postcards received so far is featured here:

http://postcards.miede.de/

Final Version as of May 14, 2018 (`classicthesis` version 4.2).